

BLOCKHOUSE DOSAGE CONTRIBUTIONS RESULTING FROM  
WINDOW-COLLIMATED, CEILING SCATTERED FALLOUT RADIATION

by

JAMES ANDREW BARAN

B. S., Case Institute of Technology, 1960

---

A MASTER'S THESIS

submitted in partial fulfillment of the

requirements for the degree

MASTER OF SCIENCE

Department of Nuclear Engineering

KANSAS STATE UNIVERSITY  
Manhattan, Kansas

1963

Approved by:

John O. Mingle  
Richard E. Faw

Major Professors

LD  
2668  
T4  
1963  
B34  
C.2  
Document

TABLE OF CONTENTS

NOMENCLATURE-----	iv
1.0 INTRODUCTION-----	1
2.0 THEORETICAL DEVELOPMENT-----	6
2.1 Derivation of Equations-----	6
2.2 Transformation of Integrals for Computer Utilization--	15
2.2.1 Differential Incident Dose Rate-----	16
2.2.2 Total Incident Dose Rate-----	18
2.2.3 Differential Reflected Dose Rate-----	19
2.2.4 Total Reflected Dose Rate-----	20
2.2.5 Total Dose Rate at Point (xx,yy,zz)-----	21
3.0 RESULTS OF CALCULATIONS-----	23
3.1 Discussion of Results-----	23
3.1.1 Albedos-----	23
3.1.2 Incident Dose Rates-----	25
3.1.3 Reflected Dose Rates-----	31
3.1.4 Total Dose Rate at Position (xx,yy,zz) in the KSU Blockhouse-----	35
3.2 Conclusions-----	45
3.3 Further Investigations-----	47
4.0 ACKNOWLEDGEMENT-----	49
5.0 LITERATURE CITED-----	50
6.0 APPENDICES-----	53
APPENDIX A: Determination of the Constant of Proportionality, W, for the Dose Angular Distribution Equation-----	54
APPENDIX B Albedo Study-----	57
APPENDIX C: Description and explanation of the IBM- 1620 Computer Program Used to Inter- polate Among Various Parameters-----	68
APPENDIX D: Description and Explanation of the IBM- 1620 Computer Program Used to Check the Accuracy of the Chilton-Huddleston Formula-----	73

APPENDIX E:	Description and Explanation of the IBM-1620 Computer Program Used for Calculating the Differential Dose Rate Albedo-----	84
APPENDIX F:	Discussion of Gaussian Quadrature-----	93
APPENDIX G:	Description and Explanation of the IBM-1620 Computer Program Used for Calculating the Differential Incident Dose Rate at Point (x,y) on the Ceiling of a Blockhouse-----	96
APPENDIX H:	Description and Explanation of the IBM-1620 Computer Program Used for Calculating the Total Incident Dose Rate at Point (x,y) on the Ceiling of a Blockhouse-----	111
APPENDIX J:	Description and Explanation of the IBM-1620 Computer Program Used for Calculating the Differential Reflected Dose Rate at Point (x,y) on the Ceiling of a Blockhouse-----	117
APPENDIX K:	Description and Explanation of the IBM-1620 Computer Program Used for Calculating the Total Reflected Dose Rate at Point (x,y) on the Ceiling of a Blockhouse-----	133
APPENDIX L:	Description and Explanation of the IBM-1620 Computer Program Used for Calculating the Total Dose Rate at Position (xx,yy,zz) in a Blockhouse-----	138
APPENDIX M:	Description and Explanation of the IBM-1620 Computer Program Used to Calculate the First Order Exponential Integral-----	160
APPENDIX N:	Protection Factor of the KSU Blockhouse--	162

## NOMENCLATURE

$a$	Dose angular distribution defining constant.
$\bar{a}$	Chilton-Huddleston albedo defined by eq.(71).
$\underline{a}$	Dose rate albedo defined by eq.(79).
$a'$	Build-up factor constant.
$a''$	Least-squares constant.
$a_k$	Christoffel numbers.
$b$	Build-up factor constant.
$b'$	Least-squares constant.
$B$	Dose build-up factor for a point isotropic source defined by eq.(16).
$c$	Degree of Gaussian quadrature for the emergent azimuthal angle.
$C, C'$	Chilton-Huddleston albedo constants.
$d$	Height of ceiling above contaminated plane, feet.
$D_i$	Incident dose rate at $(x,y)$ , roentgens/hour.
$D_o$	Dose rate at the standard unprotected position, roentgens/hour.
$D_r$	Reflected dose rate at $(x,y)$ , roentgens/hour.
$E$	Reflected energy in a single Compton scattering defined in eq.(74), MeV.
$E_1$	Exponential function of the first order.
$E_2$	Exponential function of the second order.
$E_o$	Incident gamma ray energy, MeV.
$E'$	Average energy of the reflected gamma ray, MeV.
$f_k$	Zeros of the Legendre Polynomials for the incident azimuthal angle variable.
$F_u$	Uncollided flux from an isotropic distributed source defined in eq.(14), photons/sec.

$g_j$	Zeroes of the Legendre Polynomials for the incident polar angle variable.
$h_m$	Zeroes of the Legendre Polynomials for the emergent polar angle variable.
$h'_m$	Zeroes of the Legendre Polynomials for the y co-ordinate of the ceiling.
H	Distance between ceiling and horizontal centerline of aperture, feet.
j	Degree of Gaussian quadrature for the incident polar angle.
$j'$	Azimuthal angular limit constant utilized in eq.(68).
k	Degree of Gaussian quadrature for the incident azimuthal angle.
$k'$	Polar angular limit constant utilized in eq.(68).
K	Ratio of Compton scattering energies multiplied by the Klein-Nishina cross section defined by eq.(23).
m	Degree of Gaussian quadrature for the emergent polar angle.
n	Degree of least-squares analysis.
N	Degree of Gaussian quadrature used in Appendix F.
p	Ratio of emergent to incident energies in a single Compton scattering process.
P	Probability that a photon of certain energy incident on a surface at a given angle will emerge from that surface into a certain solid angle.
r	Radial variable in plane surface source geometry, feet (see Figure 5).
R	One-half aperture width, feet (see Figure 3).
$R'$	Build-up distance variable, feet.
$R_o$	Distance variable between contaminated plane and position (x,y) on ceiling, feet (see Figure 5).
$R'_o$	Classical radius of electron defined by eq.(73), cm.
$s_c$	Zeroes of Legendre Polynomials for the emergent azimuthal angle variable.
$s'_c$	Zeroes of Legendre Polynomials for the x co-ordinate of the ceiling.

$S_A$	Plane source gamma ray intensity, photons/cm <sup>2</sup> -sec.
SD	Differential scattered dose rate defined by eq.(68), kev./gm.-sec.
t	Thickness of concrete floor slab, feet (see Figure 3).
u	Integration variable.
V	One-half aperture height, feet (see Figure 3).
W	Dose angular distribution proportionality constant defined by eq.(64).
x	Ceiling rectangular co-ordinate parallel to plane of the aperture; x = 0 is at the vertical centerline of the aperture, feet (see Figure 3).
xx	Detector rectangular co-ordinate parallel to plane of the aperture; xx = 0 is at the vertical centerline of the aperture, feet.
$X_{max}$	Half-width of structure measured parallel to aperture plane, feet.
y	Ceiling rectangular co-ordinate perpendicular to plane of the aperture; y = 0 is at aperture plane, feet.
yy	Detector rectangular co-ordinate perpendicular to plane of the aperture; yy = 0 is at aperture plane, feet.
$Y_{max}$	Total length of structure measured perpendicularly from the aperture plane, feet.
zz	Perpendicular distance measured positive downwards from ceiling, feet.
$\mu_a$	Energy linear macroscopic gamma ray absorption coefficient for air, cm <sup>-1</sup> .
$\mu'_a$	Energy mass macroscopic gamma ray absorption coefficient for air, cm <sup>2</sup> /gm.
$\Omega$	Solid angle, steradians.
$\Phi$	Emergent azimuthal angle, radians (see Figure 3).
$\Phi'$	Total change in azimuth between direction of incident and emergent gamma rays defined by eq.(25), radians.
$\Phi_0$	Incident azimuthal angle, radians.
$\Phi_1, \Phi_2$	Azimuthal limits of aperture, radians (see Figure 3).

$\Phi_j, \Phi_{j+1}$	Azimuthal angular intervals, radians.
$\rho$	Distance between position (x,y) on the ceiling and position (xx,yy,zz) of the detector defined by eq.(29).
$\Sigma$	General total linear macroscopic gamma ray absorption coefficient, $\text{cm}^{-1}$ .
$\Sigma_a$	Total linear macroscopic gamma ray absorption coefficient for air at standard temperature and pressure, $\text{cm}^{-1}$ .
$\Sigma_c$	Total linear macroscopic gamma ray absorption coefficient for concrete, $\text{cm}^{-1}$ .
$\Theta$	Emergent polar angle, radians (see Figure 3).
$\Theta_0$	Incident polar angle, radians (see Figure 3).
$\Theta_1, \Theta_2$	Polar limits of aperture, radians (see Figure 3).
$\Theta_k, \Theta_{k+1}$	Polar angular intervals, radians.
$\Theta_s$	Total scattering angle defined by eq.(24), radians.

## 1.0 INTRODUCTION

The increasing scale of nuclear explosive testing in various parts of the world has led to considerable public concern over the effects of fallout radiation. This concern, because of the ever-present possibility of international nuclear conflict, has led to public and private interest in the ability of existing or proposed structures to offer protection by shielding from the effects of the fallout radiation.

Methods are presented in the various design and analysis procedures presently available for estimating the direct dose rate contributions resulting from radiation entering structures through apertures (1,2,3). However no methods are available for estimation of the ceiling scattered dose rate portion of this contribution. This contribution is specifically classified as a ceiling shine problem and more generally as a vent problem. The necessity for additional research on this problem is further exemplified by the following statement made August 3, 1962 by Dr. L. V. Spencer, the leading theoretician in the field of structure shielding against fallout radiation (4): "So far as I know, no systematic investigations have been made of ceiling shine resulting from radiation which enters through a vent in one of the vertical walls of a building. I think this type of problem is currently the most important vent problem."

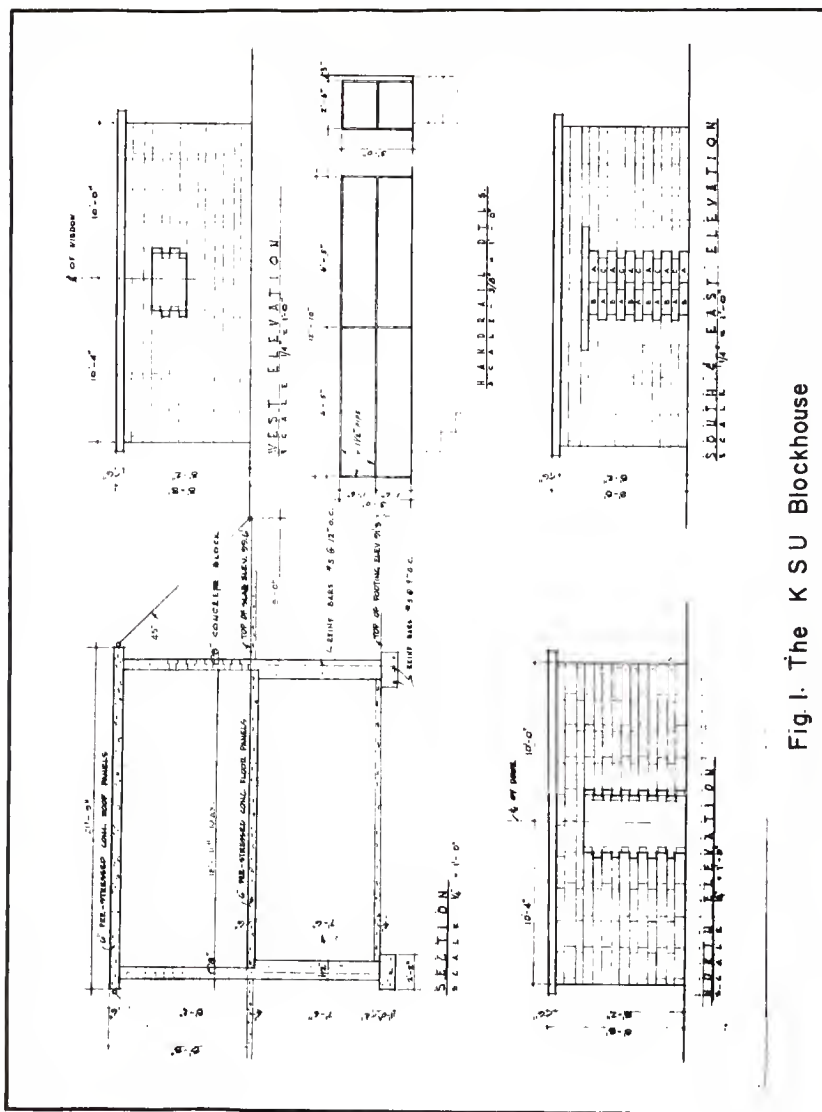
The intent of this thesis was to undertake a systematic analytical investigation of this problem utilizing the IBM-1620 computing facilities available at the Kansas State University Computing Center. FORTRAN II programming was utilized throughout the study.



The study was idealized to make it compatible with the Kansas State University Nuclear Engineering Shielding Facility blockhouse. This structure will hereinafter be called the KSU blockhouse. A blockhouse is a very elementary type of structure, consisting merely of a building with four walls and a slab roof. This study considers such a structure with a single window centered horizontally but not necessarily vertically in one of the walls. The plans for the KSU blockhouse are given on Figure 1.

The assumption was made that the fallout was uniformly distributed horizontally over exposed surfaces. This is a standard assumption made in virtually all treatments of structure shielding against fallout radiation (1, 2, 3, 4).

It is not desirable or realistic to determine the absolute radiation intensity inside a structure since this changes so rapidly following a fallout producing event. Rather, it is desirable--customary in the past few years--to measure the radiation protection afforded by a given structure in terms of a "standard unprotected position." The ratio of the dose rate at a given position in a structure to the dose rate in the unprotected position is commonly called (1, 2, 3, 4) the "reduction factor." The standard unprotected position was formerly chosen to be a few feet above a large, fallout contaminated field. However, difficulties arose in theoretically determining the absolute radiation level in such a location. The standard unprotected position is presently defined to be a detector location three feet (in dry air at 76 cm. Hg. pressure and 20°C) above a hypothetical source of the same character as the fallout on the ground. This fallout is presumed to lie on a perfectly smooth, infinite plane.



The ground is assumed to be replaced by compressed air of the same density in order to make possible an accurate theoretical analysis. This replacement of ground with compressed air is an adequate model (1). The reference dose rate can be calculated to within two to three percent accuracy, given the spectrum and strength of the gamma rays emitted per unit area of the fallout field. The accepted value of the reference dose rate for a plane contaminated with one curie/ft<sup>2</sup> of cobalt-60 is 485 roentgens per hour (5).

Radioactive fallout consists of both fission fragments and neutron activated materials. The fission fragments contribute about 95% of the total radioactivity at one hour after a fission explosion (5). The fallout material does not emit neutrons. There will be a spectrum of fallout energies varying with time since the fission material alone may contain as many as 200 radioactive nuclides, each decaying at its own rate. A different spectrum can thus be considered to be in existence at different times after fission. The differences between these spectra become significant however, only when considering extreme penetrations into matter (1). Thus a "standard" spectrum could be chosen assuming that it is a "hard" spectrum prevalent at a time that the fallout radiation has a high intensity. The 1.12 hour U-235 fission spectrum (6) was chosen to be this standard spectrum. This spectrum (4) is represented in Figure 2. The height of each box in Figure 2 is proportional to the energy content of gamma rays in the energy interval, the sum of the ordinates being unity. The two arrows in Figure 2 are positioned at the energies of the gammas given off by cobalt-60. This isotope is used in most of the fallout field experiments to simulate the standard fission spectrum. The arithmetic average energy of the cobalt-60 gammas, 1.252 Mev, was assumed to be the standard

$$\Phi = \tan^{-1}\{(x-xx)/(y-yy)\} + \pi. \quad (31)$$

The plane-source strength of gamma radiation is converted to a point-source strength of gamma radiation by integrating eq.(27) over a dA of the ceiling. The differential dose received by an isotropically responding differential detector located at (xx,yy,zz) is

$$D(xx,yy,zz;\Theta,\Phi)\rho\sin\Theta d\Phi d\Theta = \int_{A_r} D_r(x,y;\Theta,\Phi)\sin\Theta dA. \quad (32)$$

Dividing both sides of eq.(32) by  $\rho^2$ , multiplying the right side by the build-up factor and the material exponential attenuation factor and integrating over the ceiling results in an expression for the total dose rate in any position of the blockhouse resulting from aperture-collimated, ceiling scattered radiation.

$$\begin{aligned} D(xx,yy,zz) = & (1.293D_0/2\pi) \int_0^{x_{\max}} \int_0^{y_{\max}} \int_{\Theta_1}^{\Theta_2} \int_{\Phi_1}^{\Phi_2} (0.1917+0.0095\cos\Theta_0) \\ & \times \{1 + a'\Sigma_a(E_0)d \exp(b\Sigma_a(E_0)d/\cos\Theta_0)\} \exp(-\Sigma_a(E_0)d/\cos\Theta_0) \{CK(\Theta_s)+C'\} \\ & \times \{1 + a'\Sigma_a(E')(p-t/\cos\Theta)-\Sigma_c(E')t/\cos\Theta\} \exp(b\Sigma_a(E')(p-t/\cos\Theta) \\ & -\Sigma_c(E')t/\cos\Theta)\} \{ \exp(\Sigma_a(E')(p-t/\cos\Theta)-\Sigma_c(E')t/\cos\Theta) \}^{-1} \{ \rho^2(\cos\Theta_0 \\ & +\cos\Theta) \}^{-1} \sin\Theta_0 d\Theta_0 d\Phi_0 dydx. \end{aligned} \quad (33)$$

This equation was integrated numerically on the digital computer.

## 2.2 Transformation of Integrals for Computer Utilization

An IBM 1620 digital computer with a 60,000 digit memory was utilized for machine computations. FORTRAN II language was used throughout.

The approximation technique known as Gaussian quadrature (19) was

employed to integrate numerically the equations in the Section 2.1. This technique is discussed and its accuracy is checked in Appendix F. Gauss' mechanical quadrature formula is

$$\int_{-1}^1 f(x) dx = \sum_{k=1}^N a_k f(x_k) \quad (34)$$

where  $a_k$  are the Christoffel Numbers and  $x_k$  are the zeroes of the Legendre Polynomials. Eq.(34) is exact if  $f(x)$  is a polynomial of degree  $2N-1$  or less. Values of  $x_k$  and  $a_k$  for values of  $N$  through 6 are tabulated in Reference 15 and are presented in Table 12.

### 2.2.1. Differential Incident Dose Rate

The differential incident dose rate at point  $(x,y)$  of the ceiling is given by eq.(9) with a build-up term added per the previous discussion. The term

$$(0.1917 + 0.0095 \cos \Theta_0) \left\{ 1 + a' \sum_a (E_0) d \exp(b \sum_a (E_0) d / \cos \Theta_0) / \cos \Theta_0 \right\} \\ \times \left\{ 2\pi \cos \Theta_0 \exp(-a / \cos \Theta_0) \right\}^{-1} \Delta \cos \Theta_0 \Delta \Phi_0 \quad (35)$$

was computed at a given  $(x,y)$  for 56 equal solid angles in a hemisphere for radiation incident through the aperture. Here  $a = \Sigma d$  as previous. Each solid angle division is equal to  $\pi/28$  steradians. The geometry and solid-angle divisions are illustrated in Figure 6. The top half of the hemisphere in Figure 6 lies in the positive  $x$  plane of the ceiling. The midpoints of the polar angle divisions are  $7.7^\circ$ ,  $18.6^\circ$ ,  $28.3^\circ$ ,  $39.6^\circ$ ,  $49.8^\circ$ ,  $59.9^\circ$ ,  $71.1^\circ$  and  $83.8^\circ$ . The expression indicated in (35) was weighted by the fraction of each solid angle division subtended by the aperture. This fraction was determined from the known aperture limits

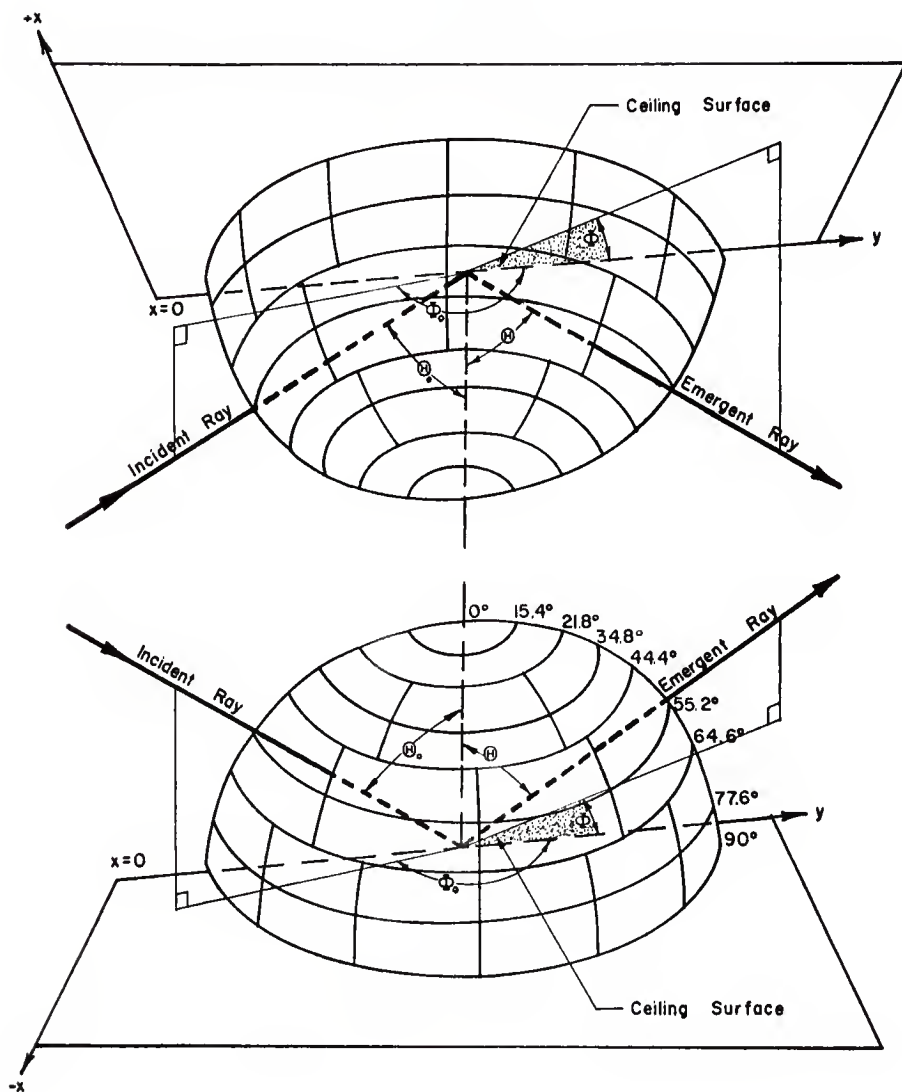


Fig. 6. Geometry and solid-angle divisions for the differential dose rate studies.

defined in eq.(1) through eq.(4). The computer program for this differential incident dose rate is presented and discussed in Appendix G.

### 2.2.2. Total Incident Dose Rate

The total incident dose rate defined by eq.(20) was solved by putting it in the Gaussian quadrature form of eq.(34). That is, letting

$$f_k = \{\Phi_{ok} - (\Phi_1 + \Phi_2)/2\} \{2/(\Phi_2 - \Phi_1)\} \quad (36)$$

thus changes the limits from -1 to +1. Therefore

$$df_k = \{2/(\Phi_2 - \Phi_1)\} d\Phi_{ok} \quad (37)$$

and eq.(20) becomes

$$\begin{aligned} D_1(x, y) = & \{D_0(\Phi_2 - \Phi_1)/4\pi\} \sum_{k=1}^{K_{\max}} \{0.1917\{E_1(\sum_a(E_o)d/\cos\Theta_{1k}) - E_1(\sum_a(E_o)d/\cos\Theta_{2k})\} \\ & + (a'/(1-b))\{\exp(-\sum_a(E_o)d(1-b)/\cos\Theta_{1k}) - \exp(-\sum_a(E_o)d(1-b)/\cos\Theta_{2k})\}\} \\ & + 0.0095\{\cos\Theta_{1k}E_2(\sum_a(E_o)d/\cos\Theta_{1k}) - \cos\Theta_{2k}E_2(\sum_a(E_o)d/\cos\Theta_{2k}) + a'\sum_a(E_o)d \\ & \times \{E_1(\sum_a(E_o)d(1-b)/\cos\Theta_{1k}) - E_1(\sum_a(E_o)d(1-b)/\cos\Theta_{2k})\}\}a_k \end{aligned} \quad (38)$$

where

$$\Theta_{1k} = \tan^{-1}\{y/(H+V)\cos(\Phi_{ok}-\pi)\} \quad (39)$$

and

$$\Theta_{2k} = \tan^{-1}\{y/(H-V)\cos(\Phi_{ok}-\pi)\}. \quad (40)$$

The angle  $\Phi_{ok}$  is obtained from eq.(36) for different values of  $f_k$ . The angles  $\Phi_1$  and  $\Phi_2$  are defined by eq.(1) and eq.(2). The computer program

for this total incident dose rate is presented and discussed in Appendix B.

### 2.2.3, Differential Reflected Dose Rate

The differential reflected dose rate was determined by evaluation of the double integral of eq.(27) for the solid angle divisions of Figure 6, i.e.,

$$\begin{aligned} & (1.293D_o/2\pi) \int_{\Phi_1}^{\Phi_2} \int_{\Theta_1}^{\Theta_2} (0.1917+0.0095\cos\Theta_o) \{1+(a'\Sigma_a(E_o)d \\ & \times \exp(b\Sigma_a(E_o)d/\cos\Theta_o))/\cos\Theta_o\} \exp\{-\Sigma_a(E_o)d/\cos\Theta_o\} \\ & \times \{CK(\Theta_s)+C'\} (\cos\Theta_o+\cos\Theta)^{-1} \sin\Theta_o d\Theta_o d\Phi_o. \end{aligned} \quad (41)$$

The  $\Phi_o$  limits are again transformed by eq.(36) and eq.(37). Letting  $\omega_o = \cos\Theta_o$ , then the limits over  $\Theta_o$  are transformed by

$$g_j = \{\omega_{oj} - (\omega_1 + \omega_2)/2\} \{2/(\omega_2 - \omega_1)\} \quad (42)$$

and

$$dg_j = \{2/(\omega_2 - \omega_1)\} d\omega_{oj}. \quad (43)$$

Expression (41) is then given by

$$\begin{aligned} & \{1.293(\Phi_2 - \Phi_1)D_o/8\pi\} \sum_{k=1}^{K_{\max}} a_k (\omega_{1k} - \omega_{2k}) \sum_{j=1}^{K_{\max}} a_j (0.1917+0.0095\omega_{oj}) \\ & \times \{1+(a'\Sigma_a(E_o)d \exp(b\Sigma_a(E_o)d/\omega_{oj}))/\omega_{oj}\} \exp\{-\Sigma_a(E_o)d/\omega_{oj}\} \\ & \times \{CK(\Theta_s)+C'\} (\omega_{oj}+\cos\Theta)^{-1} \Delta\Omega \end{aligned} \quad (44)$$

where  $\Theta_1 = \cos^{-1} \omega_1$  and  $\Theta_2 = \cos^{-1} \omega_2$  are given by eq.(39) and eq.(40),  $\Phi_1$  and  $\Phi_2$  by eq.(1) and eq.(2) and the  $\Delta\Omega$  by the emergent solid angle ( $\pi/28$  for the solid angle divisions of Figure 6).  $\cos\Theta_{oj} = \omega_{oj}$  is



obtained from eq.(42) for different values of  $g_j$ . A description and discussion of the computer program for this differential reflected dose rate is given in Appendix J.

#### 2.2.4. Total Reflected Dose Rate

The total reflected dose rate at the point (x,y) is given by eq.(28). The  $\Phi_o$  and  $\Theta_o$  limits are transformed to the -1 and +1 limits by eq.(36) and eq.(42). If  $\omega = \cos\Theta$ , then  $d\omega = -\sin\Theta d\Theta$  and the limits on  $\omega$  go from 0 to 1. This can be transformed to the desired limits by the relationships,

$$h_m = 2(\omega_m - 1/2) \quad (45)$$

and

$$dh_m = 2d\omega_m. \quad (46)$$

The  $\Phi$  transformation is

$$s_c = (\Phi_c - \pi)/\pi \quad (47)$$

and

$$ds_c = d\Phi_c/\pi. \quad (48)$$

Eq.(28) becomes

$$\begin{aligned} D_r(x,y) = \{ & 1.293(\Phi_2 - \Phi_1)D_o/16 \} \sum_{c=1}^{K_{\max}} a_c \sum_{m=1}^{K_{\max}} a_m \sum_{k=1}^{K_{\max}} a_k (\omega_{1k} - \omega_{2k}) \sum_{j=1}^{K_{\max}} a_j \\ & \times (0.1917 + 0.0095\omega_{oj}) \exp(-\sum_a (E_o)d/\omega_{oj}) (CK(\Theta_s) + C') \{ 1 + a' \sum_a (E_o)d \\ & \times \exp(b \sum_a (E_o)d/\omega_{oj}) / \omega_{oj} \} \{ \omega_{oj} + \omega_m \}^{-1}. \end{aligned} \quad (49)$$

Appendix K describes and discusses this total reflected dose rate.

### 2.2.5. Total Dose Rate at Point (xx,yy,zz)

This dose rate is given by the quadruple integral of eq.(33). The  $\Phi_0$  and  $\Theta_0$  limit transformations are given by eq.(36) and eq.(42). The x transformation is obtained from

$$s'_c = x_c / X_{\max} \quad (50)$$

and

$$ds'_c = dx_c / X_{\max} \quad (51)$$

where  $X_{\max}$  is one-half the width of the ceiling, measured parallel to the plane of the aperture, as illustrated in Figure 3. The transformation on the y limits is

$$h'_m = (2y_m - Y_{\max}) / Y_{\max} \quad (52)$$

and

$$dh'_m = 2dy_m / Y_{\max} \quad (53)$$

where  $Y_{\max}$  is the length of the ceiling, measured perpendicular to the plane of the aperture, as illustrated in Figure 3.

The total dose rate is given by Eq.(54). A description and discussion of the computer code for this total dose rate is given in Appendix L.

$$\begin{aligned}
D(xx, yy, zz) = & \left\{ 1.293(\Phi_2 - \Phi_1) X_{\max} Y_{\max} D_o / 16\pi \right\} \sum_{c=1}^{K_{\max}} a_c \sum_{m=1}^{K_{\max}} (a_m / \rho^2) \sum_{k=1}^{K_{\max}} a_k (\omega_{1k} - \\
& \omega_{2k}) \sum_{j=1}^{K_{\max}} a_j (0.1917 + 0.0095 \omega_{oj}) \left\{ 1 + a' \sum_a (E_o) d \exp(b \sum_a (E_o) d / \omega_{oj}) \right\} \exp(-\sum_a (E_o) \\
& \times d / \omega_{oj}) \left\{ CK(\Theta_g) + C' \right\} \left\{ 1 + a' (\sum_a (E') (\rho - t / \cos \Theta) - \sum_c (E') t / \cos \Theta) \right. \\
& \times \exp(b (\sum_a (E') (\rho - t / \cos \Theta) - \sum_c (E') t / \cos \Theta)) \left. \right\} \exp \left\{ -\sum_a (E') (\rho - t / \cos \Theta) \right. \\
& \left. - \sum_c (E') t / \cos \Theta \right\} \left\{ \omega_{oj} + \cos \Theta \right\}^{-1}.
\end{aligned} \tag{54}$$

### 3.0 RESULTS OF CALCULATIONS

#### 3.1 Discussion of Results

##### 3.1.1 Albedos

Albedos are discussed rather thoroughly in Appendix B. The differential dose rate albedo derived in this appendix, eq.(79), was used in this study whenever ceiling-shine was considered. Such an albedo could be obtained analytically because of the recent development of a semi-empirical formula for a differential dose albedo for gamma rays on concrete by Chilton and Huddleston (14). A comparison between the Chilton-Huddleston formula and the Monte Carlo results of Raso (12) is shown in Figure 22. It is rather difficult to obtain an accurate estimate of the statistical error of the albedos. It can be seen from Figure 22 that the biggest discrepancies appear at small emergent polar angles for total azimuthal changes of around  $50^{\circ}$ . The Chilton-Huddleston formula gives scattered dose rates too low by about a factor of two from Raso's Monte Carlo values for these angular regions. This is unfortunate as it leads to non-conservative dose rates, e.g., the ceiling scattered dose rates obtained through this formula could give dosages of one-half the "true" value. It should be emphasized here that a more extensive study of these results should be made before more general conclusions can be made. The computer code listed and explained in Appendix D would readily produce data for additional such comparisons. A limited amount of results for an incident energy of 1.252 MeV are tabulated in this appendix but could not be readily compared with Raso's results which are given at different energies.

Only a very crude estimate can be made of the statistical fluctuations of Raso's Monte Carlo results. Raso (12) states that the "statistical

percentage errors" could be roughly estimated to be inversely proportional to the square root of the product of the total number of photons back-scattered by 5000 (the number of histories run) divided by 96 (since there are 96 entries per table). The number albedo for the parameters of Figure 22 is 0.502. This results in a statistical percentage error of approximately 20%.

It would be more accurate if the Monte Carlo results were used directly in the calculations. This would require, as a minimum, an initial linear interpolation between the approximately 500 values in Rasó's 1.00 MeV table and the 500 values in his 2.00 MeV table. This would produce a table which would have to be triply interpolated (over  $\Theta$ ,  $\Theta_0$  and  $\Phi'$ ) for every albedo. This would require a computer memory and a computing time which would probably exceed the capabilities of the IBM-1620. In addition, statistical fluctuations in "Monte-Carlo" values of albedos would be carried over into scattered dose calculations. Some type of "curve-smoothing" would hence also be required in the interpolation method.

The differential dose rate albedo utilized in this thesis is defined by eq.(79). This albedo contains the albedo errors discussed above. The computer program written for this albedo is presented and discussed in Appendix E. Portions of the results tabulated in this appendix are plotted in Figures 23 through 27. The largest albedos occur with near grazing incidence and reflection. This is physically what would be expected since the photon need undergo an interaction resulting in only a small angular change to be reflected. It can readily be seen from these figures that differential dose rate albedos observed by a detector at most normal positions would lie between 1% and 20%.

A better picture of the dose rate albedo can be obtained by integrating the differential dose rate albedo over the emergent hemisphere. This was done in the computer program of Appendix E with a Gaussian quadrature of six. These total dose rate albedos were checked by multiplying each of the differential dose rate albedos by its solid angle and summing up these 96 values. The results are presented in Table 1. Better correspondence between the summed and integrated albedos

Table 1. Total dose rate albedos.

Cosine of Incident Obliquity $\cos\theta_0$	Total Dose Rate Albedo	
	Summed	Integrated
0.1	0.121	0.136
0.25	0.161	0.171
0.50	0.148	0.153
0.75	0.127	0.129
1.00	0.114	0.115

is observed with approach to perpendicular incidence. These integrated total dose rate albedos are plotted on Figure 6a. It would appear from this figure that an average total dose rate albedo from concrete would be approximately 14%. This can be compared with the 15% albedo employed by Spencer (1).

### 3.1.2 Incident Dose Rates

The computer program and results for the differential incident dose rate at point (x,y) on the ceiling of the KSU blockhouse from radiation incident on the window are presented in Appendix G. Results are tabulated for the 56 equal solid angles of Figure 6 at the (x,y) positions (0,5),

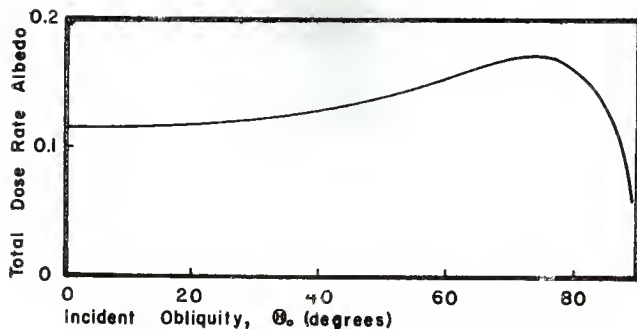


Fig. 6a. Variation of total dose rate albedos with incident polar angle.

(0,10), (0,15), (3,5), (3,10), (3,15), (6,5), (6,10) and (6,15) where the  $x$  and  $y$  have dimension of feet. The results for the three positions (0,10), (3,5) and (6,15) are presented in Figures 7 to 9.

The summation of these differential dose rates is within 4% of the value for each ceiling point obtained in the total incident dose rate program.

The total dose rate incident on any point of the ceiling of the KSU blockhouse from the window-collimated radiation is given by eq.(38). The FORTRAN II source program which solves this equation is presented in Appendix H along with the results for a two foot square mesh on the ceiling. These results are plotted in Figure 10. The dose rate is highest along the centerline of the window, as would naturally be expected. The peaking of this radiation is also to be expected since no radiation can be incident at the  $y = 0$  position. The magnitude of these incident dose rates is quite small. On the average, as can be noted on Fig. 10, less

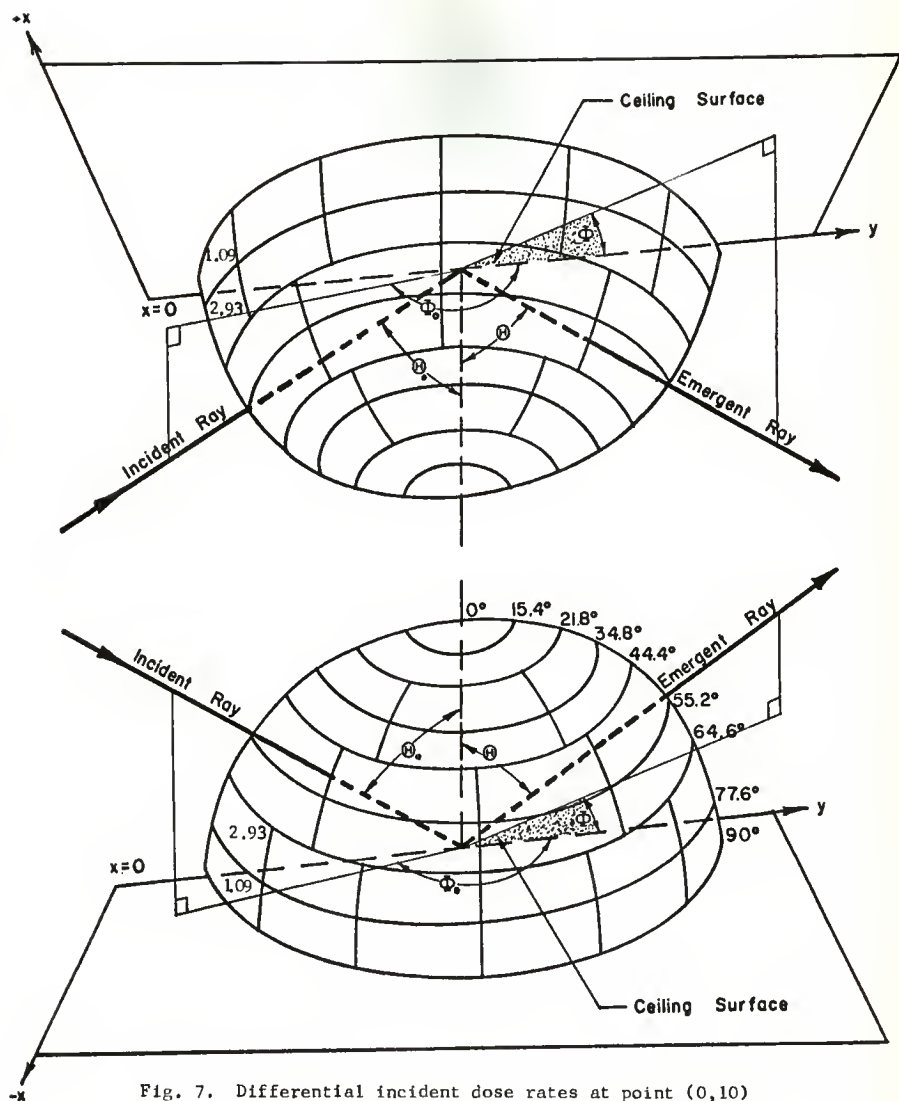


Fig. 7. Differential incident dose rates at point  $(0,10)$  on the KSU blockhouse ceiling,  $D_1(x,y;\theta_0,\Phi_0)\Delta\cos\theta_0\Delta\Phi(10^{-3}D_0)$ . The dose rates are zero unless otherwise specified.



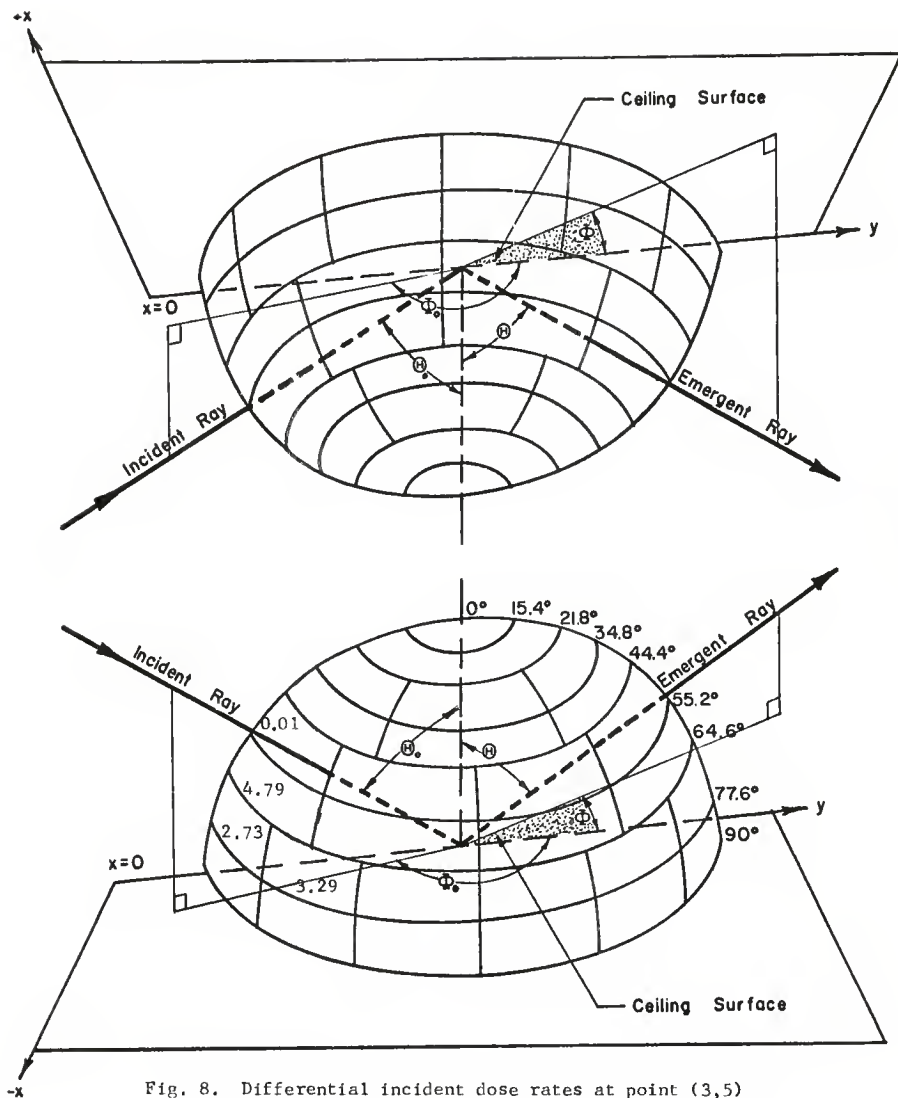


Fig. 8. Differential incident dose rates at point (3,5) on the KSU blockhouse ceiling,  $D_i(x,y;\theta_0,\phi_0)\Delta\cos\theta_0\Delta\phi$  ( $10^{-3}D_0$ ). The dose rates are zero unless otherwise specified.

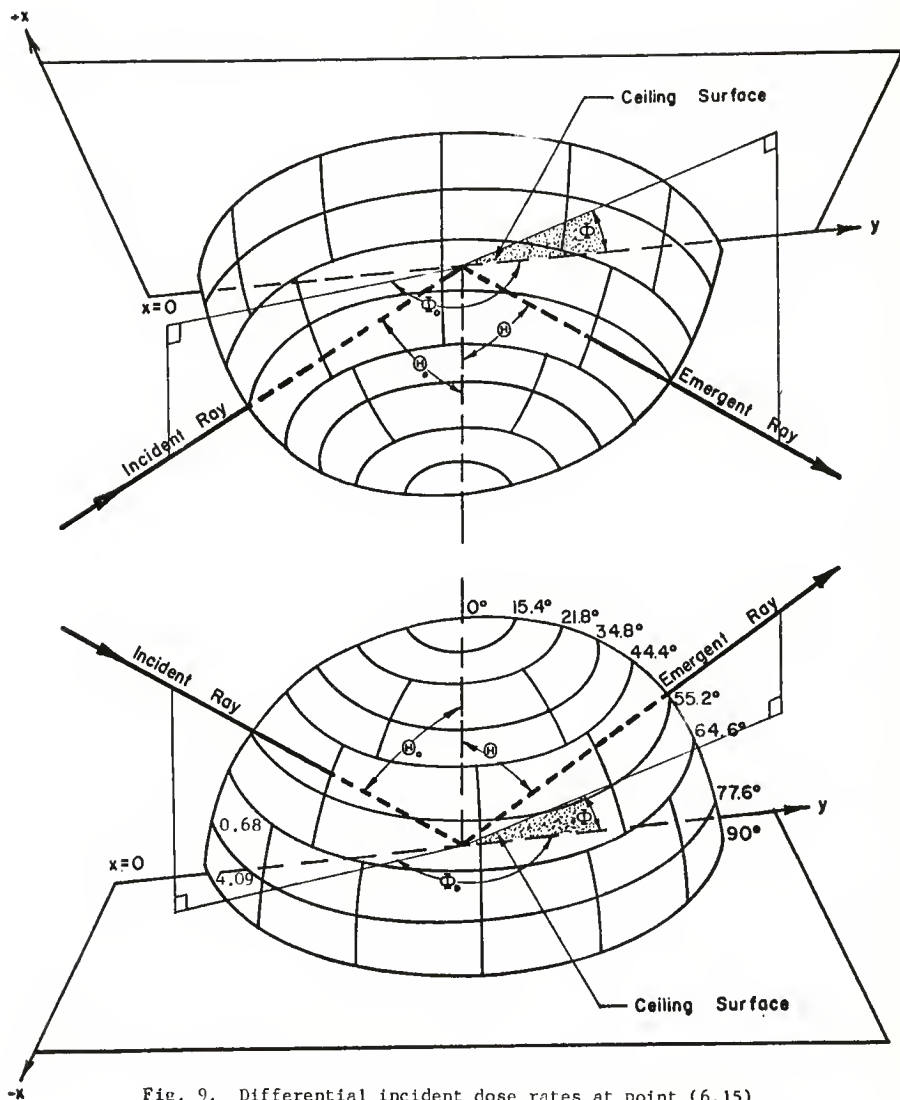


Fig. 9. Differential incident dose rates at point (6,15) on the KSU blockhouse ceiling,  $D_i(x,y;\theta,\phi)\Delta\cos\theta\Delta\phi(10^{-3}D_0)$ . The dose rates are zero unless otherwise specified.

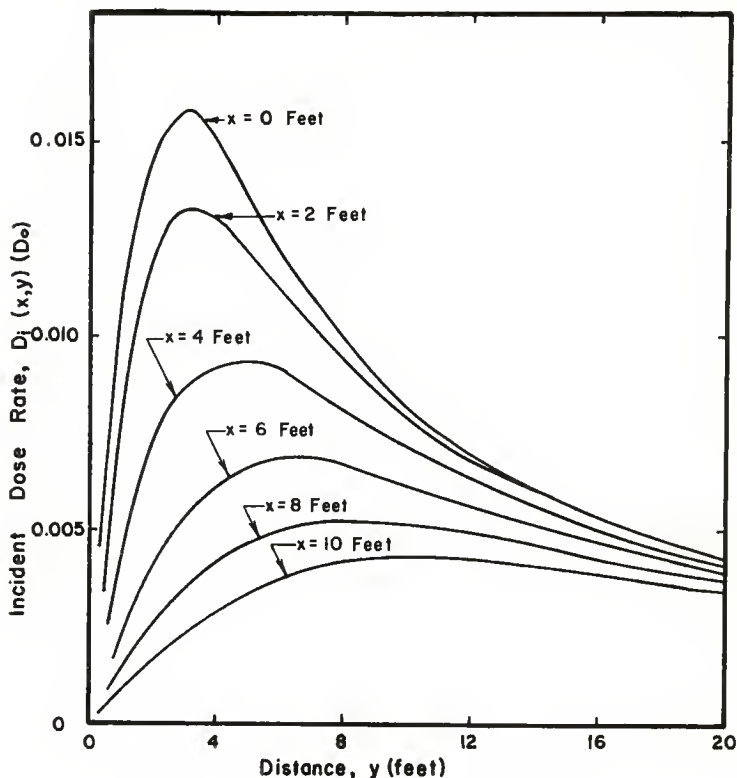


Fig. 10. Dose rates incident on ceiling of KSU blockhouse,  $D_i(x,y) (D_o)$ .

than one per cent of the reference dose rate is incident on the ceiling of the KSU blockhouse with the existing aperture (a window 26.0" high by 44.4" wide in a 20'  $\times$  20'  $\times$  8.17' blockhouse). Since the average total dose rate albedo was estimated at the end of Section 3.1.1 to be 14%, it is expected that the average total reflected dose rate at the ceil-

ing of the KSU blockhouse would be of the order of one-tenth of one per cent.

### 3.1.3 Reflected Dose Rates

The computer source program which solves the equation for the differential reflected dose rate at point (x,y) on the ceiling of a blockhouse is presented and discussed in Appendix J. Results were obtained for the 56 solid angles and the identical nine points utilized in the incident dose rate program. The results for the three positions (0,10), (3,5) and (6,15) are presented in Figures 11-13. Comparing Figures 11-13 with Figures 7-9, respectively, the forward scattering characteristic of the gamma radiation is readily noted. The magnitudes of the numbers presented in Figures 11-13 are approximately of the order of one-tenth of one per cent of the reference dose divided by 56 since there are 56 solid angles in this hemisphere.

The total dose rate reflected from any point of the ceiling, given by eq.(49), was determined in the computer program of Appendix K. The results presented in Appendix K are tabulated again in Table 2 along

Table 2. Total reflected dose rate results.

x feet	y feet	Integrated	Summed
0,00	5,00	0,0020992	0,0020559
0,00	10,00	0,0013809	0,0013193
0,00	15,00	0,0009131	0,0008542
3,00	5,00	0,0017215	0,0016866
3,00	10,00	0,0012473	0,0012183
3,00	15,00	0,0008615	0,0008200
6,00	5,00	0,0011606	0,0010697
6,00	10,00	0,0009931	0,0009810
6,00	15,00	0,0007418	0,0007273

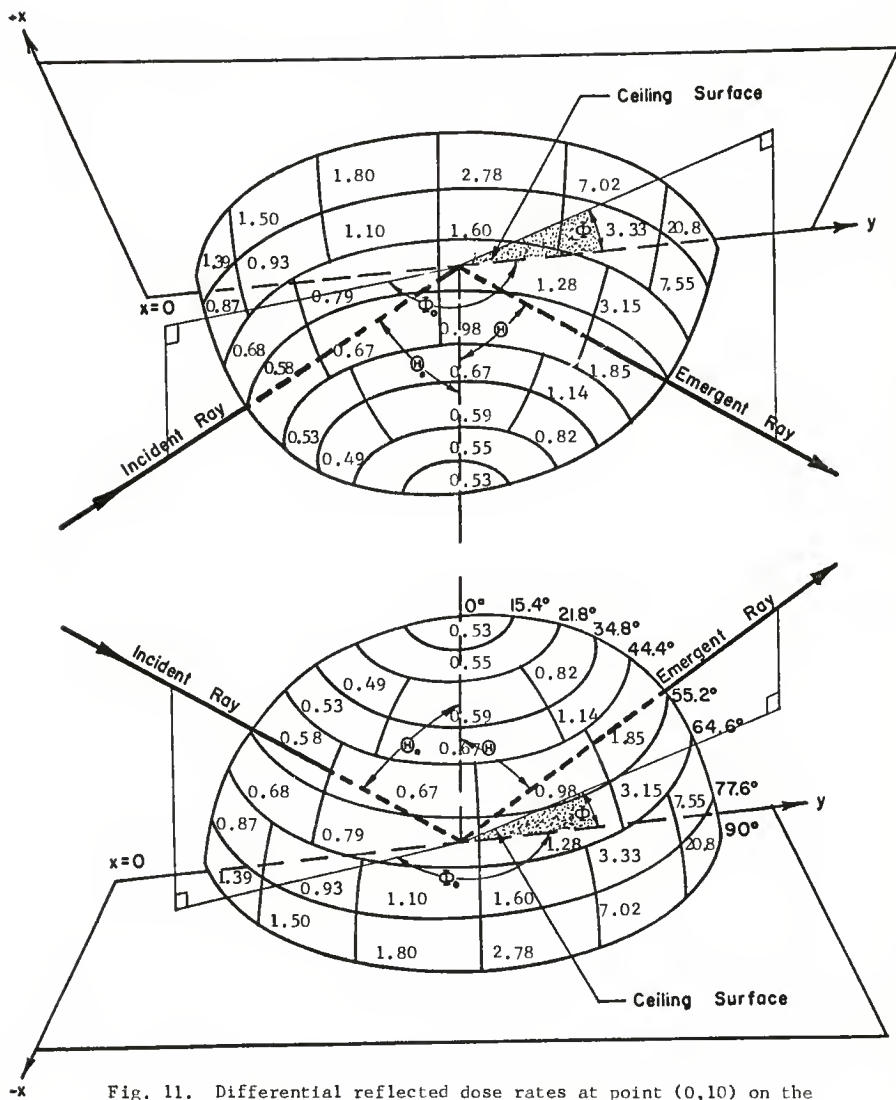


Fig. 11. Differential reflected dose rates at point (0,10) on the KSU blockhouse ceiling,  $D_r(x,y,\theta,\phi)\Delta\cos\theta\Delta\phi$  ( $10^{-5}D_0$ ).

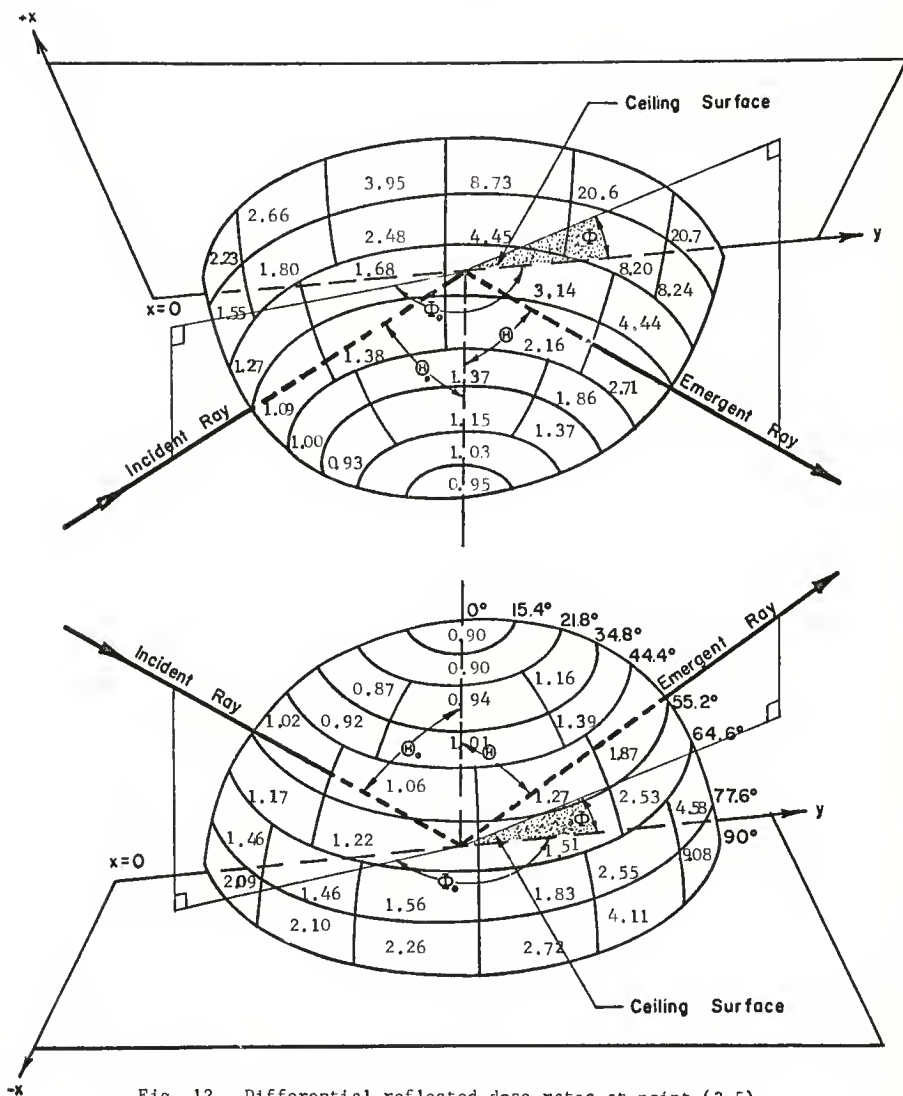


Fig. 12. Differential reflected dose rates at point (3,5) on the KSU blockhouse ceiling,  $D_r(x,y,\Theta,\Phi)\Delta\cos\Theta\Delta\Phi$  ( $10^{-5}D_0$ ).

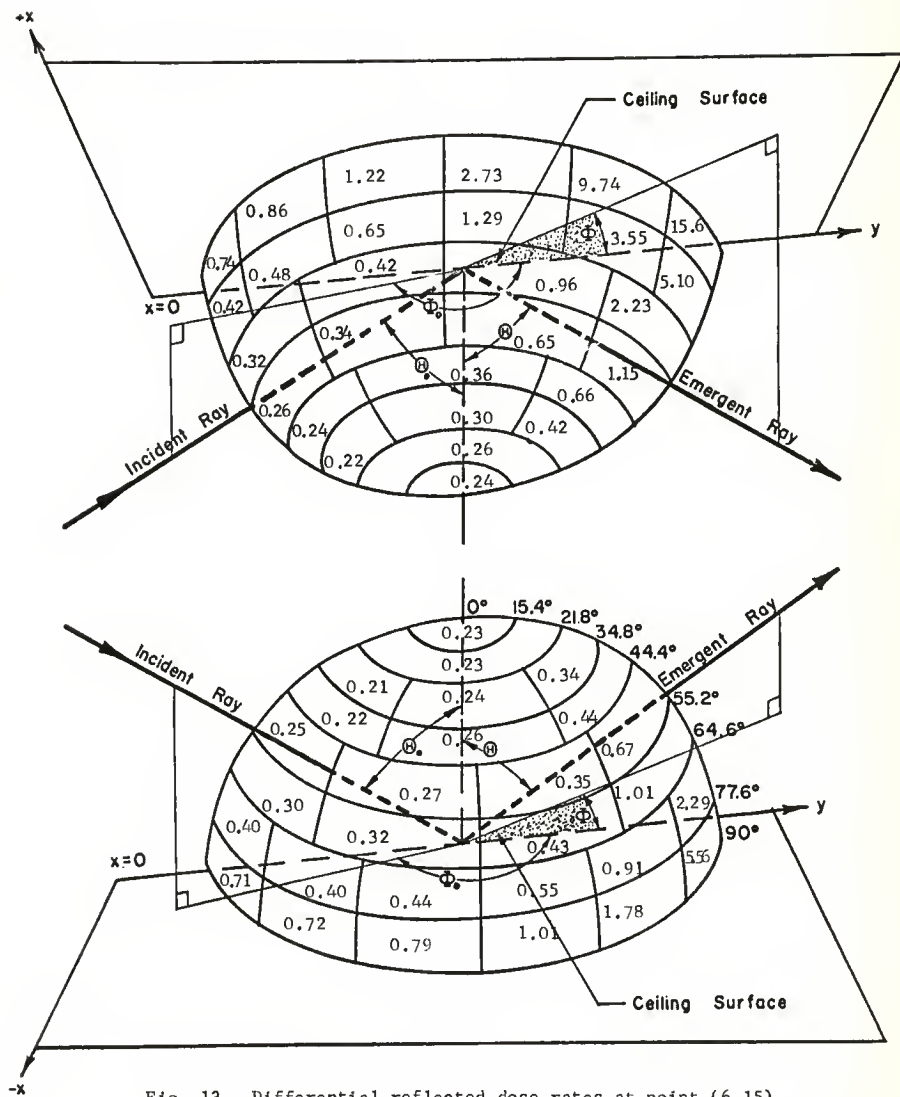


Fig. 13. Differential reflected dose rates at point (6,15) on the KSU blockhouse ceiling,  $D_r(x,y,\Theta,\Phi)\Delta\cos\Theta\Delta\Phi$  ( $10^{-5}D_0$ ).

with the summed differential reflected dose rate values. Again the dosages for a given y position are maximum along the centerline and are of the order of one-tenth of one per cent.

#### 3.1.4 Total Dose Rate at Position (xx,yy,zz) in the KSU Blockhouse

The determination of the total dose rate at any position in the KSU blockhouse was a prime objective of this thesis. This dose rate is given by eq.(54). One difficulty which was encountered in solving this equation lay in obtaining values for the average reflected gamma ray energy as a function of emergent polar and azimuthal angles. Berger and Raso (7) determined an average energy of reflected gamma photons as a function of the emergent polar angle in their Monte Carlo code. The appendix to Reference 7 (23) gives values of this average reflected energy for 1.250 MeV photons incident on a concrete slab for the incident polar angles of  $0^\circ$ ,  $30^\circ$ ,  $60^\circ$  and  $90^\circ$ . These energies are given only as a function of the emergent polar angle,  $\Theta$ . The  $30^\circ$ ,  $60^\circ$  and  $90^\circ$  average reflected energies are plotted in Figure 14.

An interpolation subroutine was revised to obtain the average reflected energy from the data of Figure 14. This computer program is discussed and presented in Appendix C. It processes data up to twenty points long and interpolations up to order seven. Longer lists and greater order interpolations can be readily obtained by modifying the program's DIMENSION statement.

The value of the average reflected energy was then utilized to interpolate to obtain the build-up parameters of reference 10 and the total linear macroscopic gamma ray absorption coefficients for air and concrete.



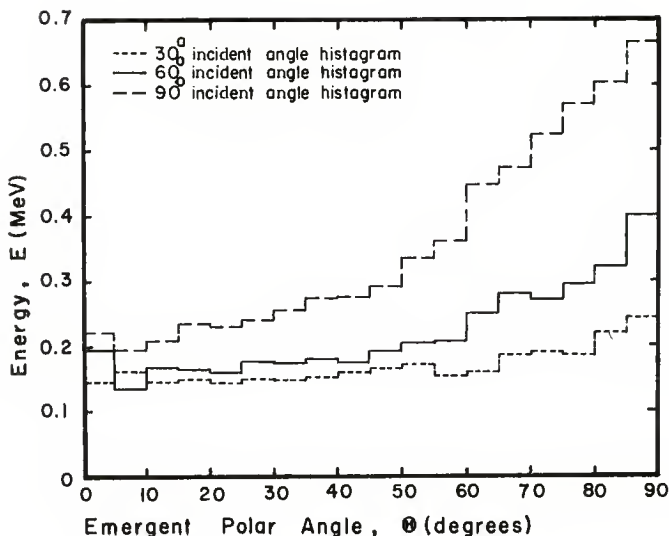


Fig. 14. Average reflected gamma ray energies, after Berger and Raso (23).

A computer program developed to solve eq.(54) is presented and discussed in Appendix L. A test of the necessary order of interpolation was made. Linear interpolation was found to be sufficiently accurate since it produced answers to within one per cent of that obtained with fifth order interpolation for the cases checked.

A test of the order of Gaussian quadrature necessary for the quadruple integration of eq.(54) was next determined. The results of this test are presented in Figure 15. This figure indicates that the value of the quadruple integrations for ceiling position (0,10,5,17) was approaching but had not yet reached a limiting value with a Gaussian quadrature of six.

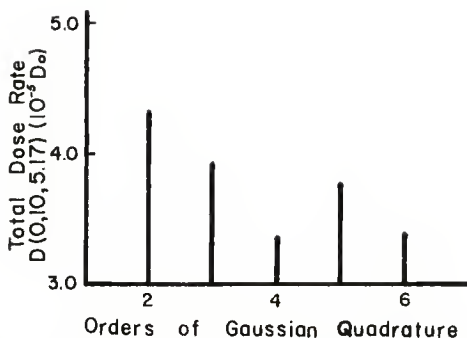


Fig. 15. Accuracy of total dose rate determinations with different orders of Gaussian quadrature for the detector position (0,10,5.17).

It was necessary to determine the accuracy of the different integrations. A quadruple integration of order seven would have required approximately five hours of computer time. Higher orders would have required correspondingly longer times. It was therefore necessary to proceed by other than this brute force method. A calculation was performed at the (0,10,5.17) position with a Gaussian quadrature order of three for the incident  $\Theta_0$  and  $\Phi_0$  variables while the x and y co-ordinates were integrated with an order of six. The result obtained was within one per cent of that obtained with all four variables of order six. The variation in intensity of the window-collimated radiation with position was thus apparently quite smooth.

The computer program in Appendix L was next modified so that the dose rate contributions from different positions along the centerline to the detector located at position (0,10,5.17) could be determined. This was accomplished by setting  $x = 0$  and printing out the dose rate contributions for  $y = 1, 2, 3 \dots 20$ . The resulting curve of dose rates versus y position on

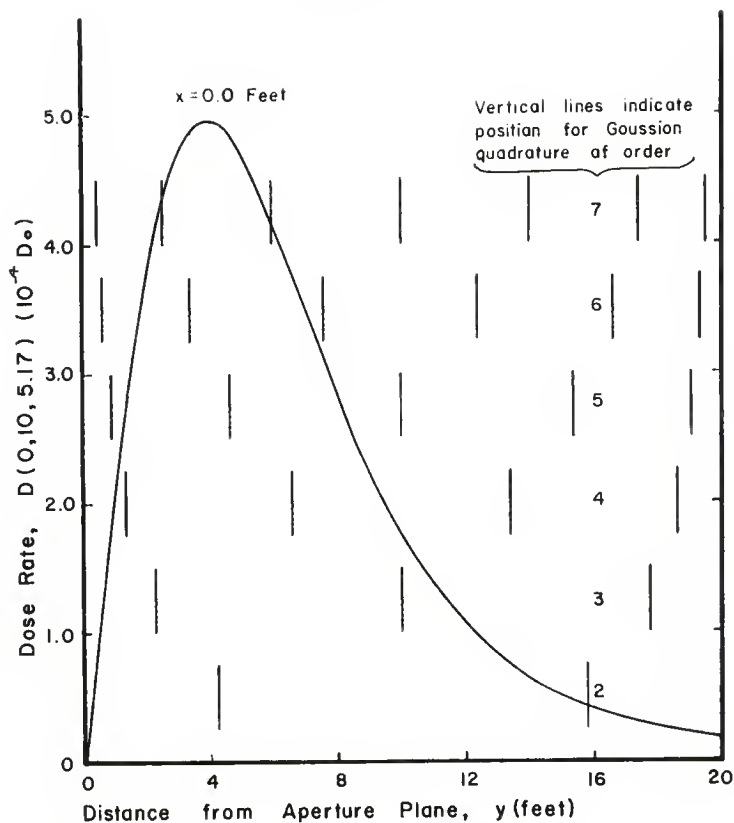


Fig. 16. Contribution to detector located at position (0,10,5.17) from centerline ( $x = 0$  feet) reflection.

the ceiling is presented in Figure 16. The general form of this curve would have been expected from the incident dose rate curves presented on Figure 10. A good feel for the numerical technique of Gaussian quadrature is obtained by noting the variation of the positions obtained with different

orders of Gaussian quadrature as illustrated in Figure 16. It is readily understood from this figure why, for example a Gaussian quadrature of two would give a high answer. The comparison between graphical integration under the curve of Figure 16 and the numerical integration obtained with different Gaussian quadrature orders is indicated in Table 3. The graphical integration value is approached with higher orders of Gaussian

Table 3. Determination of the order of Gaussian quadrature necessary for the y integration at the detector location (xx,yy,zz) of (0,10,5.17).

Method of integration	Total dose contribution at (0,10,5.17) ( $10^{-4}D_0$ )
Graphical integration of Figure 16	40.1
Gaussian quadrature integration of order	
2	53.6
3	39.6
4	39.4
5	40.5
6	40.3
7	40.2

quadrature. It was decided that a Gaussian quadrature of order six would be sufficiently accurate.

The computer program of Appendix L was written so that the symmetry about the centerline,  $x = 0$  was utilized (i.e., integration was from 0 to  $X_{\max}$  rather than  $-X_{\max}$  to  $X_{\max}$ ) when the xx co-ordinate of the detector was zero. Results obtained with a Gaussian quadrature of order six for the y integration and three for the other three integrations were within one per cent of the results obtained with sixth order quadruple Gaussian quadrature integration.

Accuracy within about ten per cent of the sixth order results was

obtained with the detector off the centerline, and the third order  $x$  integration over the entire width of the ceiling. An analysis similar to that required for the  $y$  integration was necessary. The curve obtained for an  $x$  traverse at one-half foot intervals at the  $y = 10$  foot position is presented in Figure 17. Results obtained similar to those presented

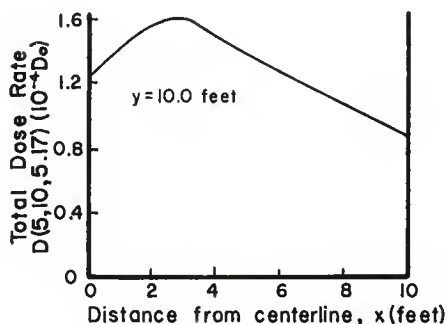


Fig. 17. Contribution to detector located at position (5,10,5.17) from radiation along the  $y = 10$  feet ceiling co-ordinate.

in Table 3 indicate that a Gaussian quadrature of order six would be required for less than one per cent error in the  $x$  integration.

Total dose rates were calculated for the detector positions three feet above the basement and first floors at the  $(x,y)$  co-ordinates (0,1), (0,6), (0,10), (0,14), (0,19), (2,10), (5, 10) and (10,10). These results are tabulated in Appendix L along with the dose rate contribution from each considered point on the ceiling to the dose rate at the detector. These dose rate contributions are the dose rates reaching the detector weighted by the appropriate Christoffel numbers. The total dose rate results are presented in Figure 18 through 21. The curve of Figure 18 displays

the variation in total dose rate seen by a detector on the centerline three feet above the first floor. This increases from a value of about  $1.7 \times 10^{-4} D_0$  underneath the window to a value of about  $2.4 \times 10^{-4} D_0$  at a distance of one foot from the plane of the window. The dose rate then increases slowly as the detector is moved from the window due to the forward scattering nature of the radiation. Figure 19 illustrates that the maximum ceiling scattered dose rate would be along the centerline on the first floor. This is again something that would be expected from the geometry of the KSU blockhouse. The maximum dose rate measured by a detector at the three foot level on the first floor of the KSU blockhouse from window-collimated, ceiling scattered fallout radiation would therefore be at the far wall directly opposite the window. The value at this position is approximately  $3.8 \times 10^{-4} D_0$ .

The plot of the total dose rate of the radiation along the basement centerline reaches a broad maximum at the center of the blockhouse and then decreases as it approaches the wall opposite to that containing the window. This is a result of the fact that the greater the polar angle between detector and ceiling position, the greater the thickness of concrete floor traversed by the radiation and consequently the greater the attenuation of the radiation. Figure 21 indicates that the maximum is again along the centerline. The maximum dose rate along the three foot level in the basement is located in the center of the blockhouse with a maximum value of about  $1.6 \times 10^{-5} D_0$ .

It is desirable to compare the total dose rate contributions from the window-collimated, ceiling scattered radiation with the total dose rates received by a detector from radiation directly penetrating the walls and from skyshine. These latter contributions are discussed in

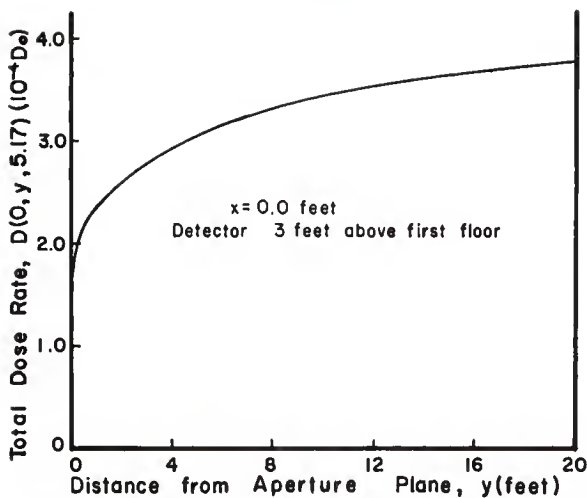


Fig. 18. Total dose rates three feet above the first floor centerline of the KSU blockhouse,  $10^{-4} D_0$ .

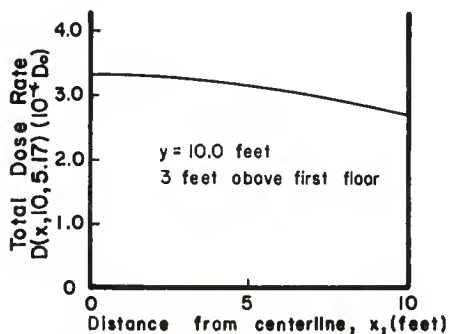


Fig. 19. Total dose rates three feet above the first floor of the KSU blockhouse along the y = 10 feet traverse,  $10^{-4} D_0$ .

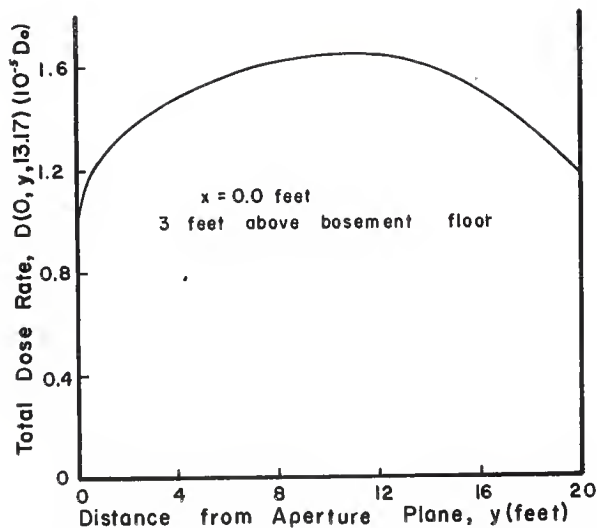


Fig. 20. Total dose rates three feet above the basement floor centerline of the KSU blockhouse,  $10^{-5}D_0$ .

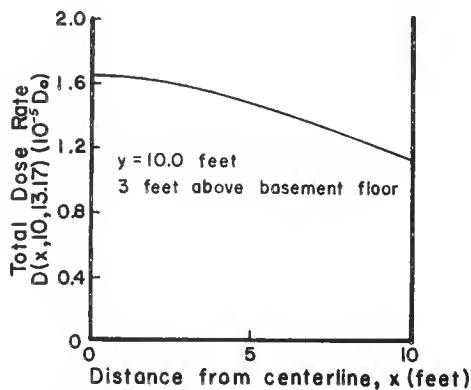


Fig. 21. Total dose rates three feet above the basement floor of the KSU blockhouse along the  $y = 10$  feet traverse,  $10^{-5}D_0$ .



Appendix N. The KSU blockhouse has an aperture fraction of approximately 0.05 in one wall (ratio of window area to wall area; the KSU blockhouse door is assumed to be filled in with concrete blocks of the same thickness as the blockhouse walls). The dose rate in the KSU blockhouse from all contributions, as discussed in Appendix N, varies only slowly with large changes in the aperture fraction if the lower sill of the aperture is a greater distance from the floor than that of the detector position. The window-collimated, ceiling scattered dose rates in the KSU blockhouse were also calculated at the detector positions (0,10,5.17) and (0,10,13.17) with essentially all of the wall above the first floor detector position removed. These results are tabulated in Appendix L. This removal of the upper five feet of wall creates an aperture fraction of 0.6. Comparisons between the window-collimated, ceiling scattered dose rate and the total dose rate incident on the detector at the two central position, (0,10,5.17) and (0,10,13.17) are presented in Table 4. The percentages presented in Table

Table 4. Ratio of window-collimated, ceiling scattered fallout radiation to total radiation received at 3 feet above the basement and first floor at the central position,  $x = 0$  feet,  $y = 10$  feet.

Contribution	Dose Rates (D)			
	Aperture Fraction			
	0.05		0.6	
	1st floor	basement	1st floor	basement
Wall penetration and skyshine (experimentally determined and adjusted for window contribution)	0.18	0.0028	0.21	0.0033
Window-collimated, ceiling scattered for one wall	0.000337	0.0000164	0.00717	0.000285
Window collimated, ceiling scattered for four walls	0.00135	0.0000656	0.0287	0.00114

Table 4. Cont.

Contribution	Dose Rates ( $D_o$ )			
	Aperture Fraction			
	0.05		0.6	
	1st floor	basement	1st floor	basement
Percent contribution of the window-collimated, ceiling scattered dose rate	0.74%	2.3%	12%	26%

4 are obtained from the ratios of the window-collimated, ceiling scattered radiation considering a window of the given aperture fraction in each of the four walls to the total amount of radiation received by the detector at the given position.

### 3.2 Conclusions

The size of the concrete blockhouse, the size and position of the aperture and the thickness of the floor are governed by the input data to the programs in this study. The output can be determined for any position in the blockhouse except directly under the window. The three main limitations inherent in these programs are the horizontal symmetry of the aperture, the height of the blockhouse ceiling of 8.17 feet above the contaminated plane and the energy of the incoming gamma.

The first of these limitations could be removed by revising the angular co-ordinate system. This would merely necessitate the defining of a new variable, the off-center position of the window vertical center-line, and adding this to the x co-ordinate in eqs.(1) and (2). The window of the KSU blockhouse is horizontally centered so the dose rates were calculated only for the positive x half of the ceiling.

The limitation of the blockhouse ceiling height above the contaminated plane to the specific height of 8.17' was inherent in Appendix A in the determination of the constant of proportionality,  $W$ , for the dose angular distribution equation. The third limitation on the incident energy is also involved with this dose angular distribution. Spencer (1) presents curves of the dose angular distributions for different heights above the contaminated plane both for a plane contaminated with cobalt-60 and a plane contaminated with the 1.12 hour spectrum of fission products. These curves would have to be put in analytical forms akin to that obtained in Appendix A to remove these limitations on the problem.

An assumption that was made in this study was that of reciprocity (11). That is, the incident gamma photons were assumed to emerge from the slab at the point of impingement. This is of course not the true situation since the photons do travel some distance in the concrete before undergoing an interaction. This concept of reciprocity was accepted in this study since no practical alternative was available.

The assumption was also made in utilizing Raso's results (12) that the 6" concrete ceiling slab was a semi-infinite reflective medium. This assumption is quite good since the Monte Carlo results of Leimdörfer (25) indicate that for practical purposes even a 10 cm. concrete wall can be regarded as infinitely thick as far as being considered to have reached the infinite-thickness albedo.

The theoretical differential dose rate albedo results obtained and graphed in this study provide a good indication of what would be experimentally obtained from gamma ray scattering off concrete slabs. An average total dose rate albedo of 14% was obtained. The figures and tabulations of the differential incident, total incident, differential reflected and

total reflected dose rates on the ceiling of the KSU blockhouse presented a good picture of the behaviour of this window-collimated dose rate contribution on the ceiling of a typical concrete structure. The per cent contributions of this radiation tabulated in Table 4 range from about 1% to 25%. These contributions, while small, are accurate and can be very useful in determining protection factors for buildings such as stores with large aperture fractions.

### 3.3 Further Investigations

Excellent opportunities for further worthwhile investigations in this field are foreseen utilizing this study as a basis. Structure shielding analysis presently treats backscattering from interior surfaces by a simple corrective factor. This factor is presently estimated by utilizing the fact that about 15% of the radiation energy incident on a surface is backscattered (1). The suggestion is herewith made that a detailed study be undertaken of the amounts, angular distributions and energies of all the backscattered radiations in simple concrete structures leading to a determination of the total backscattered dose rates in such structures. This would involve not only the window-collimated, ceiling scattered radiation but also the radiation which penetrates a wall and is backscattered off the opposite wall, and other backscattered radiations.

Once a standard computational scheme for calculation of the total backscattered dose rate contributions is prepared, it is necessary to verify it through measurements made in the KSU blockhouse surrounded by a simulated plane fallout field. One of the initial determinations to be made is that of both the polar and azimuthal variation of the average reflected energy. Such a determination is necessary to obtain accurate

answers for the further attenuation and reflective properties of the photons.

The results should finally be presented in the form of simplified design curves.

## 4.0 ACKNOWLEDGEMENT

The author wishes to express his gratitude to Dr. R. E. Faw and Dr. J. O. Mingle under whose direction this study has been accomplished. Thanks are extended to Professor J. R. Fagan for his help in the different phases of this thesis and to the staff of the Kansas State University computing center for their co-operation with the use of the IBM-1620 digital computer. Sincere appreciation is also extended to Dr. W. R. Kimel, Head of the Kansas State University Department of Nuclear Engineering, for his advice and encouragement during the course of this work.

## 5.0 LITERATURE CITED

1. Spencer, L. V.  
Structure Shielding Against Fallout Radiation from Nuclear Weapons.  
National Bureau of Standards Monograph 42 (June 1, 1962).
2. Design and Review of Structures for Protection from Fallout Gamma  
Radiation. U. S. Army. Fort Belvoir, Va. (revised October 1, 1962).
3. Fallout Shelter Surveys: Guide for Architects and Engineers. Office  
of Civil and Defense Mobilization. National Plan Appendix Series  
NP-10-2 (May, 1960).
4. Baran, J. A. et. al.  
Proceedings and Final Report of the 1962 Kansas State University-  
Department of Defense Summer Institute on Fundamental Radiation  
Shielding Problems as Applied to Nuclear Defense Planning. (November,  
1962).
5. Clarke, E. T. and Buchanan, J. O.  
Radiation Shielding Against Fallout. Nucleonics, 20, No. 8, pp.  
143-6 (1962).
6. Nelms, A. T. and Cooper, J. W.  
U<sup>235</sup> Fission Product Decay Spectra at Various Times After Fission.  
Health Physics, 1, pp. 427-41 (1959).
7. Berger, M. J. and Raso, D. J.  
Monte Carlo Calculations of Gamma-Ray Backscattering. Radiation  
Research, 12, pp. 20-37 (1960).
8. Berger, M. J.  
Effects of Boundaries and Inhomogeneities on the Penetration of  
Gamma Radiation. Proceedings of the Shielding Symposium held at  
the Naval Radiological Defense Laboratory 17-19 October 1956,  
Volume 1, pp. 47-92 (1956).
9. Goldstein, H. and Wilkins, J. E. Jr.  
Calculations of the Penetration of Gamma Rays. AEC NYO-3075  
(1954).
10. Chilton, A. B., Holoviak, D. and Donovan, L. K.  
Determination of Parameters in an Empirical Function for Build-  
up Factors for Various Photon Energies. U. S. Naval Civil  
Engineering Laboratory Technical Note N-389 (August, 1960).
11. Davisson, C. M.  
Interpretation and Applications of Monte Carlo Gamma Ray Albedo  
Values. private communication.

12. Raso, D. J.  
Monte Carlo Calculations on the Reflection and Transmission of Scattered Gamma Radiations. Technical Operations, Incorporated Report No. TO-B 61-39 (May, 1962).
13. Statement by A. B. Chilton made in reference 11.
14. Chilton, A. B. and Huddleston, C. M.  
A Semi-Empirical Formula for Differential Dose Albedo for Gamma Rays on Concrete. To be published.
15. Bellman, R. E., Kalaba, R. E. and Prestrud, M. C.  
Invariant Imbedding and Radiation Transfer in Slabs of Finite Thickness. The Rand Corporation R-3BB-ARPA (February, 1962).
16. Crotenhuis, M.  
Lecture Notes on Reactor Shielding. Argonne National Laboratory ANL-6000 (March, 1959).
17. Mickley, H. S., Sherwood, T. K., and Reed, C. E.  
Applied Mathematics in Chemical Engineering. McCraw-Hill Book Company, Inc., New York (1957).
18. LeDoux, J. C. and Donovan, L. K.  
Compilation of Exponential Functions for Arguments From 2 through 50. U. S. Naval Civil Engineering Laboratory, Y-F011-05-401 (July 25, 1960).
19. Hildebrand, F. B.  
Introduction to Numerical Analysis. McCraw-Hill Book Company, Inc., New York (1956).
20. Rockwell, Theodore III  
Reactor Shielding Design Manual. D. Van Nostrand Company, Inc. Princeton, New Jersey (1956).
21. IBM Publication  
IBM 1620 FORTRAN II Specifications, International Business Machine Corporation, Product Publications Department, San Jose, California (1962).
22. Rash, Larry A.  
Uncollided Flux from Finite Right-Circular Cylinder Viewed Endwise. Kansas Engineering Experiment Station Special Report Number 12 (December, 1961).
23. Berger, M. J. and Raso, D. J.  
Backscattering of Gamma Rays. National Bureau of Standards Report Number 5982 (February 8, 1960).
24. LeDoux, J. C.  
Equivalent Building Method of Fallout Radiation Shielding Analysis and Design. Office of Civil Defense (February, 1963).



25. Leimdörfer, M.  
The Backscattering of Gamma Radiation from Plane Concrete Walls.  
Aktipbolaget Atomenergi Arbetsrapport RFA-84 (3.7.62).
26. Hastings, Cecil Jr.  
Approximations for Digital Computers. Princeton University Press,  
Princeton, New Jersey (1955).

## 6.0 APPENDICES

## APPENDIX A

## Determination of the Constant of Proportionality, W, for the Dose Angular Distribution Equation

The dose angular distribution defined by L. V. Spencer (1) for an idealized plane fallout source can be expressed empirically in an equation of the form

$$I(d, \cos \Theta_0) = W B(\Sigma_a(E_0)d / \cos \Theta_0) \{ \cos \Theta_0 \exp(\Sigma_a(E_0)d / \cos \Theta_0) \}^{-1} \quad (55)$$

where  $d$  is the height in air above the source,  $\Theta_0$  is the incident polar angle,  $W$  is the constant of proportionality,  $B(\Sigma_a(E_0)d / \cos \Theta_0)$  is the build-up factor and  $\Sigma_a(E_0)$  is the total linear gamma ray absorption coefficient at incident energy  $E_0$ . It is desired in this appendix to determine the value of the constant of proportionality,  $W$ , for a constant height of the ceiling above the contaminated plane,  $d$ . This height,  $d$ , is taken here to be that of the KSU blockhouse, 8.17'. The total linear gamma ray absorption coefficient is tabulated in Reference 16 to be

$$\Sigma_a(1.252\text{MeV}) = 0.0567 \text{ cm}^2/\text{gm} \times 1.293 \times 10^{-3} \text{ gm/cc} = 7.331 \times 10^{-5} \text{ cm}^{-1} \quad (56)$$

and

$$\Sigma_a(E_0)d = 0.01825. \quad (57)$$

The build-up factor,  $B(\Sigma_a(E_0)d / \cos \Theta_0)$ , is given in Reference 10 to be

$$B(\Sigma_a(E_0)d / \cos \Theta_0) = 1 + a' \Sigma_a(E_0)d \exp(b \Sigma_a(E_0)d / \cos \Theta_0) / \cos \Theta_0 \quad (58)$$

where  $a'$  and  $b$  are parameters which are functions of energy. For the 1.252 MeV energy,  $a' = 0.89562$  and  $b = 0.062518$ . The  $I(d, \cos \Theta_0)$  values

were obtained from Figure B1 of Reference 1 for cobalt-60 gamma rays incident on concrete.

The values of the parameters of eq.(55) for five values of  $\cos\Theta_0$  are determined in Table 5. It is desirable to develop an equation

Table 5. Determination of W in eq.(62).

$\cos\Theta_0$	$\sum_a (E_0)d/\cos\Theta_0$	$e^{-\sum_a (E_0)d/\cos\Theta_0}$	$B(\sum_a (E_0)d/\cos\Theta_0)$	$f(d, \cos\Theta_0)$	W
1.00	0.01825	0.98191	1.0165	0.19	0.1904
0.75	0.02433	0.97596	1.0218	0.275	0.2069
0.50	0.03650	0.96416	1.0328	0.405	0.2034
0.25	0.07300	0.92960	1.0657	0.82	0.2069
0.10	0.18250	0.83318	1.1653	1.71	0.1761

to give W as a function of  $\cos\Theta_0$ . A straight line can fit these results (17) through the equation

$$W = a'' + b'(\cos\Theta_0 - \overline{\cos\Theta_0}) \quad (59)$$

where

$$\overline{\cos\Theta_0} = \left\{ \sum_{i=1}^n \cos\Theta_{0i} \right\} / n = 0.52, \quad (60)$$

$$a'' = \left\{ \sum_{i=1}^n W_i \right\} / n = 0.1967, \quad (61)$$

and

$$b' = \left\{ \sum_{i=1}^n W_i (\cos\Theta_{0i} - \overline{\cos\Theta_0}) \right\} \left\{ \sum_{i=1}^n (\cos\Theta_{0i} - \overline{\cos\Theta_0})^2 \right\}^{-1} = 0.0095. \quad (62)$$

Therefore, eq.(59) becomes

$$W = 0.1967 + 0.0095(\cos\Theta_0 - 0.52) \quad (63)$$

and

$$W = 0.1917 + 0.0095\cos\Theta_0. \quad (64)$$

Eq.(55) thus becomes

$$\begin{aligned} I(d, \cos\Theta_0) = & (0.1917 + 0.0095\cos\Theta_0) B(\sum_a (E_0) d / \cos\Theta_0) \\ & \times \{ \cos\Theta_0 \exp(\sum_a (E_0) d / \cos\Theta_0) \}^{-1}. \end{aligned} \quad (65)$$

This equation for the dose-angular distribution is utilized throughout this study.

## APPENDIX B

## Albedo Study

The total albedo is a measure of the efficiency of a surface in reflecting incident radiation. This paper concerns only gamma radiation albedos. The three most commonly used total albedos are the total number albedo, the total energy albedo and the total dose albedo. The total number albedo is simply the ratio of the number of photons reflected to the number of photons incident. The total energy albedo is the ratio of the product of the number of reflected photons by their energies to the product of the incident photons by their energies. The total dose albedo is similarly defined except that the number of photons is multiplied by the linear (or mass) energy absorption coefficient for air (at the standard temperature and pressure) at the appropriate energy along with the energy itself. Thus the dose albedo "weighs" the photons in accordance with their efficiency of detection in an air-equivalent detector.

The differential albedo is most commonly used in albedo calculations. The differential number albedo is a measure of the fraction of the photons of energy  $E_0$  incident on a surface at given  $\Theta_0$  and  $\Phi_0$  which emerge from that surface into a certain solid angle,  $d\Omega$ , about  $\Omega$ . The probability of this occurring is designated (11) as  $P(E_0, \Theta_0, \Phi_0; E, \Theta, \Phi)$ . The differential number albedo is a ratio of currents since it is a measure of the number of photons penetrating a given surface. The differential energy albedo is simply  $(E/E_0)P(E_0, \Theta_0, \Phi_0; E, \Theta, \Phi)$  and the differential dose albedo is

$$a_d(E_0, \Theta_0, \Phi_0; E, \Theta, \Phi)d\Omega = \{\mu_a(E)/\mu_a(E_0)E_0\}P(E_0, \Theta_0, \Phi_0; E, \Theta, \Phi)d\Omega. \quad (66)$$

The dose albedo is not the ratio of emergent dose rate to incident dose rate since dose is proportional to energy flux. This ratio of dose

rates is given by the differential dose rate albedo,

$$\underline{a}(\Theta_o, \Phi_o; \Theta, \Phi) d\Omega = \int_0^E (\cos \Theta_o / \cos \Theta) a_d d\Omega dE. \quad (67)$$

Albedos can be theoretically computed on electronic computers by means of the Monte Carlo method. The Monte Carlo method is a theoretical experiment whereby the paths in a medium of interest of a large number of particles are followed. The probability distribution for each type of interaction being known, the distance traveled, type and result of interaction can be chosen out of a set of random numbers. The term "Monte Carlo" has been applied to this effect because of the utilization of random numbers.

The results of a Monte Carlo study of the backscattering of gamma rays from a semi-infinite concrete medium (12) are utilized in this study. A quantity determined in reference 12, called the "differential scattered dose rate," is given by the equation

$$SD(E_o, \Theta_o, \Phi_o; E, \Theta, \Phi)_{j, k'} = \int_{\Phi_{j'}}^{\Phi_{j'+1}} \int_{\Theta_{k'}}^{\Theta_{k'+1}} \int_0^{E_o} \{E \mu_a(E) P(E_o, \Theta_o, \Phi; E, \Theta, \Phi) d\Omega dE\} \times \{(\cos \Theta_{k'} + \cos \Theta_{k'+1})/2\}^{-1} \text{ kev./gm.-sec.} \quad (68)$$

These  $SD_{j, k'}$  are tabulated for different values of  $\Omega_{j, k'}$  and represent the dose rate per incident gamma ray per  $\text{cm.}^2$  produced by the emergent flux whose directions of flow lie within a certain solid angle,  $2\Delta\Omega$ . The factor of 2 takes into account the fact that the tabular results for the angular interval  $\{\Phi_{j'}, \Phi_{j'+1}\}$  include also the mirror contribution from  $\{360^\circ - \Phi_{j'}, 360^\circ - \Phi_{j'+1}\}$ . Utilizing eq.(66), eq.(68) becomes

$$SD(E_o, \Theta_o, \Phi_o; E, \Theta, \Phi)_{j', k'} = \{\mu_a(E_o) E_o / (\text{average } \cos \Theta)\} \quad (69)$$

$$\times \int_{\Phi_{j'}}^{\Phi_{j'+1}} \int_{\Theta_{k'}}^{\Theta_{k'+1}} \int_0^{E_o} a_d(E_o, \Theta_o, \Phi_o; E, \Theta, \Phi) d\Omega dE \quad \text{kev./gm.-sec.}$$

The value of the triple integral in eq.(69) gives the ratio of the average energy absorbed in one centimeter of air per second from the radiation back-scattered into  $\Omega_{j', k'}$ , to the average energy absorbed in one centimeter of air per second from the photons incident on one square centimeter of the slab (11).

Chilton (13) defines a total dose albedo,  $a_T$ , as "the ratio of two instrument readings. The first is the reading that an isotropically responding dose-rate meter would record above an infinite plane, when it is uniformly illuminated by a broad parallel beam of gamma rays; the second is the reading of the meter due solely to the direct radiation." This ratio is the  $\underline{a}$  defined by eq.(67). Substituting eq.(69) into eq.(67) results in

$$\underline{a}(\Theta_o, \Phi_o; \Theta, \Phi) d\Omega = \{\cos \Theta_o / \mu_a(E_o) E_o\} SD(E_o, \Theta_o, \Phi_o; E, \Theta, \Phi) d\Omega. \quad (70)$$

The differential dose rate albedo symbolized by  $\underline{a}(\Theta_o, \Phi_o; \Theta, \Phi) d\Omega$  was utilized in computing the reflected dose rates in this study. Because of the large number of  $\underline{a}$ 's required for the different  $\Theta$ 's and  $\Phi$ 's, it was deemed inadvisable to attempt to interpolate among the tabulated results of reference 12. A semi-empirical formula developed by A. B. Chilton and C. M. Huddleston (14) which yields values for a somewhat different differential dose rate albedo of gamma rays on concrete was used instead. The theoretical derivation of this albedo assumed that the actual scattering process can be approximated by a term involving a single Compton scattering event and



another term involving isotropic scattering. The resultant formula, hereinafter called the Chilton-Huddleston formula, is

$$\bar{\alpha}(\Theta_0, \Theta, \Phi') = \{CK(\Theta_s) + C'\} \{1 + \cos\Theta_0 \sec\Theta\}^{-1} \quad (71)$$

where  $C$  and  $C'$  are empirical constants and  $K(\Theta_s)$  is  $E/E_0$  times the Klein-Nishina differential energy scattering cross section (20) for the total scattering angle  $\Theta_s$  and the incident photon energy,  $E_0$ . The differential cross section per unit solid angle,  $\Omega$ , derived by Klein and Nishina is given by

$$d\sigma/d\Omega = (R'_0 p)^2 \{ (1/p) + p - \sin^2\Theta_s \} / 2 \quad \text{cm}^2/\text{electron-steradian} \quad (72)$$

where  $R'_0$  is the classical radius of the electron,

$$R'_0 = e^2/mc^2 = 2.818 \times 10^{-13} \text{ cm}. \quad (73)$$

The  $K(\Theta_s)$  defined in reference 14 is equal to  $p \, d\sigma/d\Omega$ . The  $p$  is equal to  $E/E_0$  where the Compton scattered energy is

$$E = E_0 \{ 1 + E_0 (1 - \cos\Theta_s) / 0.511 \text{ MeV} \}^{-1}. \quad (74)$$

The  $\cos\Theta_s$  term in eq.(74) is equal to

$$\cos\Theta_s = \sin\Theta_0 \cos\Phi' \sin\Theta - \cos\Theta_0 \cos\Theta. \quad (75)$$

The azimuthal angle,  $\Phi'$ , given in eq.(71) and eq.(75) is equal to (see Figure 3),

$$\Phi' = \Phi - \Phi_0 + \pi. \quad (76)$$

The weakest part in the development of the Chilton-Huddleston formula is the assumption that the gamma ray mass absorption coefficient remains constant during a scattering history. Although this approximation initially appears rather poor, the comparison between the results of this two-parameter formula and the Monte Carlo results of reference 12 presented in a latter portion of this appendix indicate a satisfactory agreement.

The relationship between the differential dose rate albedo,  $\bar{a}$ , of the Chilton-Huddleston formula and the differential scattered dose rate, SD, of reference 12 is derived in reference 14 to be

$$\bar{a} = SD \{ (\cos \Theta_{k,i} + \cos \Theta_{k',i+1}) / 2 \} \{ 1000 E_o \mu_a'(E_o) 2 \Delta \Phi (\cos \Theta_{k,i} + \cos \Theta_{k',i+1}) \}^{-1} \quad (77)$$

where  $\Delta \Phi = \Phi_{j,i+1} - \Phi_{j,i} = 15^\circ$  for the results of reference 12.

The best values for the empirical constants, C and C', of eq.(71) were determined in reference 14 by a least-square computer analysis from the results of reference 12. The computed best values are given in Table 6. The best values of C and C' for the energy of the average cobalt-60

Table 6. Parameters for a semi-empirical formula for the differential gamma ray dose albedo.

Energy, $E_o$ (MeV)	C( $\times 10^{26}$ )	C'
0.2	0.022126134	0.035648111
0.5	0.033556571	0.022152990
1	0.054677888	0.011132052
2	0.086899748	0.0077462231
4	0.123811030	0.0075919821
6	0.148975400	0.0074920140
10	0.16600843	0.0070037501

gamma ray (1.252 MeV) were obtained through the interpolation subroutine to be  $C = 6.4501 \times 10^{24}$  and  $C' = 0.0089295$ . This interpolation subroutine is described in Appendix C.

The SD albedo can therefore be obtained by utilizing these best value results in eq.(71) and substituting this value of  $\bar{a}$  into eq.(77). The resultant equation is

$$\begin{aligned} SD(E_o, \Theta_o, \Phi_o; E, \Theta, \Phi) = 1000 E_o \mu'_a(E_o) \{CK(\Theta_s) + C'\} \{2\Delta\Phi(\cos\Theta_{k'} - \cos\Theta_{k'+1})\} \\ \times \{1 + \cos\Theta_o \sec\Theta\}^{-1} \{(\cos\Theta_{k'} + \cos\Theta_{k'+1})/2\}^{-1} \text{ MeV/gm.-sec.} \end{aligned} \quad (78)$$

This equation is plotted for three different emergent azimuthal angles on Figure 22. These are for an  $E_o$  of 1.00 MeV and an incident polar angle of  $\Theta_o = \cos^{-1}0.25$ . An excellent correlation is shown in Figure 22 between the plot of eq.(78) and the plotted results of reference 12. The main difference between the two appears at large emergent polar angles--an angular region which will contribute little to the total dose at pertinent points in the building. However, even here the curves obtained through the Chilton-Huddleston formula give a higher, and therefore more conservative, albedo. The computer program which determines the Chilton-Huddleston albedo is presented in Appendix D.

The differential dose rate albedo which was utilized in computing the reflected dose rates at the ceiling in this monograph is obtained by combining eq.(70) and eq.(78) and dividing through by  $2\Delta\Omega$  so as to make the resultant albedo dimensionless. i.e.,

$$\underline{a}(\Theta_o, \Phi_o; \Theta, \Phi) d\Omega = 1.293 \{CK(\Theta_s) + C'\} \{1 + \cos\Theta \sec\Theta_o\}^{-1} d\Omega \quad (79)$$

The factor of 1.293 is obtained from the product of 1000 times the density

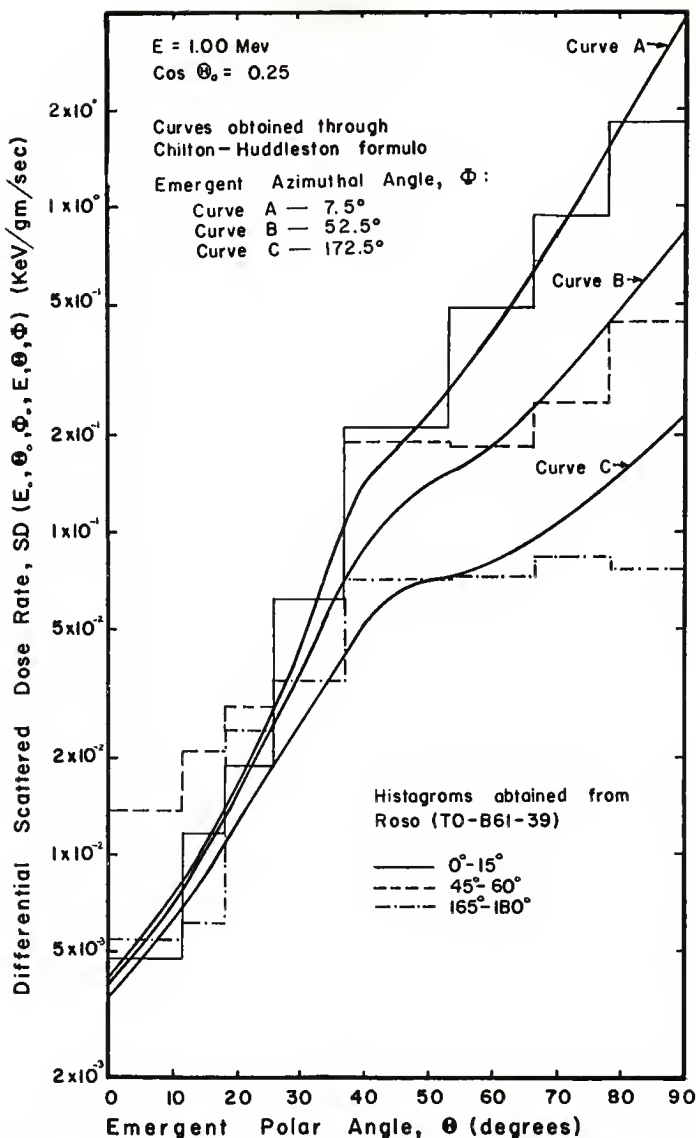


Fig. 22. Comparison between scattered dose rates obtained from Chilton-Huddleston formula and Raso's Monte Carlo results.

of air at standard temperature and pressure. The density of air is introduced because the air attenuation coefficient in eq.(70) has  $\text{cm}^{-1}$  units while that in eq.(78) has  $\text{cm}^2/\text{gm}$  units. The computer program written for  $\underline{a}$  is described in Appendix E. The variation of the dose rate albedo,  $\underline{a}$ , with emergent polar angle,  $\Theta$ , is plotted in Figures 23 through 27 for three values of  $\Phi'$  and the five incident polar angles:  $\cos\Theta_0 = 0.1, 0.25, 0.5, 0.75$  and  $1.00$ .

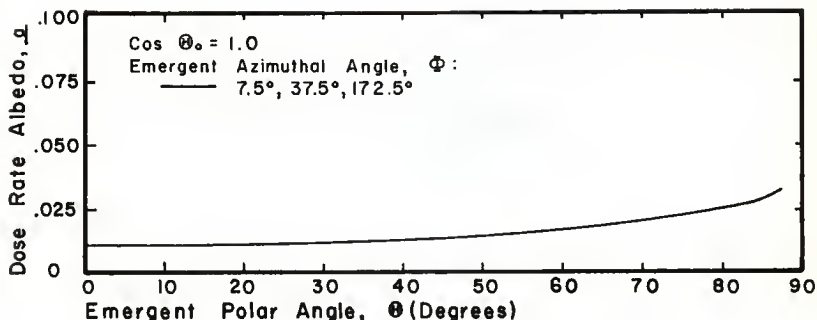


Fig. 23. Variance of dose rate albedo,  $\underline{a}$  with emergent angles for perpendicular incidence.

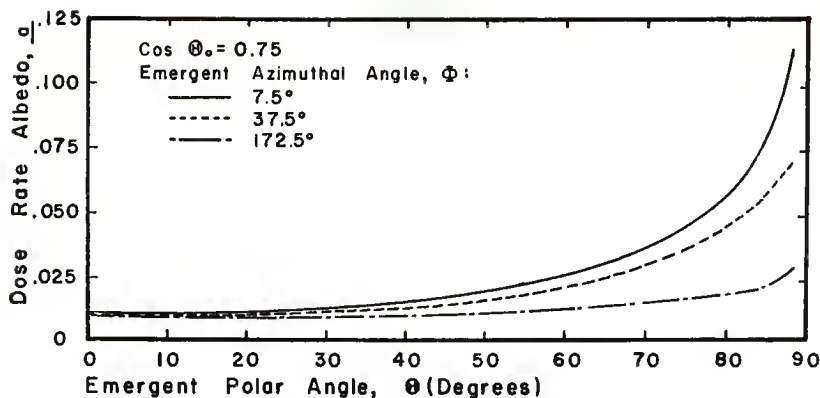


Fig. 24. Variance of dose rate albedo,  $\underline{a}$ , with emergent angles for an incident polar angle of  $41.4^\circ$ .

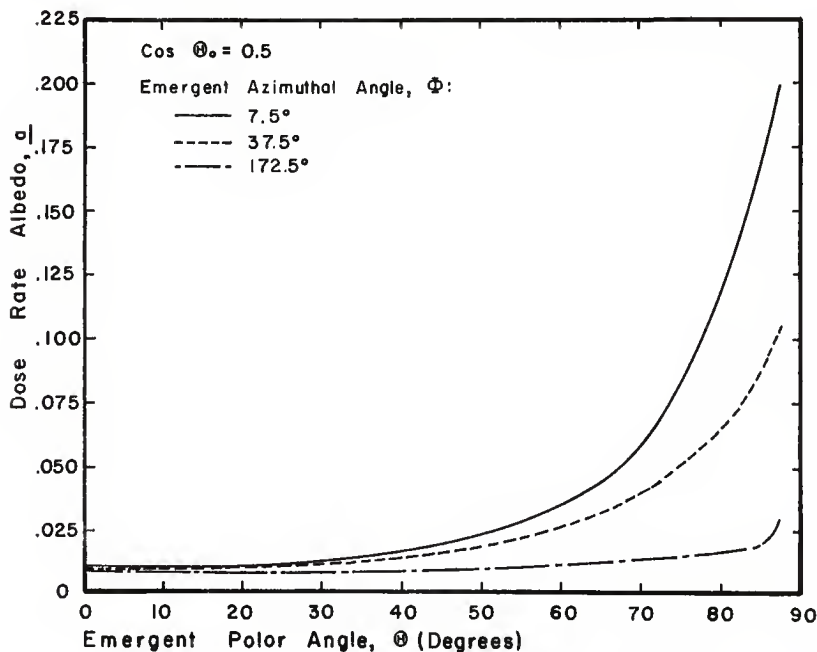


Fig. 25. Variance of dose rate albedo,  $\underline{a}$ , with emergent angles for an incident polar angle of  $60^\circ$ .

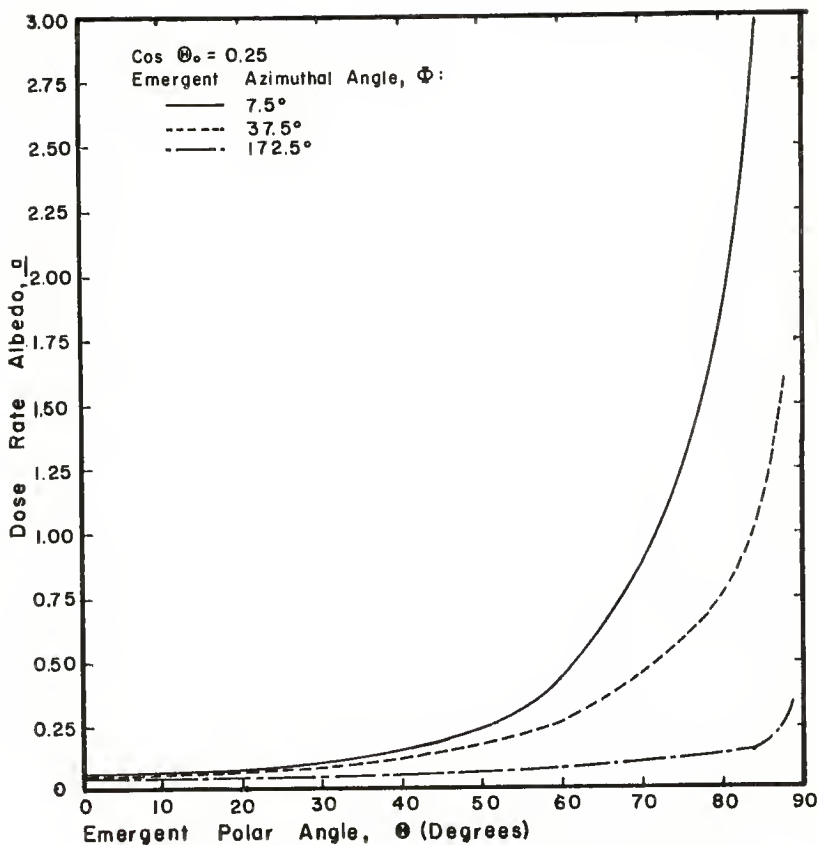


Fig. 26. Variance of dose rate albedo,  $\underline{a}$ , with emergent angles for an incident polar angle of  $75.5^\circ$ .

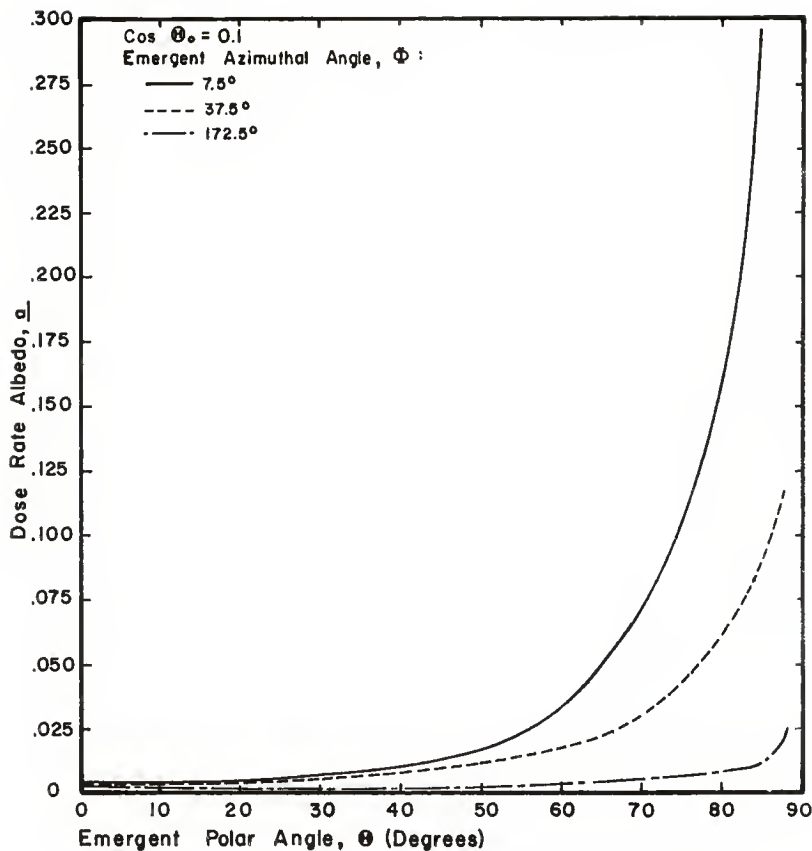


Fig. 27. Variance of dose rate albedo,  $a$ , with emergent angles for an incident polar angle of  $84.3^\circ$ .



## APPENDIX C

Description and Explanation of the IBM-1620  
Computer Program Used to Interpolate Among  
Various Parameters.

This computer code was written to interpolate among the various parameters required for the main programs. This program is a revision of one written by V. Cain during the summer of 1962 (4) and is rewritten in the form of a Subroutine Subprogram (entitled INTERP) in FORTRAN II language. The source program is listed and the logic diagram shown in this appendix.

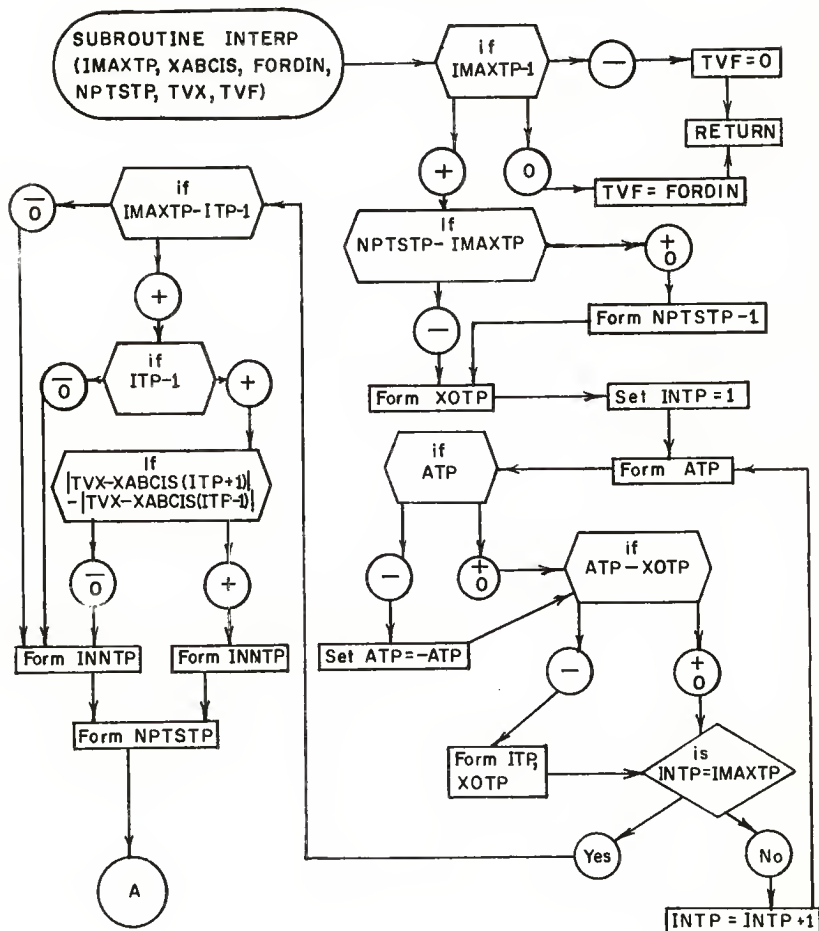
Interpolation for a given point-of-interest was made in this program over a number of interpolation points one less than the length of the interpolation list. The Gaussian arrangement was used whereby points on alternate sides of the point-of-interest are successively used. A polynomial of the same degree as the number of interpolation points minus one was passed through the list points.

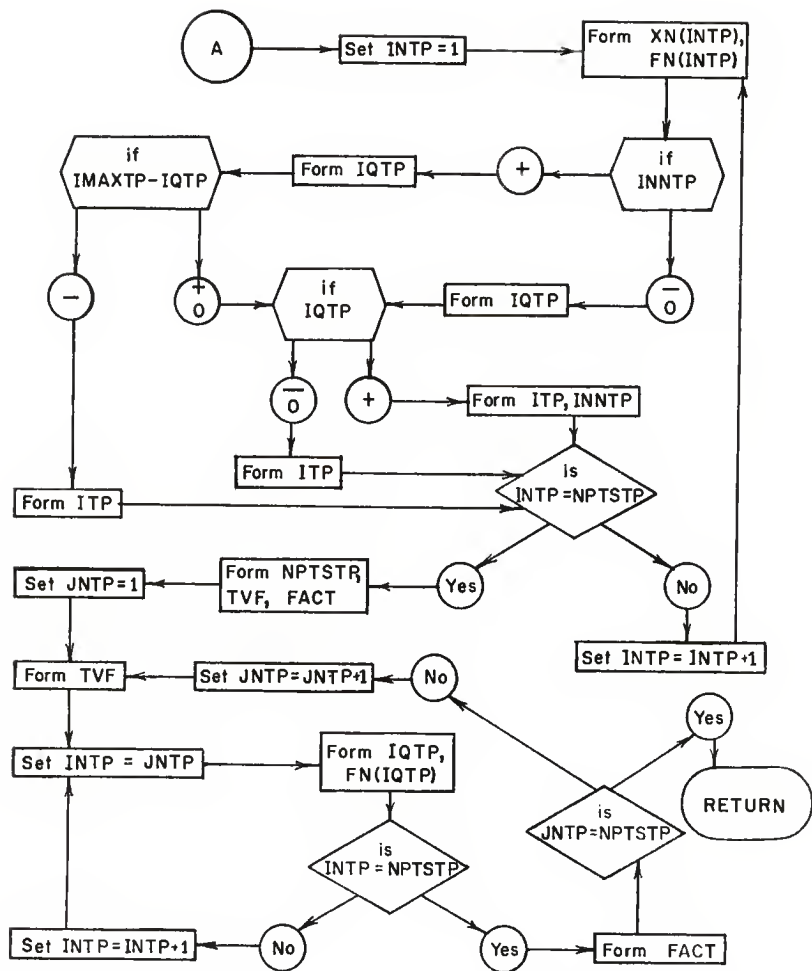
A Subroutine Subprogram is written in the general form, SUBROUTINE Name ( $a_1, a_2, \dots, a_n$ ) where Name is the symbolic name of a subprogram and each argument,  $a_1, a_2, \dots, a_n$ , if any, is either a subscripted or a non-subscripted variable name (21). This particular subroutine form is SUBROUTINE INTERP(IMAXTP, XABCIS, FORDIN, NPTSTP, TVX, TVF). This subroutine accepts lists up to twenty points long and interpolations up to order seven. Longer lists and greater order interpolations can be readily obtained by modifying the DIMENSION statement. Arrangements are made for extremely short lists and for interpolations near one end of the list. Table 7 lists the various input data and variables utilized in this subroutine.

Table 7. Input data and variables required for  
the IBM-1620 interpolation program.

Symbol	Explanation
INTERP	Symbolic Name of the Subroutine Subprogram
IMAXTP	Length of Interpolation List
XABCIS	Abscissa of Interpolation List; Must be Entered into Computer in Either Ascending or Descending Order
FORDIN	Ordinate of Interpolation List
NETSTP	Number of Interpolation Points
TVX	Interpolation Point in Abscissa List
TVF	Desired Interpolated Value in Ordinate List
XOTP	Floating Point Variable Used in Ordering Interpolation Points
INTP	Fixed Point Variable Used in Ordering Interpolation Points; INTP = 1 is the Argument of the XABCIS (and FORDIN) Nearest TVX, INTP = 2 is Next Nearest, Etc.
ATP	Variable Used in Ordering Interpolation Points Made Equal to Absolute Value of Difference Between TVX and Each XABCIS
ITP	Position in List of XABCIS Nearest TVX
INNTP	Integer Oscillating Between +1 and -1 to Obtain the Gaussian Arrangement
XN	Abscissa List Ordered So That Successive Values are at Greater Distances from TVX
FN	Ordinate List Ordered So That Successive Values are at Greater Distances from TVF
IQTP	Variable Which Determines if End of List Has Been Reached
FACT	Factor Which Modifies the Divided Differences

# LOGIC DIAGRAM FOR THE INTERPOLATION SUBROUTINE





```

C      INTERPOLATION SUBROUTINE, FIX)      V. CAINS REWRITTEN 1/63 BY J. BARAN
C      INPUT DATA--IMAXTP=LENGTH OF INTERPOLATION LIST, XABCIS=ABSCISSA,
C      FCRDIN=ORDINATE LIST, NPTSTP=NUMBER OF INTERPOLATION POINTS, TVX=
C      VALUE INTO X LIST AT WHICH INTERPOLATED F VALUE (TVF) IS DESIRED
C      SUBROUTINE INTERP(IMAXTP,XABCIS,FCRDIN,NPTSTP,TVX,TVF)
      DIMENSION XABCIS(20), FCRDIN(20), XN(7), FN(7)
      IF(IMAXTP-1) 810, 820, 830
800     TVF=0.
810     GO TO 1000
820     TVF=FCRDIN(1)
      GO TO 1000
C      THESE ORDERS TAKE CARE OF ECCENTRICALLY SHORT LISTS
830     IF(NPTSTP-IMAXTP) 850, 840, 840
840     NPTSTP=IMAXTP-1
C      ORDER OF INTERPOLATION IS DECREASED IF LIST IS TOO SHORT
850     XCTP=1.E90
      DO 890 I=1, IMAXTP
      ATP=TVX-XABCIS(I)
      IF(ATP) 860, 870, 870
860     ATP=-ATP
870     IF(ATP-XCTP) 880, 890, 890
880     ITP=INTP
      XCTP=ATP
890     CONTINUE
C      THIS LOOP SELECTS THE VALUE OF XABCIS CLOSEST TO TVX
      IF (IMAXTP-ITP-1) 892, 892, 889
889     IF (ABS(F(TVX-XABCIS(ITP+1)) - ABS(F(TVX - XABCIS(ITP-1)))) 892, 892
      1, 893
892     INNTP=1
      GO TO 894
893     INNTP = -1
894     NPTSTP=NPTSTP+1
C      THESE ORDERS DETERMINE ON WHICH SIDE OF TVX IS THE NEXT XABCIS
      DO 970 I=1, NPTSTP
      XN(ITP)=XABCIS(ITP)
      FN(ITP)=FCRDIN(ITP)
      IF(INNTP) 900, 900, 910
900     IQTP=ITP-INTP
      GO TO 940
910     IQTP=ITP+INTP
920     IF(IMAXTP-IQTP) 930, 940, 940
930     ITP=ITP-1
      GO TO 970
940     IF(IQTP) 950, 950, 960
950     ITP=ITP+1
      GO TO 970
960     ITP=IQTP
      INNTP=-INNTP
970     CONTINUE
C      THIS LOOP ORDERS THE INTERPOLATION POINTS
C      FOR INCREASING DISTANCES FROM TVX
      NPTSTP=NPTSTP-1
      TVF=0.
      FACT=1.
      DO 990 J=1, NPTSTP
      TVF=TVF+FACT*FN(J)
      DO 980 I=J, NPTSTP
      IQTP=INTP-J+1
880     FN(IQTP)=(FN(IQTP+1)-FN(IQTP))/(XN(ITP+1)-XN(IQTP))
890     FACT=FACT*(TVX-XN(JNTPT))
C      THIS IS THE MAIN LOOP FOR CALCULATING THE DIVIDED DIFFERENCES
1000    RETURN
      END

```

## APPENDIX D

Description and Explanation of the IBM-1620  
Computer Program Used to Check the Accuracy  
of the Chilton-Huddleston Formula.

This computer code was written to check the accuracy of the Chilton-Huddleston formula. The program was written in FORTRAN II language. The source program is listed, the logic diagram shown and pertinent results tabulated for five incident polar angles in this appendix.

It was deemed advisable to check the accuracy of the Chilton-Huddleston formula defined by eq.(71),

$$\bar{a}(\Theta_0, \Theta, \Phi') = \{CK(\Theta_s) + C'\} \{1 + \cos\Theta_0 \sec\Theta\}^{-1}, \quad (71)$$

since the results of this formula are utilized throughout this work. This was accomplished by comparing the results obtained by adapting this formula to give the scattered dose rate values defined by eq.(78),

$$SD(E_0, \Theta_0, \Phi_0; E, \Theta, \Phi) = 1000E_0 \mu'_a(E_0) \{CK(\Theta_s) + C'\} \{2\Delta(\cos\Theta_{k'} - \cos\Theta_{k'+1})\} \\ \times \{1 + \cos\Theta_0 \sec\Theta\}^{-1} \{(\cos\Theta_{k'} + \cos\Theta_{k'+1})/2\}^{-1} \text{ MeV/gm.-sec.} \quad (78)$$

with those obtained by Raso (12) through the Monte Carlo technique. The Chilton-Huddleston formula was derived (14) from the Raso results.

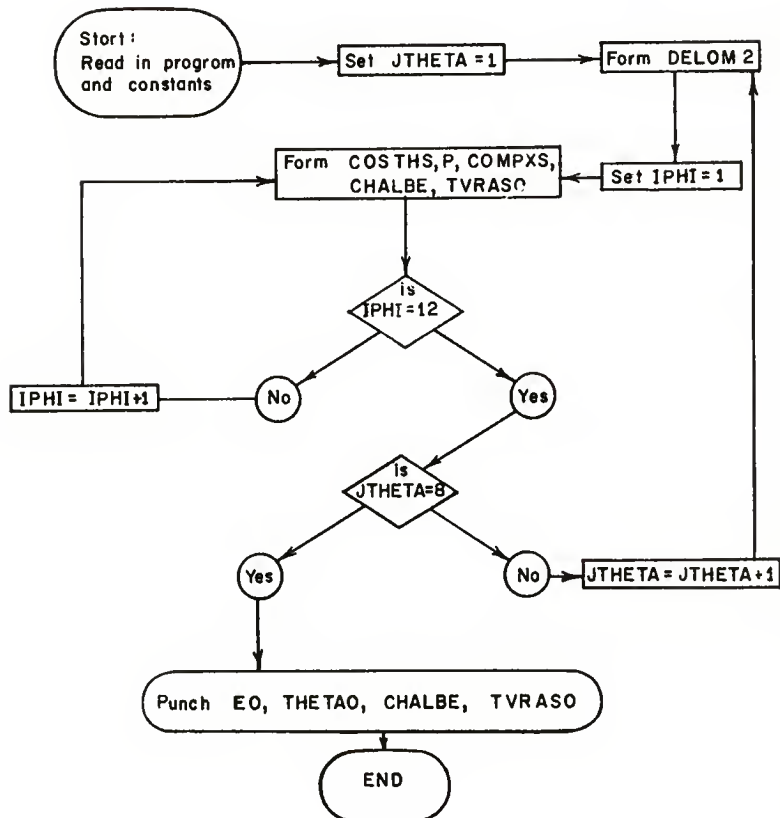
Table 8 lists the various input data and variables utilized in this program. Both the Chilton-Huddleston differential dose rate albedo results and the Raso differential scattered dose rate results are tabulated in this appendix for an incident energy of 1.252 MeV and the five incident polar angles,  $\cos\Theta_0 = 0.1, 0.25, 0.5, 0.75$  and  $1.0$ . Both of these results are also obtained for an incident energy of 1.00 MeV and an

incident polar angle of  $\cos\Theta_0 = 0.25$ . The Raso scattered dose rate for this input data is compared with Raso's Monte Carlo results in Figure 22.

Table 8. Input data and variables required for the IBM-1620 Chilton-Huddleston formula check.

Symbol	Explanation
EO	Incident Photon Energy, $E_0$ (MeV)
THETAO	Incident Polar Angle, $\Theta_0$ (Radians)
EACAE0	Energy Mass Macroscopic Gamma Ray Absorption Coefficient for Air, $\mu_a^0(E_0)$ ( $\text{cm}^2/\text{gm}$ )
C	Chilton-Huddleston Parameter, C
CPRIME	Chilton-Huddleston Parameter, C'
THETAK	Polar Angular Limits, $\Theta_k$ (radians)
THETA	Emergent Polar Angle, $\Theta$ (radians)
PHI	Emergent Azimuthal Angle, $\Phi$ (radians)
JTHETA	Fixed Point Variable Defining Theta Values
IPHI	Fixed Point Variable Defining Phi Values
COSTHS	Cosine of Total Scattering Angle, $\cos\Theta_s$
P	Ratio of Emergent to Incident Energies in a Simple Compton Scattering Process, p
COMPS	Klein-Nishina Cross Section Times p, $K(\Theta_s)$
CHALBE	Chilton-Huddleston Albedo
TVRASO	Raso's Scattered Dose Rate, $\text{kev/gm.-sec.}$

LOGIC DIAGRAM FOR ALBEDO DETERMINATIONS  
BY THE CHILTON-HUDDLESTON FORMULA





```

C      CHILTON-HUDDLESTON FORMULA ACURACY CHECK--J.BARAN, DEC., 1962
C      INPUT DATA--EO=INITIAL PHOTON ENERGY (MEV), THETA=INITIAL
C      OBLIQUITY (RADIAN), EACAEO=ENERGY ABS. COEFF. FOR AIR AT EO
C      CM.SQ/GM), C AND CPRIME=CHILTON-HUDDLESTON PARAMETERS.
C      DIMENSION THETA(9), THETA(8), PHI(12), CHALBE(12,8),
      1TVRASO(12,8)
10  FORMAT (F5.2,F9.6,F7.4)
20  FORMAT (F12.9,F13.10)
60  FORMAT (6F9.6/6F9.6)
80  FORMAT(24H      BACKSCATTERING OF      ,F6.3, 35H MEV PHOTONS FROM A
      1CONCRETE MEDIUM )
87  FORMAT(50H      CHILTON-HUDDLESTON DIFFERENTIAL DOSE ALBEDO:
90  FORMAT      (69H      AZIMUTH      7.5      22.5      37.5
      1      52.5      /15H      POLAR )
95  FORMAT      (70H      AZIMUTH      67.5      82.5      97.5
      1      112.5      ,/15H      POLAR )
100 FORMAT      (70H      AZIMUTH      127.5      142.5      157.5
      1      172.5      /15H      POLAR )
102 FORMAT (52H      RASO DIFFERENTIAL SCATTERED DOSE RATE (KEV/GM-SEC))
115 FORMAT (27H      INCIDENT OBLIQUITY = F9.6, 8H RADIAN, //)
120 FORMAT (13H      8      ,4(F13.5)/ 13H      15      ,4F13.5/
      113H      22      , 4(F13.5)/ 13H      32      ,4F13.5/
      113H      45      , 4(F13.5)/ 13H      60      ,4F13.5/
      113H      72      , 4(F13.5)/ 13H      84      ,4F13.5//)
30  READ 10, EO, THETA, EACAEO
C      INPUT ABOVE IS 1 CARD
C      READ 20, C, CPRIME
C      INPUT ABOVE IS 1 CARD
C      READ 60, THETA
C      INPUT ABOVE IS 2 CARDS
C      READ 60, THETA
C      INPUT ABOVE IS 2 CARDS
C      READ 60, PHI
C      INPUT ABOVE IS 2 CARDS
C      DO 70 JTHETA=1,8
      DELOM2=EO*EACAEO*0.523599*(COSF(THETA(JTHETA))-COSF(THETA(JTHETA
      1+1)))
      DO 65 IPHI=1,12
C      THIS LOOP CALCULATES THE CHILTON-HUDDLESTON ALBEDO AND RASOS
C      SCATTERED DOSE RATE FOR EACH EMERGENT POLAR AND AZIMUTHAL ANGLE
      COSTHS=SINF(THETA)*COSF(PHI(IPHI))*SINF(THETA(JTHETA))
      1-COSF(THETA)*COSF(THETA(JTHETA))
      P=1./(1.+(EO*(1.-COSTHS)/0.511))
      COMPS=(3.970562      )*(P**2)*(1.+(P**2)-P*(1.-(COSTHS**2)))
      CHALBE(IPHI,JTHETA)=(C*COMPS+CPRIME)/(1.+(COSF(THETA)/
      1COSF(THETA(JTHETA))))
65  TVRASO(IPHI,JTHETA)=CHALBE(IPHI,JTHETA)*2000.*DELOM2/
      1(COSF(THETA(JTHETA))+COSF(THETA(JTHETA+1)))
70  CONTINUE
      PUNCH 80, EO
      PUNCH 115, THETA
      PUNCH 87

```

```

PUNCH 90
PUNCH 120, ((CHALBE(IPHI,JTHETA),IPHI=1,4 ),JTHETA=1,8)
PUNCH 95
PUNCH 120, ((CHALBE(IPHI,JTHETA),IPHI=5,8 ),JTHETA=1,8)
PUNCH 100
PUNCH 120, ((CHALBE(IPHI,JTHETA),IPHI=9,12),JTHETA=1,8)
PUNCH 102
PUNCH 90
PUNCH 120, ((TVRASC(IPHI,JTHETA),IPHI=1,4 ),JTHETA=1,8)
PUNCH 95
PUNCH 120, ((TVRASC(IPHI,JTHETA),IPHI=5,8 ),JTHETA=1,8)
PUNCH 100
PUNCH 120, ((TVRASC(IPHI,JTHETA),IPHI=9,12),JTHETA=1,8)
GO TO 30
END

```

# INPUT DATA

```

1.25 1.318146 0.0268
.064501061 0.0089294690
.000000 0.200713 0.317650 0.450295 0.644026 0.926770
1.158899 1.370033 1.570796
.139626 0.261800 0.383973 0.558506 0.785399 1.047198
1.256638 1.466077
.130900 0.392699 0.654499 0.916298 1.178098 1.439897
1.701697 1.963496 2.225296 2.487095 2.748895 3.010694

```

TABLE 9.  
CHILTON-HUDDLESTON ALBEDO RESULTS

BACKSCATTERING OF 1.250 MEV PHOTONS FROM A CONCRETE MEDIUM  
INCIDENT OBLIQUITY = 0.000000 RADIAN

CHILTON-HUDDLESTON DIFFERENTIAL DOSE ALBEDO

AZIMUTH	7.5	22.5	37.5	52.5
POLAR				
8	.00823	.00823	.00823	.00823
15	.00818	.00818	.00818	.00818
22	.00809	.00809	.00809	.00809
32	.00788	.00788	.00788	.00788
45	.00742	.00742	.00742	.00742
60	.00644	.00644	.00644	.00644
72	.00498	.00498	.00498	.00498
84	.00227	.00227	.00227	.00227
AZIMUTH	67.5	82.5	97.5	112.5
POLAR				
8	.00823	.00823	.00823	.00823
15	.00818	.00818	.00818	.00818
22	.00809	.00809	.00809	.00809
32	.00788	.00788	.00788	.00788
45	.00742	.00742	.00742	.00742
60	.00644	.00644	.00644	.00644
72	.00498	.00498	.00498	.00498
84	.00227	.00227	.00227	.00227
AZIMUTH	127.5	142.5	157.5	172.5
POLAR				
8	.00823	.00823	.00823	.00823
15	.00818	.00818	.00818	.00818
22	.00809	.00809	.00809	.00809
32	.00788	.00788	.00788	.00788
45	.00742	.00742	.00742	.00742
60	.00644	.00644	.00644	.00644
72	.00498	.00498	.00498	.00498
84	.00227	.00227	.00227	.00227

RASC DIFFERENTIAL SCATTERED DOSE RATE (KEV/GM-SEC)

AZIMUTH	7.5	22.5	37.5	52.5
POLAR				
8	.00293	.00293	.00293	.00293
15	.00445	.00445	.00445	.00445
22	.00761	.00761	.00761	.00761
32	.01637	.01637	.01637	.01637
45	.03706	.03706	.03706	.03706
60	.04518	.04518	.04518	.04518
72	.05865	.05865	.05865	.05865
84	.07963	.07963	.07963	.07963
AZIMUTH	67.5	82.5	97.5	112.5
POLAR				
8	.00293	.00293	.00293	.00293
15	.00445	.00445	.00445	.00445
22	.00761	.00761	.00761	.00761
32	.01637	.01637	.01637	.01637
45	.03706	.03706	.03706	.03706
60	.04518	.04518	.04518	.04518
72	.05865	.05865	.05865	.05865
84	.07963	.07963	.07963	.07963
AZIMUTH	127.5	142.5	157.5	172.5
POLAR				
8	.00293	.00293	.00293	.00293
15	.00445	.00445	.00445	.00445
22	.00761	.00761	.00761	.00761
32	.01637	.01637	.01637	.01637
45	.03706	.03706	.03706	.03706
60	.04518	.04518	.04518	.04518
72	.05865	.05865	.05865	.05865
84	.07963	.07963	.07963	.07963

TABLE 9 CONT.  
CHILTON-HUDDLESTON ALBEDO RESULTS

BACKSCATTERING OF 1.250 MEV PHOTONS FROM A CONCRETE MEDIUM  
INCIDENT SBLIQUITY = .722730 RADIAN

CHILTON-HUDDLESTON DIFFERENTIAL DOSE ALBEDO

AZIMUTH	7.5	22.5	37.5	52.5
PCLAR				
8	.01038	.01036	.01032	.01026
15	.01064	.01059	.01051	.01039
22	.01091	.01083	.01069	.01049
32	.01133	.01119	.01093	.01060
45	.01197	.01169	.01120	.01062
60	.01271	.01214	.01121	.01019
72	.01252	.01162	.01023	.00882
84	.00793	.00705	.00580	.00465
AZIMUTH	67.5	82.5	97.5	112.5
PCLAR				
8	.01019	.01012	.01004	.00997
15	.01025	.01010	.00996	.00983
22	.01027	.01005	.00984	.00965
32	.01024	.00990	.00959	.00932
45	.01003	.00950	.00905	.00869
60	.00925	.00849	.00789	.00745
72	.00766	.00678	.00615	.00570
84	.00379	.00320	.00281	.00255
AZIMUTH	127.5	142.5	157.5	172.5
PCLAR				
8	.00991	.00986	.00983	.00981
15	.00972	.00963	.00958	.00955
22	.00950	.00938	.00930	.00926
32	.00911	.00895	.00885	.00880
45	.00841	.00821	.00809	.00802
60	.00713	.00690	.00676	.00670
72	.00539	.00519	.00506	.00500
84	.00238	.00227	.00220	.00217

RASC DIFFERENTIAL SCATTERED DOSE RATE (KEV/GM-SEC)

AZIMUTH	7.5	22.5	37.5	52.5
PCLAR				
8	.00369	.00368	.00367	.00365
15	.00579	.00577	.00572	.00565
22	.01027	.01020	.01006	.00988
32	.02354	.02324	.02271	.02202
45	.05978	.05838	.05595	.05303
60	.08915	.08516	.07865	.07148
72	.14725	.13661	.12029	.10378
84	.27836	.24763	.20370	.16340
AZIMUTH	67.5	82.5	97.5	112.5
PCLAR				
8	.00362	.00360	.00357	.00354
15	.00558	.00550	.00542	.00535
22	.00967	.00946	.00926	.00909
32	.02128	.02056	.01991	.01936
45	.05009	.04743	.04519	.04339
60	.06494	.05956	.05539	.05227
72	.09007	.07974	.07231	.06707
84	.13319	.11252	.09878	.08968
AZIMUTH	127.5	142.5	157.5	172.5
PCLAR				
8	.00352	.00350	.00349	.00349
15	.00529	.00524	.00521	.00520
22	.00894	.00883	.00876	.00872
32	.01892	.01859	.01838	.01827
45	.04201	.04102	.04039	.04007
60	.05001	.04845	.04746	.04699
72	.06344	.06102	.05952	.05881
84	.08367	.07978	.07743	.07633

TABLE 9 CONT.  
CHILTON-HUDDLESTON ALBEDO RESULTS

BACKSCATTERING OF 1.250 MEV PHOTONS FROM A CONCRETE MEDIUM  
INCIDENT CBLIQUITY = 1.047198 RADIAN

CHILTON-HUDDLESTON DIFFERENTIAL DOSE ALBEDO				
AZIMUTH	7.5	22.5	37.5	52.5
POLAR				
8	.01357	.01352	.01342	.01328
15	.01429	.01417	.01395	.01365
22	.01518	.01495	.01456	.01405
32	.01684	.01638	.01560	.01467
45	.02014	.01907	.01735	.01552
60	.02647	.02370	.01976	.01616
72	.03250	.02721	.02048	.01514
84	.02589	.01997	.01328	.00872
AZIMUTH	67.5	82.5	97.5	112.5
POLAR				
8	.01312	.01295	.01278	.01263
15	.01332	.01298	.01267	.01239
22	.01351	.01299	.01252	.01213
32	.01374	.01292	.01224	.01169
45	.01390	.01262	.01165	.01094
60	.01346	.01160	.01035	.00952
72	.01168	.00957	.00828	.00747
84	.00615	.00475	.00397	.00352
AZIMUTH	127.5	142.5	157.5	172.5
POLAR				
8	.01250	.01239	.01232	.01229
15	.01216	.01199	.01187	.01181
22	.01182	.01159	.01144	.01136
32	.01128	.01099	.01080	.01071
45	.01043	.01008	.00987	.00976
60	.00896	.00859	.00837	.00827
72	.00696	.00663	.00644	.00635
84	.00324	.00307	.00297	.00292
RASC DIFFERENTIAL SCATTERED DOSE RATE (KEV/GM-SEC)				
AZIMUTH	7.5	22.5	37.5	52.5
POLAR				
8	.00482	.00481	.00477	.00472
15	.00778	.00771	.00759	.00743
22	.01429	.01408	.01370	.01323
32	.03498	.03403	.03240	.03047
45	.10060	.09522	.08664	.07749
60	.18570	.16627	.13862	.11335
72	.38211	.31996	.24078	.17807
84	.90824	.70085	.46615	.30602
AZIMUTH	67.5	82.5	97.5	112.5
POLAR				
8	.00466	.00460	.00454	.00449
15	.00725	.00707	.00689	.00674
22	.01272	.01223	.01179	.01142
32	.02855	.02684	.02542	.02429
45	.06942	.06300	.05816	.05462
60	.09441	.08137	.07263	.06677
72	.13734	.11252	.09737	.08790
84	.21579	.16690	.13959	.12356
AZIMUTH	127.5	142.5	157.5	172.5
POLAR				
8	.00444	.00440	.00438	.00437
15	.00662	.00652	.00646	.00643
22	.01112	.01091	.01077	.01069
32	.02344	.02283	.02244	.02225
45	.05209	.05037	.04929	.04877
60	.06285	.06029	.05874	.05801
72	.08186	.07803	.07576	.07470
84	.11376	.10773	.10421	.10258

TABLE 9 CONT.  
CHILTON-HUDDLESTON ALBEDO RESULTS

BACKSCATTERING OF 1.250 MEV PHOTONS FROM A CONCRETE MEDIUM  
INCIDENT OBLIQUITY = 1.318146 RADIAN

CHILTON-HUDDLESTON DIFFERENTIAL DOSE ALBEDO

AZIMUTH	7.5	22.5	37.5	52.5
POLAR				
8	.01902	.01890	.01867	.01836
15	.02082	.02052	.01997	.01927
22	.02322	.02262	.02158	.02032
32	.02827	.02688	.02461	.02211
45	.03990	.03598	.03029	.02494
60	.06650	.05442	.03955	.02828
72	.09815	.07268	.04567	.02859
84	.09059	.06084	.03328	.01842
AZIMUTH	67.5	82.5	97.5	112.5
POLAR				
8	.01801	.01764	.01728	.01696
15	.01851	.01777	.01710	.01654
22	.01905	.01789	.01691	.01613
32	.01985	.01800	.01658	.01553
45	.02083	.01794	.01598	.01465
60	.02126	.01714	.01469	.01318
72	.01960	.01496	.01245	.01101
84	.01160	.00843	.00684	.00596
AZIMUTH	127.5	142.5	157.5	172.5
POLAR				
8	.01669	.01648	.01634	.01627
15	.01608	.01575	.01552	.01541
22	.01553	.01510	.01482	.01469
32	.01478	.01426	.01393	.01378
45	.01376	.01318	.01283	.01266
60	.01224	.01164	.01129	.01113
72	.01014	.00960	.00929	.00915
84	.00545	.00515	.00497	.00489

RASO DIFFERENTIAL SCATTERED DOSE RATE (KEV/GM-SEC)

AZIMUTH	7.5	22.5	37.5	52.5
POLAR				
8	.00676	.00672	.00664	.00653
15	.01133	.01117	.01087	.01049
22	.02186	.02130	.02032	.01913
32	.05872	.05582	.05110	.04593
45	.19923	.17967	.15125	.12455
60	.46644	.38170	.27739	.19835
72	1.15391	.85453	.53695	.33623
84	3.17828	2.13434	1.16781	.64639
AZIMUTH	67.5	82.5	97.5	112.5
POLAR				
8	.00640	.00627	.00614	.00603
15	.01008	.00967	.00931	.00900
22	.01793	.01684	.01592	.01518
32	.04123	.03739	.03445	.03226
45	.10402	.08960	.07980	.07319
60	.49114	.32021	.20302	.09248
72	.23048	.17955	.14646	.12648
84	.40712	.29598	.24009	.20943
AZIMUTH	127.5	142.5	157.5	172.5
POLAR				
8	.00593	.00586	.00581	.00578
15	.00876	.00857	.00845	.00839
22	.01462	.01421	.01395	.01383
32	.03069	.02961	.02894	.02862
45	.06874	.06584	.06407	.06324
60	.08584	.08167	.07921	.07806
72	.11922	.11294	.10929	.10760
84	.19147	.18069	.17450	.17166

TABLE 9 CONT.  
CHILTON-HUDDLESTON ALBEDO RESULTS

BACKSCATTERING OF 1.250 MEV PHOTONS FROM A CONCRETE MEDIUM  
INCIDENT OBLIQUITY = 1.470630 RADIAN

CHILTON-HUDDLESTON DIFFERENTIAL DOSE ALBEDO				
AZIMUTH	7.5	22.5	37.5	52.5
POLAR				
8	.02448	.02427	.02388	.02336
15	.02765	.02711	.02614	.02493
22	.03208	.03096	.02904	.02679
32	.04198	.03915	.03469	.03004
45	.06644	.05771	.04575	.03537
60	.12638	.09734	.06456	.04227
72	.20220	.13963	.07937	.04539
84	.21149	.13379	.06752	.03489
AZIMUTH	67.5	82.5	97.5	112.5
POLAR				
8	.02277	.02217	.02159	.02107
15	.02364	.02242	.02134	.02045
22	.02459	.02267	.02110	.01987
32	.02606	.02299	.02073	.01913
45	.02803	.02325	.02019	.01821
60	.02975	.02298	.01920	.01699
72	.02919	.02146	.01750	.01530
84	.02102	.01491	.01196	.01037
AZIMUTH	127.5	142.5	157.5	172.5
POLAR				
8	.02065	.02032	.02010	.01999
15	.01974	.01923	.01889	.01873
22	.01896	.01832	.01792	.01772
32	.01801	.01726	.01680	.01658
45	.01694	.01612	.01563	.01540
60	.01564	.01480	.01432	.01410
72	.01401	.01323	.01278	.01257
84	.00945	.00891	.00860	.00845
RASC DIFFERENTIAL SCATTERED DOSE RATE (KEV/GM-SEC)				
AZIMUTH	7.5	22.5	37.5	52.5
POLAR				
8	.00870	.00863	.00849	.00831
15	.01505	.01476	.01423	.01357
22	.03020	.02915	.02734	.02522
32	.08718	.08130	.07205	.06240
45	.33173	.28813	.22842	.17663
60	.88637	.68271	.45284	.29649
72	2.37728	1.64158	.93320	.53364
84	7.41934	4.69351	2.36873	1.22425
AZIMUTH	67.5	82.5	97.5	112.5
POLAR				
8	.00810	.00788	.00768	.00749
15	.01287	.01220	.01162	.01113
22	.02315	.02134	.01986	.01871
32	.05413	.04774	.04306	.03973
45	.13998	.11609	.10080	.09096
60	.20865	.16117	.13469	.11917
72	.34724	.23222	.20580	.17997
84	.73748	.52340	.41960	.36394
AZIMUTH	127.5	142.5	157.5	172.5
POLAR				
8	.00734	.00722	.00715	.00711
15	.01075	.01047	.01028	.01019
22	.01785	.01725	.01687	.01668
32	.03741	.03585	.03490	.03444
45	.08457	.08049	.07805	.07691
60	.10969	.10386	.10046	.09889
72	.16473	.15555	.15026	.14782
84	.33181	.31269	.30176	.29676

TABLE 9 CONT.  
CHILTON-HUDDLESTON ALBEDO RESULTS

BACKSCATTERING OF 1.000 MEV PHOTONS FROM A CONCRETE MEDIUM  
INCIDENT OBLIQUITY = 1.318146 RADIAN

CHILTON-HUDDLESTON DIFFERENTIAL DOSE ALBEDO				
AZIMUTH	7.5	22.5	37.5	52.5
PCLAR				
8	.02240	.02227	.02203	.02171
15	.02428	.02396	.02339	.02265
22	.02681	.02617	.02507	.02374
32	.03215	.03066	.02825	.02559
45	.04433	.04022	.03421	.02852
60	.07076	.05883	.04369	.03187
72	.09855	.07540	.04933	.03185
84	.08453	.05998	.03503	.02028
AZIMUTH	67.5	82.5	97.5	112.5
PCLAR				
8	.02134	.02095	.02058	.02025
15	.02186	.02108	.02039	.01980
22	.02240	.02119	.02016	.01935
32	.02320	.02126	.01977	.01868
45	.02414	.02109	.01903	.01766
60	.02440	.02002	.01745	.01589
72	.02233	.01740	.01476	.01326
84	.01313	.00976	.00808	.00717
AZIMUTH	127.5	142.5	157.5	172.5
PCLAR				
8	.01997	.01975	.01960	.01953
15	.01933	.01898	.01875	.01864
22	.01873	.01829	.01800	.01787
32	.01790	.01737	.01704	.01688
45	.01675	.01615	.01579	.01561
60	.01492	.01431	.01395	.01378
72	.01236	.01181	.01150	.01135
84	.00664	.00633	.00615	.00606
RASC DIFFERENTIAL SCATTERED DOSE RATE (KEV/GM-SEC)				
AZIMUTH	7.5	22.5	37.5	52.5
PCLAR				
8	.00666	.00662	.00655	.00645
15	.01105	.01090	.01064	.01031
22	.02109	.02059	.01973	.01868
32	.05581	.05323	.04903	.04443
45	.18501	.16788	.14276	.11901
60	.41483	.34490	.25612	.18684
72	.96848	.74094	.48474	.31304
84	2.47880	1.75887	1.02739	.59488
AZIMUTH	67.5	82.5	97.5	112.5
PCLAR				
8	.00634	.00623	.00612	.00602
15	.00994	.00959	.00928	.00901
22	.01762	.01667	.01587	.01523
32	.04027	.03690	.03433	.03243
45	.10075	.08802	.07945	.07372
60	.14308	.11741	.10233	.09320
72	.21951	.17102	.14508	.13035
84	.38521	.28633	.23702	.21036
AZIMUTH	127.5	142.5	157.5	172.5
PCLAR				
8	.00593	.00587	.00582	.00580
15	.00879	.00864	.00853	.00848
22	.01474	.01439	.01417	.01406
32	.03108	.03015	.02958	.02930
45	.06990	.06740	.06589	.06517
60	.08749	.08391	.08180	.08081
72	.12152	.11614	.11300	.11155
84	.19485	.18564	.18033	.17788



## APPENDIX E

Description and Explanation of the IBM-1620  
Computer Program Used for Calculating the  
Differential Dose Rate Albedo

This computer code was written to calculate the differential dose rate albedo defined by eq.(79), i.e.,

$$a(\Theta_o, \Phi_o; \Theta, \Phi) d\Omega = 1.293 \{CK(\Theta_s) + C'\} \{1 + \cos\Theta \sec\Theta_o\}^{-1} d\Omega \quad (79)$$

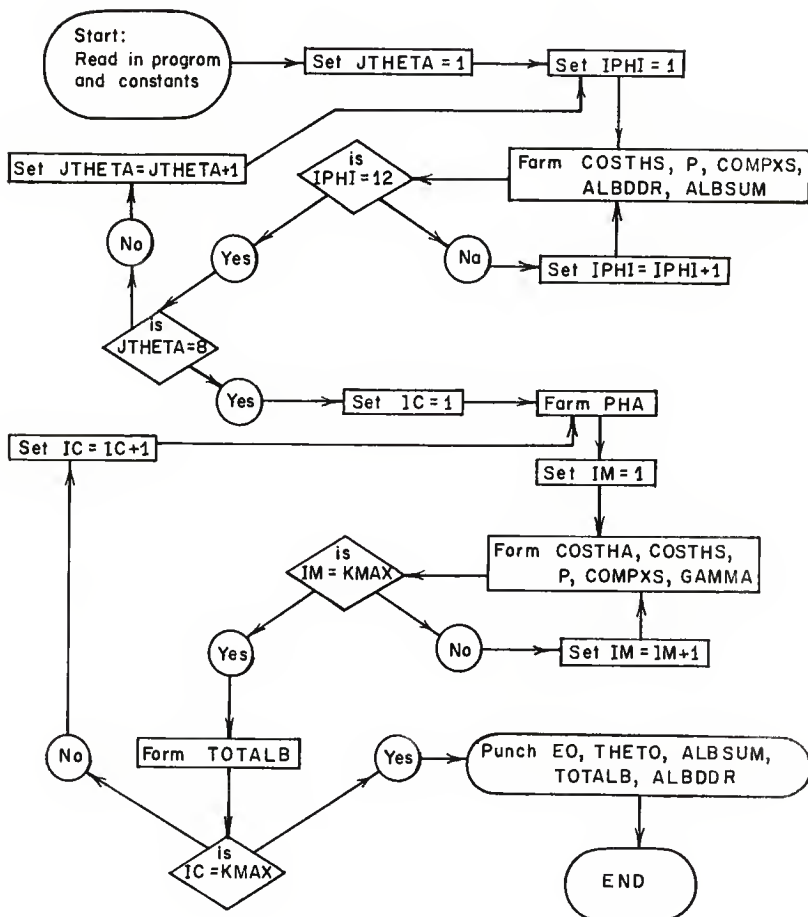
The program was written in FORTRAN II language. The source program is listed, the logic diagram shown and pertinent results tabulated in this appendix. The results are tabulated for the five incident polar angles,  $\cos\Theta_o = 0.1, 0.25, 0.5, 0.75$  and  $1.00$ . Selected portions of these results are plotted in Figures 23 through 27. Table 10 defines the various symbols utilized in this computer code.

Table 10. Input data and variables required for the IBM-1620 differential dose rate albedo computer program.

Symbol*	Explanation
KMAX	Degree of Gaussian Quadrature Utilized, k
DELOME	Solid Angle Subtended, $(\Phi_{k'+1} - \Phi_{k'}) (\cos\Theta_{k'} - \cos\Theta_{k'+1}), \Delta\Omega_{j', k'}$
CHRTNO	Christoffel Numbers
OLEGNP	Zeros of the Legendre Polynomials
TOTALB	Total Dose Rate Albedo (Integrated)
ALBSUM	Total Dose Rate Albedo (Summed)
ALBDDR	Dose Rate Albedo (Dose Rate Out/Dose Rate In)
PHA	Emergent Azimuthal Angle, $\Phi$ (Radians)
GAMMA	Integration Variable
COSTHA	Cosine of the Emergent Polar Angle, $\cos\Theta$
SINTHA	Sine of the Emergent Polar Angle, $\sin\Theta$
GAMMAL	Integration Variable
IM	Fixed Point Emergent Polar Angle Integration Variable
IC	Fixed Point Emergent Azimuthal Angle Integration Variable

\* Additional utilized symbols are defined in Table 8.

# LOGIC DIAGRAM FOR THE DIFFERENTIAL DOSE RATE ALBEDO



```

C      DIFFERENTIAL DOSE RATE ALBEDO BY J.A. BARAN MARCH,63
C      INPUT DATA--EC=INITIAL PHOTON ENERGY (MEV), THETAC=INITIAL
C      OBLIQUITY, C AND CPRIME=CHILTON-HUDDLESTON PARAMETERS.
      DIMENSION CLEGNP(10),THETA(8), PHI(12), ALBDDR(12,8),CHRTNC(10),
      IDELCME(8)
10  FORMAT (F6.3,F9.6,I3)
20  FORMAT (F12.9,F13.10)
22  FORMAT(F11.8)
60  FORMAT (6F9.6/6F9.6)
80  FORMAT(24H      BACKSCATTERING OF ,F6.3, 35H MEV PHOTONS FROM A
      1CONCRETE MEDIUM )
90  FORMAT      (69H      AZIMUTH      7.5      22.5      37.5
      1      52.5      /15H      POLAR )
95  FORMAT      (70H      AZIMUTH      67.5      82.5      97.5
      1      112.5      ,/15H      POLAR )
100 FORMAT      (70H      AZIMUTH      127.5      142.5      157.5
      1      172.5      /15H      POLAR )
105 FORMAT (44H      TOTAL DOSE RATE ALBEDO (SUMMATION) = F7.5)
110 FORMAT (75H      DOSE RATE ALBEDO--DOSE RATE CUT/DOSE RATE IN,
      1PER STERADIAN      //)
115 FORMAT (27H      INCIDENT OBLIQUITY = F9.6, 8H RADIANS ,//)
120 FORMAT (13H      8      ,4(F13.5)/ 13H      15      ,4F13.5/
      113H      22      , 4(F13.5)/ 13H      32      ,4F13.5/
      113H      45      , 4(F13.5)/ 13H      60      ,4F13.5/
      113H      72      , 4(F13.5)/ 13H      84      ,4F13.5//)
125 FORMAT (44H      TOTAL DOSE RATE ALBEDO (INTEGRATED) = F7.5,//)
30  READ 10, EC, THETAC, KMAX
C      INPUT ABOVE IS 1 CARD
      READ 20, C, CPRIME
C      INPUT ABOVE IS 1 CARD
      READ 60, THETA
C      INPUT ABOVE IS 2 CARDS
      READ 60, PHI
C      INPUT ABOVE IS 2 CARDS
      READ 60, DELCME
C      INPUT ABOVE IS 2 CARDS
      DO16I=1,KMAX
      READ22,CHRTNC(I)
16  READ22,CLEGNP(I)
C      INPUT ABOVE IS 12 CARDS
      TOTALB = 0.
      ALBSUM = 0.0
      DO 70 JTHETA=1,8
      DO 65 IPHI=1,12
      COSTHS=SINF(THETAC)*COSF(PHI(IPHI))*SINF(THETA(JTHETA))
      1-COSF(THETAC)*COSF(THETA(JTHETA))
      P=1./(1.+(EC*(1.-COSTHS)/0.511))
      COMPS=(3.970562      )*(P**2)*(1.+(P**2)-P*(1.-(COSTHS**2)))
      ALBDDR(IPHI,JTHETA) = ( 1.293      *COSF(THETAC)*(C*COMPS+CPRIME))/
      1COSF(THETA(JTHETA))+COSF(THETAC))
65  ALBSUM = ALBSUM + DELCME(JTHETA) * ALBDDR(IPHI,JTHETA) * 2.
C      THIS LOOP CALCULATES THE DOSE RATE ALBEDO

```

70 CONTINUE

DO 7 IC=1,KMAX

C THIS IC LOOP INTEGRATES OVER THE EMERGENT AZIMUTHAL ANGLES

PHA=(CLEGNP(IC)\*3.1415927) + 3.1415927

GAMMA = 0.

DO 6 IM=1,KMAX

C THIS IM LOOP INTEGRATES OVER THE EMERGENT POLAR ANGLES

COSTHA=(CLEGNP(IM)/2.)\*0.5

SINTHA=SQRT(1.-COSTHA\*COSTHA)

COSTHS=SINF(THETAC)\*COSF(PHA)\*SINTHA - (COSF(THETAC)\*COSTHA)

P=1./(1.+(EQ\*(1.-COSTHS)/0.511))

COMPXS=(3.970562 )\*(P\*\*2)\*(1.+(P\*\*2)-P\*(1.-COSTHS\*\*2))

GAMMA1=((2.03104\*COSF(THETAC)\*(C\*COMPXS+CPRIME))/(COSTHA+COSF(THETAC))) \* CHRINC(IM)

6 GAMMA=GAMMA + GAMMA1

7 TOTALB = TOTALB + (GAMMA \* CHRINC(IC))

PUNCH 80, EQ

PUNCH 115, THETAC

PUNCH 105, ALBSUM

PUNCH 125, TOTALB

PUNCH 110

PUNCH 90

PUNCH 120, ((ALBDDR(IPHI,JTHETA),IPHI=1,4 ),JTHETA=1,8)

PUNCH 95

PUNCH 120, ((ALBDDR(IPHI,JTHETA),IPHI=5,8 ),JTHETA=1,8)

PUNCH 100

PUNCH 120, ((ALBDDR(IPHI,JTHETA),IPHI=9,12),JTHETA=1,8)

GO TO 30

END

# INPUT DATA

1.252 1.318146 6

.064501061 0.0089294690

.139626 0.261800 0.383973 0.558506 0.785399 1.047198

1.256638 1.466077

.130900 0.392699 0.654499 0.916298 1.178098 1.439897

1.701697 1.963496 2.225296 2.487095 2.748895 3.010694

.00525 .00785 .0131 .026 .0525 .0525

.0525 .0525

.46791393

.23861919

.36076157

.66120939

.17132449

.93246951

.17132449

- .93246951

.36076157

- .66120939

.46791393

- .23861919

TABLE 11.  
DIFFERENTIAL DOSE RATE ALBEDO RESULTS

BACKSCATTERING OF 1.252 MEV PHOTONS FROM A CONCRETE MEDIUM  
INCIDENT OBLIQUITY = 0.000000 RADIAN

TOTAL DOSE RATE ALBEDO (SUMMATION) = .11410  
TOTAL DOSE RATE ALBEDO (INTEGRATED) = .11509

DOSE RATE ALBEDO--DOSE RATE OUT/DOSE RATE IN, PER STERADIAN

AZIMUTH POLAR	7.5	22.5	37.5	52.5
8	.01074	.01074	.01074	.01074
15	.01094	.01094	.01094	.01094
22	.01127	.01127	.01127	.01127
32	.01200	.01200	.01200	.01200
45	.01355	.01355	.01355	.01355
60	.01663	.01663	.01663	.01663
72	.02084	.02084	.02084	.02084
84	.02804	.02804	.02804	.02804
AZIMUTH POLAR	67.5	82.5	97.5	112.5
8	.01074	.01074	.01074	.01074
15	.01094	.01094	.01094	.01094
22	.01127	.01127	.01127	.01127
32	.01200	.01200	.01200	.01200
45	.01355	.01355	.01355	.01355
60	.01663	.01663	.01663	.01663
72	.02084	.02084	.02084	.02084
84	.02804	.02804	.02804	.02804
AZIMUTH POLAR	127.5	142.5	157.5	172.5
8	.01074	.01074	.01074	.01074
15	.01094	.01094	.01094	.01094
22	.01127	.01127	.01127	.01127
32	.01200	.01200	.01200	.01200
45	.01355	.01355	.01355	.01355
60	.01663	.01663	.01663	.01663
72	.02084	.02084	.02084	.02084
84	.02804	.02804	.02804	.02804

TABLE 11 CONT.  
DIFFERENTIAL DOSE RATE ALBEDO RESULTS

BACKSCATTERING OF 1.252 MEV PHOTONS FROM A CONCRETE MEDIUM  
INCIDENT OBLIQUITY = .722730 RADIAN

TOTAL DOSE RATE ALBEDO (SUMMATION) = .12711  
TOTAL DOSE RATE ALBEDO (INTEGRATED) = .12905

DOSE RATE ALBEDO--DOSE RATE OUT/DOSE RATE IN, PER STERADIAN

AZIMUTH POLAR	7.5	22.5	37.5	52.5
8	.01016	.01013	.01009	.01004
15	.01067	.01062	.01053	.01041
22	.01140	.01131	.01116	.01096
32	.01294	.01278	.01248	.01211
45	.01640	.01601	.01535	.01454
60	.02462	.02351	.02172	.01974
72	.03924	.03641	.03206	.02766
84	.07350	.06538	.05379	.04314
AZIMUTH POLAR	67.5	82.5	97.5	112.5
8	.00997	.00989	.00982	.00975
15	.01027	.01013	.00998	.00986
22	.01073	.01050	.01028	.01008
32	.01170	.01130	.01095	.01065
45	.01374	.01301	.01239	.01190
60	.01793	.01645	.01529	.01443
72	.02400	.02125	.01927	.01788
84	.03517	.02971	.02608	.02368
AZIMUTH POLAR	127.5	142.5	157.5	172.5
8	.00969	.00964	.00961	.00959
15	.00975	.00966	.00960	.00957
22	.00992	.00980	.00972	.00967
32	.01040	.01022	.01011	.01005
45	.01152	.01125	.01108	.01099
60	.01381	.01338	.01311	.01298
72	.01691	.01626	.01586	.01568
84	.02210	.02107	.02045	.02016

TABLE 11 CONT.  
DIFFERENTIAL DOSE RATE ALBEDO RESULTS

BACKSCATTERING OF 1.252 MEV PHOTONS FROM A CONCRETE MEDIUM  
INCIDENT OBLIQUITY = 1.047198 RADIAN

TOTAL DOSE RATE ALBEDO (SUMMATION) = .14837  
TOTAL DOSE RATE ALBEDO (INTEGRATED) = .15259

DOSE RATE ALBEDO--DOSE RATE OUT/DOSE RATE IN, PER STERADIAN

AZIMUTH POLAR	7.5	22.5	37.5	52.5
8	.00885	.00881	.00875	.00866
15	.00955	.00947	.00932	.00912
22	.01057	.01041	.01013	.00978
32	.01282	.01247	.01187	.01117
45	.01839	.01741	.01584	.01417
60	.03418	.03060	.02551	.02086
72	.06789	.05685	.04278	.03164
84	.15992	.12339	.08206	.05387
AZIMUTH POLAR	67.5	82.5	97.5	112.5
8	.00855	.00844	.00833	.00823
15	.00890	.00868	.00847	.00828
22	.00941	.00904	.00872	.00844
32	.01046	.00984	.00931	.00890
45	.01269	.01152	.01063	.00998
60	.01738	.01498	.01337	.01229
72	.02440	.01999	.01730	.01562
84	.03798	.02938	.02457	.02175
AZIMUTH POLAR	127.5	142.5	157.5	172.5
8	.00815	.00808	.00803	.00801
15	.00813	.00801	.00793	.00789
22	.00823	.00807	.00796	.00791
32	.00859	.00837	.00822	.00815
45	.00952	.00921	.00901	.00892
60	.01157	.01110	.01081	.01068
72	.01454	.01386	.01346	.01327
84	.02003	.01897	.01835	.01806

TABLE 11 CONT.  
DIFFERENTIAL DOSE RATE ALBEDO RESULTS

BACKSCATTERING OF 1.252 MEV PHOTONS FROM A CONCRETE MEDIUM  
INCIDENT OBLIQUITY = 1.318146 RADIAN

TOTAL DOSE RATE ALBEDO (SUMMATION) = .16153

TOTAL DOSE RATE ALBEDO (INTEGRATED) = .17116

DOSE RATE ALBEDO--DOSE RATE OUT/DOSE RATE IN, PER STERADIAN

AZIMUTH POLAR	7.5	22.5	37.5	52.5
8	.00620	.00616	.00608	.00598
15	.00695	.00685	.00667	.00644
22	.00808	.00787	.00751	.00707
32	.01076	.01023	.00936	.00841
45	.01821	.01642	.01382	.01138
60	.04293	.03512	.02552	.01825
72	.10254	.07592	.04769	.02986
84	.27995	.18793	.10279	.05688
AZIMUTH POLAR	67.5	82.5	97.5	112.5
8	.00587	.00574	.00563	.00552
15	.00618	.00594	.00571	.00552
22	.00663	.00623	.00588	.00561
32	.00755	.00685	.00631	.00591
45	.00951	.00819	.00729	.00669
60	.01372	.01106	.00948	.00851
72	.02047	.01563	.01301	.01150
84	.03583	.02605	.02113	.01843
AZIMUTH POLAR	127.5	142.5	157.5	172.5
8	.00544	.00537	.00532	.00530
15	.00537	.00526	.00518	.00515
22	.00540	.00525	.00516	.00511
32	.00562	.00542	.00530	.00524
45	.00628	.00602	.00585	.00578
60	.00790	.00751	.00729	.00718
72	.01059	.01003	.00971	.00956
84	.01685	.01590	.01536	.01511



TABLE 11 CONT.  
DIFFERENTIAL DOSE RATE ALBEDO RESULTS

BACKSCATTERING OF 1.252 MEV PHOTONS FROM A CONCRETE MEDIUM  
INCIDENT OBLIQUITY = 1.470630 RADIAN

TOTAL DOSE RATE ALBEDO (SUMMATION) = .12092

TOTAL DOSE RATE ALBEDO (INTEGRATED) = .13555

DOSE RATE ALBEDO--DOSE RATE OUT/DOSE RATE IN, PER STERADIAN

AZIMUTH POLAR	7.5	22.5	37.5	52.5
8	.00319	.00316	.00311	.00304
15	.00369	.00362	.00349	.00333
22	.00446	.00431	.00404	.00373
32	.00639	.00596	.00528	.00457
45	.01213	.01053	.00835	.00645
60	.03264	.02513	.01667	.01091
72	.08454	.05835	.03316	.01896
84	.26152	.16536	.08341	.04310
AZIMUTH POLAR	67.5	82.5	97.5	112.5
8	.00296	.00289	.00281	.00274
15	.00316	.00299	.00285	.00273
22	.00342	.00315	.00293	.00276
32	.00396	.00350	.00315	.00291
45	.00511	.00424	.00368	.00332
60	.00768	.00593	.00495	.00438
72	.01219	.00896	.00731	.00639
84	.02596	.01842	.01477	.01281
AZIMUTH POLAR	127.5	142.5	157.5	172.5
8	.00269	.00265	.00262	.00260
15	.00263	.00257	.00252	.00250
22	.00264	.00255	.00249	.00246
32	.00274	.00262	.00255	.00252
45	.00309	.00294	.00285	.00281
60	.00403	.00382	.00369	.00364
72	.00585	.00552	.00534	.00525
84	.01168	.01101	.01062	.01045

## APPENDIX F

## Discussion of Gaussian Quadrature

The complexity of the required integrations in this thesis precluded all but the simplest of direct integrations. It was necessary to fit the data with an empirical expression and then use formal analytical methods. This technique is commonly called numerical integration. A rather efficient method of numerical integration called Gaussian quadrature is used in this study (15, 17). This general procedure notes values of the ordinate  $y$  at  $n$  predetermined values of  $x$ . The sum of the products of the ordinate  $y$  multiplied by a predetermined constant is multiplied by the difference in the integration limits of  $x$  to give the desired integral. Utilizing  $n$  predetermined values of  $x$ , a polynomial of  $(2n-1)$ st degree would be exactly fitted.

Consider the derivation for the special case of a fifth-degree function per reference 17. A fifth-degree function is of the form,

$$y = a_0 + a_1x + a_2x^2 + a_3x^3 + a_4x^4 + a_5x^5. \quad (80)$$

The desired integration of  $y$  from  $d'$  to  $c'$  must be transformed to limits of  $-1$  to  $+1$ . This can be achieved by the relationship,

$$x = \{(c'+d')/2\} + \{(c'-d')/2\}u. \quad (81)$$

The integral therefore becomes

$$\int_{d'}^{c'} y dx = \{(c'-d')/2\} \int_{-1}^{+1} y du = N'(c'-d') \quad (82)$$

where  $N'$  is the average value of  $y$  over the interval  $d'$  to  $c'$ . From eq. (80) and eq. (81),

$$y = a'_0 + a'_1 u + a'_2 u^2 + a'_3 u^3 + a'_4 u^4 + a'_5 u^5. \quad (83)$$

Substituting eq.(83) into eq.(82) yields

$$N' = a'_0 + (a'_2/3) + (a'_4/5). \quad (84)$$

With the methodology outlined at the beginning of this appendix, the  $N'$  of eq.(84) may be obtained from the three constants  $C_1$ ,  $C_2$  and  $C_3$  and the three ordinates  $y_1$ ,  $y_2$ , and  $y_3$  by

$$N' = C_1 y_1 + C_2 y_2 + C_3 y_3. \quad (85)$$

Substituting the power series of eq.(83) into eq.(85) results in

$$\begin{aligned} N' = & a'_0(C_1+C_2+C_3) + a'_1(C_1u_1+C_2u_2+C_3u_3) \\ & + a'_2(C_1u_1^2+C_2u_2^2+C_3u_3^2) + a'_3(C_1u_1^3+C_2u_2^3+C_3u_3^3) \\ & + a'_4(C_1u_1^4+C_2u_2^4+C_3u_3^4) + a'_5(C_1u_1^5+C_2u_2^5+C_3u_3^5). \end{aligned} \quad (86)$$

Comparing this result with that of eq.(84), the following equalities must be true.

$$\begin{aligned} C_1+C_2+C_3 &= 1 \\ C_1u_1 + C_2u_2 + C_3u_3 &= 0 \\ C_1u_1^2 + C_2u_2^2 + C_3u_3^2 &= 1/3 \\ C_1u_1^4 + C_2u_2^4 + C_3u_3^4 &= 1/5 \\ C_1u_1^5 + C_2u_2^5 + C_3u_3^5 &= 0 \end{aligned} \quad (87)$$

These equations are simultaneously solved to give the results,

$$C_1 = C_3 = 5/18$$

$$C_2 = 4/9$$

$$u_1 = -(3/5)^{\frac{1}{2}} = -0.7746 \quad (88)$$

$$u_2 = 0$$

$$u_3 = (3/5)^{\frac{1}{2}} = 0.7746$$

These results are combined by eq.(85) and the value of the integral given by  $N'(c'-d')$ . Table 12 gives  $u_k$  (or  $x_k$ ) and  $C_k$  (or  $a_k$ ) values for values of  $n$  up through  $n = 6$  (15). Since  $x_k = x_{n-k+1}$  and  $a_k = a_{n-k+1}$ , only half of the values are tabulated.

Table 12. Parameters utilized in Gauss' mechanical quadrature formula (15).

$n$	$k$	$x_k$	$a_k$
2	1	0.577350269189626	1.000000000000000
3	1	0.774596669241483	0.555555555555556
	2	0.000000000000000	0.888888888888889
4	1	0.339981043584856	0.652145154862546
	2	0.861136311594053	0.347854845137454
5	1	0.538469310105683	0.478628670499366
	2	0.906179845938664	0.236926885056189
	3	0.000000000000000	0.568888888888889
6	1	0.238619186083197	0.467913934572691
	2	0.661209386466265	0.360761573048139
	3	0.932469514203152	0.171324492379170

## APPENDIX G

Description and Explanation of the IBM-1620  
Computer Program Used for Calculating the  
Differential Incident Dose Rate at Point (x,y)  
on the Ceiling of a Blockhouse

This computer code was written to calculate the differential incident dose rate defined by expression (35),

$$(0.1917 + 0.0095 \cos \Theta_0) \left\{ 1 + a' \sum_a (E_0)_d \exp(b \sum_a (E_0)_d / \cos \Theta_0) / \cos \Theta_0 \right\} \quad (35)$$

$$\times \{ 2\pi \cos \Theta_0 \exp(-a / \cos \Theta_0) \}^{-1} \Delta \cos \Theta_0 \Delta \Phi_0.$$

The program was written in FORTRAN II language. The source program is listed and the logic diagram is shown in this appendix.

Results are obtained for the KSU blockhouse for 56 equal solid angles at the (x,y) positions: (0,5), (0,10), (0,15), (3,5), (3,10), (3,15), (6,5), (6,10) and (6,15) with the dimensions of feet. These results are presented in this appendix as Table 14. Selected portions of these results are presented in the format of Figure 6 in the main body of this work. Table 13 defines the various symbols utilized in this computer code.

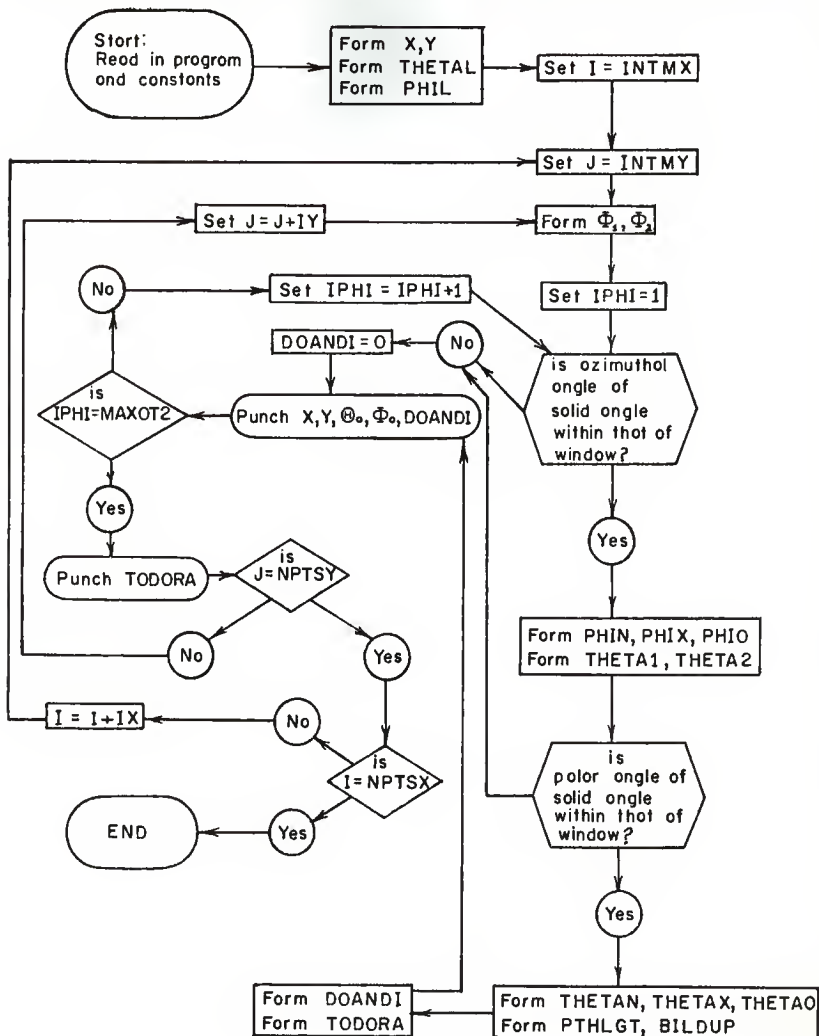
Table 13. Input data and variables required for the IBM-1620 differential incident dose rate computer program.

Symbol	Explanation
ACHD	Build-up Parameter, a'
BCHD	Build-up Parameter, b
R	One-half Aperture Width (feet)
H	Distance Between Ceiling and Horizontal Centerline of Aperture (feet)
V	One-half Aperture Height (feet)
X	x Co-ordinate
NFTSX	Maximum x Co-ordinate Calculated (feet)

Table 13 cont.

Symbol	Explanation
Y	y Co-ordinate
NPTSY	Maximum y Co-ordinate Calculated (feet)
INTMX	Initial Value of x Co-ordinate Calculated (feet)
INTMY	Initial Value of y Co-ordinate Calculated (feet)
IX	Interval Between Calculated x Values (feet)
IY	Interval Between Calculated y Values (feet)
MAXOME	One-half the Number of Solid Angles Calculated About a Point on the Ceiling
THEDEG	Average Polar Angle for Each Solid Angle (degrees)
PHIDEG	Average Azimuthal Angle for Each Solid Angle (degrees)
THETA	Average Polar Angle for Each Solid Angle (radians)
PHI	Average Azimuthal Angle for Each Solid Angle (radians)
THETAG	Polar Angular Limits of Each Solid Angle (degrees)
PHIG	Azimuthal Angular Limits of Each Solid Angle (degrees)
THETAL	Polar Angular Limits of Each Solid Angle (radians)
PHIL	Azimuthal Angular Limits of Each Solid Angle (radians)
PHI1	Azimuthal Limit of Aperture in the Positive x Plane (radians)
PHI2	Azimuthal Limit of Aperture in the Negative x Plane (radians)
PHIN	Minimum Value of Azimuthal Angle Subtended by the Aperture for Each Solid Angle (radians)
PHIX	Maximum Value of Azimuthal Angle Subtended by the Aperture for Each Solid Angle (radians)
PHIO	Arithmetic Average of Maximum and Minimum Values of Azimuthal Angles Subtended by the Aperture for Each Solid Angle (radians)
THETA1	Polar Angle Subtended by Bottom of Aperture at the Determined PHIO (radians)
THETA2	Polar Angle Subtended by Top of Aperture at the Determined PHIO (radians)
THETAN	Minimum Value of Polar Angle Subtended by the Aperture for Each Solid Angle (radians)
COSTHN	Cosine of THETAN
THETAX	Maximum Value of Polar Angle Subtended by the Aperture for Each Solid Angle (radians)
COSTHX	Cosine of THETAX
COSTHO	Cosine of Arithmetic Average of Maximum and Minimum Polar Angles Subtended by the Aperture for Each Solid Angle
PTHILCT	Mean Free Paths of Incident Gamma Ray Photon from Given Point on the Contaminated Plane to (x,y) on the Ceiling
BILDUP	Dose Build-up Factor for a Point Isotropic Source, B
DOANDI	Differential Incident Dose Rate, $D_1(x,y;\Theta_0\Phi_0)(D_0)$
TODORA	Summation of DOANDI ( $D_0$ )

# LOGIC DIAGRAM FOR THE DIFFERENTIAL INCIDENT DOSE RATE AT ANY POINT ON A BLOCKHOUSE CEILING



```

C      DIFFERENTIAL INCIDENT DOSE RATE DIST.--3/11/63 BY J.A. BARAN
      DIMENSION THEDEG(56), PHIDEG(56), X(51), Y(100), PHI(56), THETA(56
1), THETAG(56), PHIG(56), THETAL(112), PHIL(112)
17  FORMAT (6F10.1)
18  FORMAT (20I3)
19  FORMAT (2F7.2)
700  FORMAT(4E18.10)
710  FORMAT(/,48H
      18,/)
      SUM OF DIFFERENTIAL DOSE RATES = F10.
714  FORMAT (60H
      1RAIN ,//)
      X          Y          THETA      PHI      DIFF.DO
715  FORMAT (10H
      F6.2, F9.2, F10.2, F10.2, F13.9)
30  READ 700,
      ACHD,BCHD,R,H,V
C      INPUT ABOVE IS 2 CARDS
      READ 18,
      NPTSX, NPTSY, INTMX, INTMY,IX,IY,
      MAXCME
C      INPUT ABOVE IS 1 CARD
      DO 21 I=1,MAXCME
      J = MAXCME + I
      READ 19, THEDEG(I), PHIDEG(I)
      THEDEG(J) = THEDEG(I)
21  PHIDEG(J) = 180. + PHIDEG(I)
C      INPUT ABOVE IS 28 CARDS
      MAXCT2 = MAXCME * 2
      READ 17, THETAG
C      INPUT ABOVE IS 10 CARDS
      READ 17, PHIG
C      INPUT ABOVE IS 10 CARDS
      DO 14 I=INTMX, NPTSX, IX
14  X(I)= I-1
      DO 15 I=INTMY, NPTSY, IY
15  Y(I) = I
C      THESE LOOPS CALCULATE THE X AND Y CO-ORDINATES OF INTEREST
C      WHERE THE DIFFERENTIAL INCIDENT DOSE RATES ARE CALCULATED
      DO 76JTHETA=1,MAXCT2
      THETAL(JTHETA) = THETAG(JTHETA) / 57.295779
      PHIL(JTHETA) = PHIG(JTHETA) / 57.295779
      J = MAXCT2 + JTHETA
      THETAL(J) = THETAL(JTHETA)
76  PHIL(J) = 3.1415927 + PHIL(JTHETA)
C      THIS LOOP CONVERTS THE SOLID ANGLE LIMITS TO RADIANS AND UTILIZES
C      SYMMETRY TO EXPAND THE SOLID ANGLES TO COVER THE HEMISPHERE
      DO 760 I=INTMX, NPTSX, IX
      DO 720 J=INTMY, NPTSY, IY
C      THESE LOOPS REPEAT THE ENTIRE CALCULATION FOR DIFFERENT (X,Y)
      IF (SENSE SWITCH 1) 86, 87
86  PAUSE
87  PHI1=ATANF((X(I)-R)/Y(J)) + 3.1415927
      PHI2=ATANF((X(I)+R)/Y(J)) + 3.1415927
      TDCORA = 0.
      PUNCH 714
      DO 65 IPHI = 1, MAXCT2
C      THIS LOOP REPEATS THE CALCULATIONS FOR EACH SOLID ANGLE

```



```

      IF(PHIL(2*IPHI)-PHI1) 101,101,104
104  IF(PHI2-PHIL( 2*IPHI -1)) 101, 101, 111
C    THESE TWO ORDERS DETERMINE IF THE AZIMUTHAL LIMITS OF THE SOLID
C    ANGLE SUBTEND ANY PORTION OF THE APERTURE
111  IF(PHIL( 2*IPHI -1) - PHI1) 112, 112, 113
101  DCANDI=0.
      GO TO 65
112  PHIN=PHI1
      GO TO 114
113  PHIN=PHIL( 2*IPHI -1)
114  IF(PHI2-PHIL(2*IPHI))115,116,116
115  PHIX=PHI2
      GO TO 118
116  PHIX=PHIL(2*IPHI)
C    THE PORTION OF THE AZIMUTHAL INTERVAL OF THE SOLID ANGLE
C    SUBTENDING THE APERTURE IS DETERMINED BY THESE ORDERS
118  PHIC = (PHIX+PHIN)/2.
      THETA1=ATANF(Y(J)/((H+V)*ABSF(COSF(PHIC-3.1415927))))
      THETA2=ATANF(Y(J)/((H-V)*ABSF(COSF(PHIC-3.1415927))))
      IF(THETA2-THETA1) 101,101,102
102  IF(THETA2-THETA1) 101,101,105
C    THESE TWO ORDERS DETERMINE IF THE POLAR LIMITS OF THE SOLID
C    ANGLE SUBTEND ANY PORTION OF THE APERTURE
105  IF(THETA2-THETA1) 106,106,107
106  THETA1 = THETA1
      COSTHN=COSF(THETA1)
      GO TO 108
107  THETA1 = THETA1(2*IPHI-1)
      COSTHN=COSF(THETA1(2*IPHI-1))
108  IF(THETA2-THETA1(2*IPHI))109,110,110
109  THETA2 = THETA2
      COSTHX=COSF(THETA2)
      GO TO 117
110  THETA2 = THETA2(2*IPHI)
      COSTHX=COSF(THETA2(2*IPHI))
C    THE PORTION OF THE POLAR INTERVAL OF THE SOLID ANGLE
C    SUBTENDING THE APERTURE IS DETERMINED BY THESE ORDERS
117  COSTHC = COSF((THETA1+THETA2)/2.)
      PTHLGT=0.01825/COSTHC
      BILDUP=1.+ACHD*PTHLGT*EXPF(BCHD*PTHLGT)
      DCANDI=(0.1917+0.0095*COSTHC)*BILDUP*(PHIX-PHIN)*(COSTHN-
1    COSTHX)/(6.2831853 * COSTHC * EXPF(PTHLGT))
      TODORA = DCANDI + TODORA
65  PUNCH 715,X(I),Y(J), THEDEG(IPHI), PHIDEG(IPHI), DCANDI
      PUNCH 710, TODORA
720  CONTINUE
760  CONTINUE
      GO TO 30
END

```

## INPUT DATA

89.562-2		62.518-3		1.85+0		2.88+0
1.08+0						
7 15 1 5 3 5 28						
7.70 90.00						
18.60 90.00						
28.30 30.00						
28.30 90.00						
28.30 150.00						
39.60 30.00						
39.60 90.00						
39.60 150.00						
49.80 22.50						
49.80 67.50						
49.80 112.50						
49.80 157.50						
59.90 22.50						
59.90 67.50						
59.90 112.50						
59.90 157.50						
71.10 15.00						
71.10 45.00						
71.10 75.00						
71.10 105.00						
71.10 135.00						
71.10 165.00						
83.80 15.00						
83.80 45.00						
83.80 75.00						
83.80 105.00						
83.80 135.00						
83.80 165.00						
.0 15.4	15.4	21.8	21.8	34.8		
21.8 34.8	21.8	34.8	34.8	44.4		
34.8 44.4	34.8	44.4	44.4	55.2		
44.4 55.2	44.4	55.2	55.2	64.6		
55.2 64.6	55.2	64.6	64.6	77.6		
55.2 64.6	64.6	77.6	77.6	90.0		
64.6 77.6	64.6	77.6	64.6	90.0		
64.6 77.6	77.6	90.0	77.6	90.0		
77.6 90.0	77.6	90.0	77.6	90.0		
77.6 90.0	90.0					
.0 180.0	0.0	180.0	0.0	60.0		
60.0 120.0	120.0	180.0	0.0	60.0		
60.0 120.0	120.0	180.0	0.0	45.0		
45.0 90.0	90.0	135.0	135.0	180.0		
.0 45.0	45.0	90.0	90.0	135.0		
135.0 180.0	0.0	30.0	30.0	60.0		
60.0 90.0	90.0	120.0	120.0	150.0		
150.0 180.0	0.0	30.0	30.0	60.0		
60.0 90.0	90.0	120.0	120.0	150.0		
150.0 180.0						

TABLE 14.  
DIFFERENTIAL INCIDENT DCSE RATE RESULTS

X	Y	THETA	PHI	DIFF.DCRAIN
.00	5.00	7.70	90.00	0.00000000
.00	5.00	18.60	90.00	0.00000000
.00	5.00	28.30	30.00	0.00000000
.00	5.00	28.30	90.00	0.00000000
.00	5.00	28.30	150.00	0.00000000
.00	5.00	39.60	30.00	0.00000000
.00	5.00	39.60	90.00	0.00000000
.00	5.00	39.60	150.00	0.00000000
.00	5.00	49.80	22.50	0.00000000
.00	5.00	49.80	112.50	0.00000000
.00	5.00	49.80	157.50	.00082519
.00	5.00	59.90	22.50	0.00000000
.00	5.00	59.90	67.50	0.00000000
.00	5.00	59.90	112.50	0.00000000
.00	5.00	59.90	157.50	.00311931
.00	5.00	71.10	15.00	0.00000000
.00	5.00	71.10	45.00	0.00000000
.00	5.00	71.10	75.00	0.00000000
.00	5.00	71.10	105.00	0.00000000
.00	5.00	71.10	135.00	0.00000000
.00	5.00	71.10	165.00	.00272201
.00	5.00	83.80	15.00	0.00000000
.00	5.00	83.80	45.00	0.00000000
.00	5.00	83.80	75.00	0.00000000
.00	5.00	83.80	105.00	0.00000000
.00	5.00	83.80	135.00	0.00000000
.00	5.00	83.80	165.00	0.00000000
.00	5.00	83.80	270.00	0.00000000
.00	5.00	18.60	270.00	0.00000000
.00	5.00	28.30	270.00	0.00000000
.00	5.00	28.30	330.00	0.00000000
.00	5.00	39.60	210.00	0.00000000
.00	5.00	39.60	270.00	0.00000000
.00	5.00	39.60	330.00	0.00000000
.00	5.00	49.80	202.50	.00082519
.00	5.00	49.80	247.50	0.00000000
.00	5.00	49.80	292.50	0.00000000
.00	5.00	49.80	337.50	0.00000000
.00	5.00	59.90	202.50	.00311931
.00	5.00	59.90	247.50	0.00000000
.00	5.00	59.90	292.50	0.00000000
.00	5.00	59.90	337.50	0.00000000
.00	5.00	71.10	195.00	.00272201
.00	5.00	71.10	225.00	0.00000000
.00	5.00	71.10	255.00	0.00000000
.00	5.00	71.10	285.00	0.00000000
.00	5.00	71.10	315.00	0.00000000
.00	5.00	71.10	345.00	0.00000000
.00	5.00	83.80	195.00	0.00000000
.00	5.00	83.80	225.00	0.00000000
.00	5.00	83.80	255.00	0.00000000
.00	5.00	83.80	285.00	0.00000000
.00	5.00	83.80	315.00	0.00000000
.00	5.00	83.80	345.00	0.00000000

SUM OF DIFFERENTIAL DCSE RATES = .01333303

TABLE 14 CONT.  
DIFFERENTIAL INCIDENT DOSE RATE RESULTS

X	Y	THETA	PHI	DIFF.DCRAIN
.00	10.00	7.70	90.00	0.00000000
.00	10.00	18.60	90.00	0.00000000
.00	10.00	28.30	30.00	0.00000000
.00	10.00	28.30	90.00	0.00000000
.00	10.00	28.30	150.00	0.00000000
.00	10.00	39.60	30.00	0.00000000
.00	10.00	39.60	90.00	0.00000000
.00	10.00	39.60	150.00	0.00000000
.00	10.00	49.80	22.50	0.00000000
.00	10.00	49.80	67.50	0.00000000
.00	10.00	49.80	112.50	0.00000000
.00	10.00	49.80	157.50	0.00000000
.00	10.00	59.90	22.50	0.00000000
.00	10.00	59.90	67.50	0.00000000
.00	10.00	59.90	112.50	0.00000000
.00	10.00	59.90	157.50	0.00000000
.00	10.00	71.10	15.00	0.00000000
.00	10.00	71.10	45.00	0.00000000
.00	10.00	71.10	75.00	0.00000000
.00	10.00	71.10	105.00	0.00000000
.00	10.00	71.10	135.00	0.00000000
.00	10.00	71.10	165.00	.00292936
.00	10.00	83.80	15.00	0.00000000
.00	10.00	83.80	45.00	0.00000000
.00	10.00	83.80	75.00	0.00000000
.00	10.00	83.80	105.00	0.00000000
.00	10.00	83.80	135.00	0.00000000
.00	10.00	83.80	165.00	.00108949
.00	10.00	7.70	270.00	0.00000000
.00	10.00	18.60	270.00	0.00000000
.00	10.00	28.30	210.00	0.00000000
.00	10.00	28.30	270.00	0.00000000
.00	10.00	28.30	330.00	0.00000000
.00	10.00	39.60	210.00	0.00000000
.00	10.00	39.60	270.00	0.00000000
.00	10.00	39.60	330.00	0.00000000
.00	10.00	49.80	202.50	0.00000000
.00	10.00	49.80	247.50	0.00000000
.00	10.00	49.80	292.50	0.00000000
.00	10.00	49.80	337.50	0.00000000
.00	10.00	59.90	202.50	0.00000000
.00	10.00	59.90	247.50	0.00000000
.00	10.00	59.90	292.50	0.00000000
.00	10.00	59.90	337.50	0.00000000
.00	10.00	71.10	195.00	.00292936
.00	10.00	71.10	225.00	0.00000000
.00	10.00	71.10	255.00	0.00000000
.00	10.00	71.10	285.00	0.00000000
.00	10.00	71.10	315.00	0.00000000
.00	10.00	71.10	345.00	0.00000000
.00	10.00	83.80	195.00	.00108949
.00	10.00	83.80	225.00	0.00000000
.00	10.00	83.80	255.00	0.00000000
.00	10.00	83.80	285.00	0.00000000
.00	10.00	83.80	315.00	0.00000000
.00	10.00	83.80	345.00	0.00000000

SUM OF DIFFERENTIAL DOSE RATES = .00803773

TABLE 14 CONT.  
DIFFERENTIAL INCIDENT DOSE RATE RESULTS

X	Y	THETA	PHI	DIFF.DORAIN
.00	15.00	7.70	90.00	0.00000000
.00	15.00	18.60	90.00	0.00000000
.00	15.00	28.30	30.00	0.00000000
.00	15.00	28.30	90.00	0.00000000
.00	15.00	28.30	150.00	0.00000000
.00	15.00	39.60	30.00	0.00000000
.00	15.00	39.60	90.00	0.00000000
.00	15.00	39.60	150.00	0.00000000
.00	15.00	49.80	22.50	0.00000000
.00	15.00	49.80	67.50	0.00000000
.00	15.00	49.80	112.50	0.00000000
.00	15.00	49.80	157.50	0.00000000
.00	15.00	59.90	22.50	0.00000000
.00	15.00	59.90	67.50	0.00000000
.00	15.00	59.90	112.50	0.00000000
.00	15.00	59.90	157.50	0.00000000
.00	15.00	71.10	15.00	0.00000000
.00	15.00	71.10	45.00	0.00000000
.00	15.00	71.10	75.00	0.00000000
.00	15.00	71.10	105.00	0.00000000
.00	15.00	71.10	135.00	0.00000000
.00	15.00	71.10	165.00	.00063981
.00	15.00	83.80	15.00	0.00000000
.00	15.00	83.80	45.00	0.00000000
.00	15.00	83.80	75.00	0.00000000
.00	15.00	83.80	105.00	0.00000000
.00	15.00	83.80	135.00	0.00000000
.00	15.00	83.80	165.00	.00213256
.00	15.00	7.70	270.00	0.00000000
.00	15.00	18.60	270.00	0.00000000
.00	15.00	28.30	210.00	0.00000000
.00	15.00	28.30	270.00	0.00000000
.00	15.00	28.30	330.00	0.00000000
.00	15.00	39.60	210.00	0.00000000
.00	15.00	39.60	270.00	0.00000000
.00	15.00	39.60	330.00	0.00000000
.00	15.00	49.80	202.50	0.00000000
.00	15.00	49.80	247.50	0.00000000
.00	15.00	49.80	292.50	0.00000000
.00	15.00	49.80	337.50	0.00000000
.00	15.00	59.90	202.50	0.00000000
.00	15.00	59.90	247.50	0.00000000
.00	15.00	59.90	292.50	0.00000000
.00	15.00	59.90	337.50	0.00000000
.00	15.00	71.10	195.00	.00063981
.00	15.00	71.10	225.00	0.00000000
.00	15.00	71.10	255.00	0.00000000
.00	15.00	71.10	285.00	0.00000000
.00	15.00	71.10	315.00	0.00000000
.00	15.00	71.10	345.00	0.00000000
.00	15.00	83.80	195.00	.00213256
.00	15.00	83.80	225.00	0.00000000
.00	15.00	83.80	255.00	0.00000000
.00	15.00	83.80	285.00	0.00000000
.00	15.00	83.80	315.00	0.00000000
.00	15.00	83.80	345.00	0.00000000

SUM OF DIFFERENTIAL DOSE RATES = .00554476

TABLE 14 CONT.  
DIFFERENTIAL INCIDENT DOSE RATE RESULTS

X	Y	THETA	PHI	DIFF.DCRAIN
3.00	5.00	7.70	90.00	0.000000000
3.00	5.00	18.60	90.00	0.000000000
3.00	5.00	28.30	30.00	0.000000000
3.00	5.00	28.30	90.00	0.000000000
3.00	5.00	28.30	150.00	0.000000000
3.00	5.00	39.60	30.00	0.000000000
3.00	5.00	39.60	90.00	0.000000000
3.00	5.00	39.60	150.00	0.000000000
3.00	5.00	49.80	22.50	0.000000000
3.00	5.00	49.80	67.50	0.000000000
3.00	5.00	49.80	112.50	0.000000000
3.00	5.00	49.80	157.50	0.000000000
3.00	5.00	59.90	22.50	0.000000000
3.00	5.00	59.90	67.50	0.000000000
3.00	5.00	59.90	112.50	0.000000000
3.00	5.00	59.90	157.50	0.000000000
3.00	5.00	71.10	15.00	0.000000000
3.00	5.00	71.10	45.00	0.000000000
3.00	5.00	71.10	75.00	0.000000000
3.00	5.00	71.10	105.00	0.000000000
3.00	5.00	71.10	135.00	0.000000000
3.00	5.00	71.10	165.00	0.000000000
3.00	5.00	83.80	15.00	0.000000000
3.00	5.00	83.80	45.00	0.000000000
3.00	5.00	83.80	75.00	0.000000000
3.00	5.00	83.80	105.00	0.000000000
3.00	5.00	83.80	135.00	0.000000000
3.00	5.00	83.80	165.00	0.000000000
3.00	5.00	7.70	270.00	0.000000000
3.00	5.00	18.60	270.00	0.000000000
3.00	5.00	28.30	210.00	0.000000000
3.00	5.00	28.30	270.00	0.000000000
3.00	5.00	28.30	330.00	0.000000000
3.00	5.00	39.60	210.00	0.000000000
3.00	5.00	39.60	270.00	0.000000000
3.00	5.00	39.60	330.00	0.000000000
3.00	5.00	49.80	202.50	0.00001220
3.00	5.00	49.80	247.50	0.000000000
3.00	5.00	49.80	292.50	0.000000000
3.00	5.00	49.80	337.50	0.000000000
3.00	5.00	59.90	202.50	0.00478928
3.00	5.00	59.90	247.50	0.000000000
3.00	5.00	59.90	292.50	0.000000000
3.00	5.00	59.90	337.50	0.000000000
3.00	5.00	71.10	195.00	0.00273512
3.00	5.00	71.10	225.00	0.00328693
3.00	5.00	71.10	255.00	0.000000000
3.00	5.00	71.10	285.00	0.000000000
3.00	5.00	71.10	315.00	0.000000000
3.00	5.00	71.10	345.00	0.000000000
3.00	5.00	83.80	195.00	0.000000000
3.00	5.00	83.80	225.00	0.000000000
3.00	5.00	83.80	255.00	0.000000000
3.00	5.00	83.80	285.00	0.000000000
3.00	5.00	83.80	315.00	0.000000000
3.00	5.00	83.80	345.00	0.000000000

SUM OF DIFFERENTIAL DOSE RATES = .01082353

TABLE 14 CONT.  
DIFFERENTIAL INCIDENT DOSE RATE RESULTS

X	Y	THETA	PHI	DIFF.DCRAIN
3.00	10.00	7.70	90.00	0.00000000
3.00	10.00	18.60	90.00	0.00000000
3.00	10.00	28.30	30.00	0.00000000
3.00	10.00	28.30	90.00	0.00000000
3.00	10.00	28.30	150.00	0.00000000
3.00	10.00	39.60	30.00	0.00000000
3.00	10.00	39.60	90.00	0.00000000
3.00	10.00	39.60	150.00	0.00000000
3.00	10.00	49.80	22.50	0.00000000
3.00	10.00	49.80	67.50	0.00000000
3.00	10.00	49.80	112.50	0.00000000
3.00	10.00	49.80	157.50	0.00000000
3.00	10.00	59.90	22.50	0.00000000
3.00	10.00	59.90	67.50	0.00000000
3.00	10.00	59.90	112.50	0.00000000
3.00	10.00	59.90	157.50	0.00000000
3.00	10.00	71.10	15.00	0.00000000
3.00	10.00	71.10	45.00	0.00000000
3.00	10.00	71.10	75.00	0.00000000
3.00	10.00	71.10	105.00	0.00000000
3.00	10.00	71.10	135.00	0.00000000
3.00	10.00	71.10	165.00	0.00000000
3.00	10.00	83.80	15.00	0.00000000
3.00	10.00	83.80	45.00	0.00000000
3.00	10.00	83.80	75.00	0.00000000
3.00	10.00	83.80	105.00	0.00000000
3.00	10.00	83.80	135.00	0.00000000
3.00	10.00	83.80	165.00	0.00000000
3.00	10.00	7.70	270.00	0.00000000
3.00	10.00	18.60	270.00	0.00000000
3.00	10.00	28.30	210.00	0.00000000
3.00	10.00	28.30	270.00	0.00000000
3.00	10.00	28.30	330.00	0.00000000
3.00	10.00	39.60	210.00	0.00000000
3.00	10.00	39.60	270.00	0.00000000
3.00	10.00	39.60	330.00	0.00000000
3.00	10.00	49.80	202.50	0.00000000
3.00	10.00	49.80	247.50	0.00000000
3.00	10.00	49.80	292.50	0.00000000
3.00	10.00	49.80	337.50	0.00000000
3.00	10.00	59.90	202.50	0.00000000
3.00	10.00	59.90	247.50	0.00000000
3.00	10.00	59.90	292.50	0.00000000
3.00	10.00	59.90	337.50	0.00000000
3.00	10.00	71.10	195.00	.00509215
3.00	10.00	71.10	225.00	0.00000000
3.00	10.00	71.10	255.00	0.00000000
3.00	10.00	71.10	285.00	0.00000000
3.00	10.00	71.10	315.00	0.00000000
3.00	10.00	71.10	345.00	0.00000000
3.00	10.00	83.80	195.00	.00236443
3.00	10.00	83.80	225.00	0.00000000
3.00	10.00	83.80	255.00	0.00000000
3.00	10.00	83.80	285.00	0.00000000
3.00	10.00	83.80	315.00	0.00000000
3.00	10.00	83.80	345.00	0.00000000

SUM OF DIFFERENTIAL DOSE RATES = .00745659

TABLE 14 CONT.  
DIFFERENTIAL INCIDENT DOSE RATE RESULTS

X	Y	THETA	PHI	DIFF.DOCRIN
3.00	15.00	7.70	90.00	0.00000000
3.00	15.00	18.60	90.00	0.00000000
3.00	15.00	28.30	30.00	0.00000000
3.00	15.00	28.30	90.00	0.00000000
3.00	15.00	28.30	150.00	0.00000000
3.00	15.00	39.60	30.00	0.00000000
3.00	15.00	39.60	90.00	0.00000000
3.00	15.00	39.60	150.00	0.00000000
3.00	15.00	49.80	22.50	0.00000000
3.00	15.00	49.80	67.50	0.00000000
3.00	15.00	49.80	112.50	0.00000000
3.00	15.00	49.80	157.50	0.00000000
3.00	15.00	59.90	22.50	0.00000000
3.00	15.00	59.90	67.50	0.00000000
3.00	15.00	59.90	112.50	0.00000000
3.00	15.00	59.90	157.50	0.00000000
3.00	15.00	71.10	15.00	0.00000000
3.00	15.00	71.10	45.00	0.00000000
3.00	15.00	71.10	75.00	0.00000000
3.00	15.00	71.10	105.00	0.00000000
3.00	15.00	71.10	135.00	0.00000000
3.00	15.00	71.10	165.00	0.00000000
3.00	15.00	83.80	15.00	0.00000000
3.00	15.00	83.80	45.00	0.00000000
3.00	15.00	83.80	75.00	0.00000000
3.00	15.00	83.80	105.00	0.00000000
3.00	15.00	83.80	135.00	0.00000000
3.00	15.00	83.80	165.00	0.00000000
3.00	15.00	7.70	270.00	0.00000000
3.00	15.00	18.60	270.00	0.00000000
3.00	15.00	28.30	210.00	0.00000000
3.00	15.00	28.30	270.00	0.00000000
3.00	15.00	28.30	330.00	0.00000000
3.00	15.00	39.60	210.00	0.00000000
3.00	15.00	39.60	270.00	0.00000000
3.00	15.00	39.60	330.00	0.00000000
3.00	15.00	49.80	202.50	0.00000000
3.00	15.00	49.80	247.50	0.00000000
3.00	15.00	49.80	292.50	0.00000000
3.00	15.00	49.80	337.50	0.00000000
3.00	15.00	59.90	202.50	0.00000000
3.00	15.00	59.90	247.50	0.00000000
3.00	15.00	59.90	292.50	0.00000000
3.00	15.00	59.90	337.50	0.00000000
3.00	15.00	71.10	195.00	0.0111612
3.00	15.00	71.10	225.00	0.00000000
3.00	15.00	71.10	255.00	0.00000000
3.00	15.00	71.10	285.00	0.00000000
3.00	15.00	71.10	315.00	0.00000000
3.00	15.00	71.10	345.00	0.00000000
3.00	15.00	83.80	195.00	0.00421480
3.00	15.00	83.80	225.00	0.00000000
3.00	15.00	83.80	255.00	0.00000000
3.00	15.00	83.80	285.00	0.00000000
3.00	15.00	83.80	315.00	0.00000000
3.00	15.00	83.80	345.00	0.00000000

SUM OF DIFFERENTIAL DOSE RATES = .00533093



TABLE 14 CONT.  
DIFFERENTIAL INCIDENT DOSE RATE RESULTS

X	Y	THETA	PHI	DIFF.DCRAIN
6.00	5.00	7.70	90.00	0.00000000
6.00	5.00	18.60	90.00	0.00000000
6.00	5.00	28.30	30.00	0.00000000
6.00	5.00	28.30	90.00	0.00000000
6.00	5.00	28.30	150.00	0.00000000
6.00	5.00	39.60	30.00	0.00000000
6.00	5.00	39.60	90.00	0.00000000
6.00	5.00	39.60	150.00	0.00000000
6.00	5.00	49.80	22.50	0.00000000
6.00	5.00	49.80	67.50	0.00000000
6.00	5.00	49.80	112.50	0.00000000
6.00	5.00	49.80	157.50	0.00000000
6.00	5.00	59.90	22.50	0.00000000
6.00	5.00	59.90	67.50	0.00000000
6.00	5.00	59.90	112.50	0.00000000
6.00	5.00	59.90	157.50	0.00000000
6.00	5.00	71.10	15.00	0.00000000
6.00	5.00	71.10	45.00	0.00000000
6.00	5.00	71.10	75.00	0.00000000
6.00	5.00	71.10	105.00	0.00000000
6.00	5.00	71.10	135.00	0.00000000
6.00	5.00	71.10	165.00	0.00000000
6.00	5.00	83.80	15.00	0.00000000
6.00	5.00	83.80	45.00	0.00000000
6.00	5.00	83.80	75.00	0.00000000
6.00	5.00	83.80	105.00	0.00000000
6.00	5.00	83.80	135.00	0.00000000
6.00	5.00	83.80	165.00	0.00000000
6.00	5.00	83.80	270.00	0.00000000
6.00	5.00	18.60	270.00	0.00000000
6.00	5.00	28.30	210.00	0.00000000
6.00	5.00	28.30	270.00	0.00000000
6.00	5.00	28.30	330.00	0.00000000
6.00	5.00	39.60	210.00	0.00000000
6.00	5.00	39.60	270.00	0.00000000
6.00	5.00	39.60	330.00	0.00000000
6.00	5.00	49.80	202.50	0.00000000
6.00	5.00	49.80	247.50	0.00000000
6.00	5.00	49.80	292.50	0.00000000
6.00	5.00	49.80	337.50	0.00000000
6.00	5.00	59.90	202.50	.00046940
6.00	5.00	59.90	247.50	.00023564
6.00	5.00	59.90	292.50	0.00000000
6.00	5.00	59.90	337.50	0.00000000
6.00	5.00	71.10	195.00	0.00000000
6.00	5.00	71.10	235.00	.000569038
6.00	5.00	71.10	255.00	0.00000000
6.00	5.00	71.10	285.00	0.00000000
6.00	5.00	71.10	315.00	0.00000000
6.00	5.00	71.10	345.00	0.00000000
6.00	5.00	83.80	195.00	0.00000000
6.00	5.00	83.80	225.00	0.00000000
6.00	5.00	83.80	255.00	0.00000000
6.00	5.00	83.80	285.00	0.00000000
6.00	5.00	83.80	315.00	0.00000000
6.00	5.00	83.80	345.00	0.00000000

SUM OF DIFFERENTIAL DOSE RATES = .00639543

TABLE 14 CONT.  
DIFFERENTIAL INCIDENT DOSE RATE RESULTS

X	Y	THETA	PHI	DIFF.DCRAIN
6.00	10.00	7.70	90.00	0.00000000
6.00	10.00	18.60	90.00	0.00000000
6.00	10.00	28.30	30.00	0.00000000
6.00	10.00	28.30	90.00	0.00000000
6.00	10.00	28.30	150.00	0.00000000
6.00	10.00	39.60	30.00	0.00000000
6.00	10.00	39.60	90.00	0.00000000
6.00	10.00	39.60	150.00	0.00000000
6.00	10.00	49.80	22.50	0.00000000
6.00	10.00	49.80	67.50	0.00000000
6.00	10.00	49.80	112.50	0.00000000
6.00	10.00	49.80	157.50	0.00000000
6.00	10.00	59.90	22.50	0.00000000
6.00	10.00	59.90	67.50	0.00000000
6.00	10.00	59.90	112.50	0.00000000
6.00	10.00	59.90	157.50	0.00000000
6.00	10.00	71.10	15.00	0.00000000
6.00	10.00	71.10	45.00	0.00000000
6.00	10.00	71.10	75.00	0.00000000
6.00	10.00	71.10	105.00	0.00000000
6.00	10.00	71.10	135.00	0.00000000
6.00	10.00	71.10	165.00	0.00000000
6.00	10.00	83.80	15.00	0.00000000
6.00	10.00	83.80	45.00	0.00000000
6.00	10.00	83.80	75.00	0.00000000
6.00	10.00	83.80	105.00	0.00000000
6.00	10.00	83.80	135.00	0.00000000
6.00	10.00	83.80	165.00	0.00000000
6.00	10.00	7.70	270.00	0.00000000
6.00	10.00	18.60	270.00	0.00000000
6.00	10.00	28.30	210.00	0.00000000
6.00	10.00	28.30	270.00	0.00000000
6.00	10.00	28.30	330.00	0.00000000
6.00	10.00	39.60	210.00	0.00000000
6.00	10.00	39.60	270.00	0.00000000
6.00	10.00	39.60	330.00	0.00000000
6.00	10.00	49.80	202.50	0.00000000
6.00	10.00	49.80	247.50	0.00000000
6.00	10.00	49.80	292.50	0.00000000
6.00	10.00	49.80	337.50	0.00000000
6.00	10.00	59.90	247.50	0.00000000
6.00	10.00	59.90	292.50	0.00000000
6.00	10.00	59.90	337.50	0.00000000
6.00	10.00	71.10	195.00	.00173986
6.00	10.00	71.10	225.00	.00159981
6.00	10.00	71.10	255.00	0.00000000
6.00	10.00	71.10	285.00	0.00000000
6.00	10.00	71.10	315.00	0.00000000
6.00	10.00	71.10	345.00	0.00000000
6.00	10.00	83.80	195.00	.00117133
6.00	10.00	83.80	225.00	.00159927
6.00	10.00	83.80	255.00	0.00000000
6.00	10.00	83.80	285.00	0.00000000
6.00	10.00	83.80	315.00	0.00000000
6.00	10.00	83.80	345.00	0.00000000

SUM OF DIFFERENTIAL DOSE RATES = .00611028

TABLE 14 CONT.  
 DIFFERENTIAL INCIDENT DOSE RATE RESULTS

X	Y	THETA	PHI	DIFF.DCRAIN
6.00	15.00	7.70	90.00	0.00000000
6.00	15.00	18.60	90.00	0.00000000
6.00	15.00	28.30	30.00	0.00000000
6.00	15.00	28.30	90.00	0.00000000
6.00	15.00	28.30	150.00	0.00000000
6.00	15.00	39.60	30.00	0.00000000
6.00	15.00	39.60	90.00	0.00000000
6.00	15.00	39.60	150.00	0.00000000
6.00	15.00	49.80	22.50	0.00000000
6.00	15.00	49.80	67.50	0.00000000
6.00	15.00	49.80	112.50	0.00000000
6.00	15.00	49.80	157.50	0.00000000
6.00	15.00	59.90	22.50	0.00000000
6.00	15.00	59.90	67.50	0.00000000
6.00	15.00	59.90	112.50	0.00000000
6.00	15.00	59.90	157.50	0.00000000
6.00	15.00	71.10	15.00	0.00000000
6.00	15.00	71.10	45.00	0.00000000
6.00	15.00	71.10	75.00	0.00000000
6.00	15.00	71.10	105.00	0.00000000
6.00	15.00	71.10	135.00	0.00000000
6.00	15.00	71.10	165.00	0.00000000
6.00	15.00	83.80	15.00	0.00000000
6.00	15.00	83.80	45.00	0.00000000
6.00	15.00	83.80	75.00	0.00000000
6.00	15.00	83.80	105.00	0.00000000
6.00	15.00	83.80	135.00	0.00000000
6.00	15.00	83.80	165.00	0.00000000
6.00	15.00	7.70	270.00	0.00000000
6.00	15.00	18.60	270.00	0.00000000
6.00	15.00	28.30	210.00	0.00000000
6.00	15.00	28.30	270.00	0.00000000
6.00	15.00	28.30	330.00	0.00000000
6.00	15.00	39.60	210.00	0.00000000
6.00	15.00	39.60	270.00	0.00000000
6.00	15.00	39.60	330.00	0.00000000
6.00	15.00	49.80	202.50	0.00000000
6.00	15.00	49.80	247.50	0.00000000
6.00	15.00	49.80	292.50	0.00000000
6.00	15.00	49.80	337.50	0.00000000
6.00	15.00	59.90	202.50	0.00000000
6.00	15.00	59.90	247.50	0.00000000
6.00	15.00	59.90	292.50	0.00000000
6.00	15.00	59.90	337.50	0.00000000
6.00	15.00	71.10	195.00	.00067857
6.00	15.00	71.10	225.00	0.00000000
6.00	15.00	71.10	255.00	0.00000000
6.00	15.00	71.10	285.00	0.00000000
6.00	15.00	71.10	315.00	0.00000000
6.00	15.00	71.10	345.00	0.00000000
6.00	15.00	83.80	195.00	.00409056
6.00	15.00	83.80	225.00	0.00000000
6.00	15.00	83.80	255.00	0.00000000
6.00	15.00	83.80	285.00	0.00000000
6.00	15.00	83.80	315.00	0.00000000
6.00	15.00	83.80	345.00	0.00000000

SUM OF DIFFERENTIAL DOSE RATES = .00476914

## APPENDIX H

Description and Explanation of the IBM-1620  
Computer Program Used for Calculating the  
Total Incident Dose Rate at Point (x,y) on  
the Ceiling of a Blockhouse

The total dose rate incident on any point of the ceiling of a  
blockhouse is given by eq.(38),

$$D_1(x,y) = \left\{ D_0 (\phi_2 - \phi_1) / 4\pi \right\} \sum_{k=1}^{K_{\max}} \left\{ 0.1917 \left\{ E_1 \left( \sum_a (E_0) d / \cos \theta_{1k} \right) - E_1 \left( \sum_a (E_0) d / \cos \theta_{2k} \right) \right. \right. \\ \left. \left. + (a' / (1-b)) \left\{ \exp(-\sum_a (E_0) d (1-b) / \cos \theta_{1k}) - \exp(-\sum_a (E_0) d (1-b) / \cos \theta_{2k}) \right\} \right\} \right. \\ \left. + 0.0095 \left\{ \cos \theta_{1k} E_2 \left( \sum_a (E_0) d / \cos \theta_{1k} \right) - \cos \theta_{2k} E_2 \left( \sum_a (E_0) d / \cos \theta_{2k} \right) + a' \sum_a (E_0) d \right. \right. \\ \left. \left. \times \left\{ E_1 \left( \sum_a (E_0) d (1-b) / \cos \theta_{1k} \right) - E_1 \left( \sum_a (E_0) d (1-b) / \cos \theta_{2k} \right) \right\} \right\} \right\} a_k. \quad (38)$$

The FORTRAN II source program solving this equation is listed in this appendix. A logic diagram is also shown to help clarify the program. Approximately 70 seconds of computer time were required for each point on the ceiling with a  $K_{\max}$  of six. Table 15 defines the various symbols used in this computer code. Results are presented in Table 16 for a two foot square mesh on the ceiling of the KSU blockhouse.

Table 15. Input data and variables required for the  
IBM-1620 total incident dose rate computer  
program.

Symbol*	Explanation
KMAX	Degree of Gaussian Quadrature Utilized, $K_{\max}$
CHRTNO	Christoffel Numbers, $a_k$
OLEGNP	Zeros of the Legendre Polynomials, $x_k$
PHIO	Incident Azimuthal Angle (radians)
ARGT1	Argument of $E_1$ Function

Table 15 cont.

---

Symbol

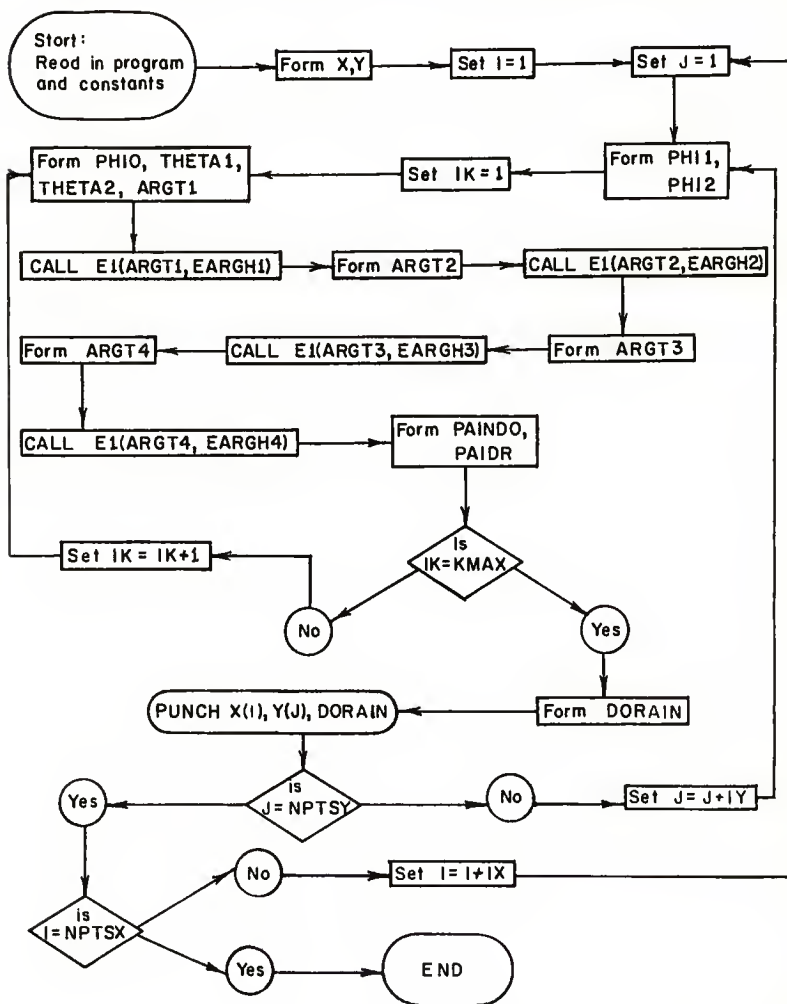
---

ARGT2	Argument of $E_1$ Function
ARGT3	Argument of $E_2$ Function
ARGT4	Argument of $E_1$ Function
EARGH1	$E_1$ (ARGT1)
EARGH2	$E_1$ (ARGT2)
EARGH3	$E_1$ (ARGT3)
EARGH4	$E_1$ (ARGT4)
DORAIN	Incident Dose Rate ( $D_o$ )

---

\*Additional utilized symbols are defined in Table 13

# LOGIC DIAGRAM FOR THE TOTAL INCIDENT DOSE RATE AT ANY POINT ON A BLOCKHOUSE CEILING



```

C      INCIDENT DOSE RATE BY J. BARAN 3/16/63
      DIMENSION X(51), Y(100), CHRTNC(10), CLEGNP(10)
      18 FORMAT (6I3)
      22 FORMAT(F11.8)
      700 FORMAT(4E18.10)
      715 FORMAT (F28.2, F18.2, F20.6)
      710 READ 700,      ACHD,BCHD,R,H,V
C      INPUT ABOVE IS 2 CARDS
      READ 18,          NPTSX, NPTSY, IX, IY, KMAX
C      INPUT ABOVE IS 1 CARD
      DC16I=1,KMAX
      READ22,CHRTNC(I)
      16 READ22,CLEGNP(I)
C      INPUT ABOVE IS 12 CARDS
      DC 14 I=1,NPTSX, IX
      14 X(I)= I-1
      DC 15 I=1,NPTSY, IY
      15 Y(I)= I
C      THESE LOOPS CALCULATE THE X AND Y CO-ORDINATES OF INTEREST
      DC 760 I=1, NPTSX, IX
      DC 720 J=1, NPTSY, IY
C      THESE LOOPS REPEAT THE ENTIRE CALCULATION FOR DIFFERENT (X,Y)
      PHI1=ATANF((X(I)-R)/Y(J)) + 3.1415927
      PHI2=ATANF((X(I)+R)/Y(J)) + 3.1415927
      PHI2M1 = PHI2 - PHI1
      PHI1P2 = PHI2 + PHI1
      PAIDR=0.
      DC 5 IK=1,KMAX
C      THIS LOOP PERFORMS THE INTEGRATION OVER INCIDENT AZIMUTHAL ANGLES
      IF (SENSE SWITCH 1) 88, 89
      88 PAUSE
      89 PHIC= (PHI2M1*CLEGNP(IK)/2.) + (PHI1P2/2.)
      THETA1=ATANF(Y(J)/((H+V)*ABSF(COSF(PHIC-3.1415927))))
      THETA2=ATANF(Y(J)/((H-V)*ABSF(COSF(PHIC-3.1415927))))
      COSTH1 = COSF(THETA1)
      COSTH2 = COSF(THETA2)
      ARG1 = 0.01825/COSTH2
      CALL E1(ARG1,EARGH1)
C      THIS ORDER TRANSFERS CONTROL TO THE E1 SUBROUTINE TO
C      CALCULATE THE EXPONENTIAL INTEGRAL OF ARG1
      ARG2 = 0.01825/COSTH1
      CALL E1(ARG2,EARGH2)
      ARG3 =-0.01825*(BCHD-1.)/COSTH2
      CALL E1(ARG3,EARGH3)
      ARG4 =-0.01825*(BCHD-1.)/COSTH1
      CALL E1(ARG4,EARGH4)
      PAINDC =0.1917*(EARGH2 - EARGH1+(ACHD*(EXPF(-ARG3)-EXPF(-ARG4))/
      1(BCHD-1.)))+ 0.0095*((COSTH1 / EXPF(ARG2)) - 0.01825*EARGH2 -
      1(COSTH2 / EXPF(ARG1)) + 0.01825*EARGH1 + ACHD * 0.01825
      1*(EARGH4 - EARGH3))
      5 PAIDR = PAIDR +(PAINDC*CHRTNC(IK))
      DRAIN = PAIDR * PHI2M1 / 12.566371

```

```

720 PUNCH 715, X(I), Y(J), DCRAIN
760 CONTINUE
GC TC 710
END

```

## INPUT DATA

89.562-2	62.518-3	1.85+0	2.88+0
1.08+0			
11 20 2 2 6			
.46791393			
.23861919			
.36076157			
.66120939			
.17132449			
.93246951			
.17132449			
- .93246951			
.36076157			
- .66120939			
.46791393			
- .23861919			



TABLE 16.  
TOTAL INCIDENT DOSE RATE RESULTS

X	Y	DCRAIN
.00	1.00	.010579
.00	3.00	.015834
.00	5.00	.013459
.00	7.00	.010895
.00	9.00	.008961
.00	11.00	.007544
.00	13.00	.006484
.00	15.00	.005670
.00	17.00	.005028
.00	19.00	.004510
2.00	1.00	.007898
2.00	3.00	.013270
2.00	5.00	.012152
2.00	7.00	.010227
2.00	9.00	.008592
2.00	11.00	.007323
2.00	13.00	.006343
2.00	15.00	.005575
2.00	17.00	.004961
2.00	19.00	.004462
4.00	1.00	.004043
4.00	3.00	.008645
4.00	5.00	.009330
4.00	7.00	.008617
4.00	9.00	.007640
4.00	11.00	.006730
4.00	13.00	.005954
4.00	15.00	.005308
4.00	17.00	.004771
4.00	19.00	.004323
6.00	1.00	.002148
6.00	3.00	.005333
6.00	5.00	.006653
6.00	7.00	.006796
6.00	9.00	.006438
6.00	11.00	.005924
6.00	13.00	.005399
6.00	15.00	.004915
6.00	17.00	.004485
6.00	19.00	.004108
8.00	1.00	.001285
8.00	3.00	.003436
8.00	5.00	.004712
8.00	7.00	.005224
8.00	9.00	.005264
8.00	11.00	.005068
8.00	13.00	.004773
8.00	15.00	.004451
8.00	17.00	.004136
8.00	19.00	.003841
10.00	1.00	.000845
10.00	3.00	.002348
10.00	5.00	.003414
10.00	7.00	.004014
10.00	9.00	.004256
10.00	11.00	.004268
10.00	13.00	.004150
10.00	15.00	.003968
10.00	17.00	.003758
10.00	19.00	.003543

## APPENDIX J

Description and Explanation of the IBM-1620  
Computer Program Used for Calculating the  
Differential Reflected Dose Rate at Point  
(x,y) on the Ceiling of a Blockhouse

The differential reflected dose rate at any point on the ceiling  
is given by expression (44),

$$\begin{aligned} & \left\{ 1.293(\Phi_2 - \Phi_1) D_0 / 8\pi \right\} \sum_{k=1}^{K_{\max}} a_k (\omega_{1k} - \omega_{2k}) \sum_{j=1}^{K_{\max}} a_j (0.1917 + 0.0095 \omega_{oj}) \\ & \times \left\{ 1 + (a' \sum_a (E_o) d \exp(b \sum_a (E_o) d / \omega_{oj})) / \omega_{oj} \right\} \exp \left\{ - \sum_a (E_o) d / \omega_{oj} \right\} \\ & \times \left\{ CK(\Theta_s) + C' \right\} (\omega_{oj} + \cos \Theta)^{-1} \Delta \Omega. \end{aligned} \quad (44)$$

The FORTRAN II source program which solves eq.(44) is listed in this appendix. A logic diagram for this program is also presented in this appendix.

The IBM-1620 computer required approximately 75 seconds to calculate the dose rate reflected into each of the solid angles with a  $K_{\max}$  of six. The total computer time required for the 56 solid angles per ceiling point and the nine ceiling points considered was  $10\frac{1}{2}$  hours. These results are tabulated as Table 18.

The alphanumeric characters utilized in this program are defined in Table 17.

Table 17. Input data and variables required for the IBM-1620 differential reflected dose rate computer program.

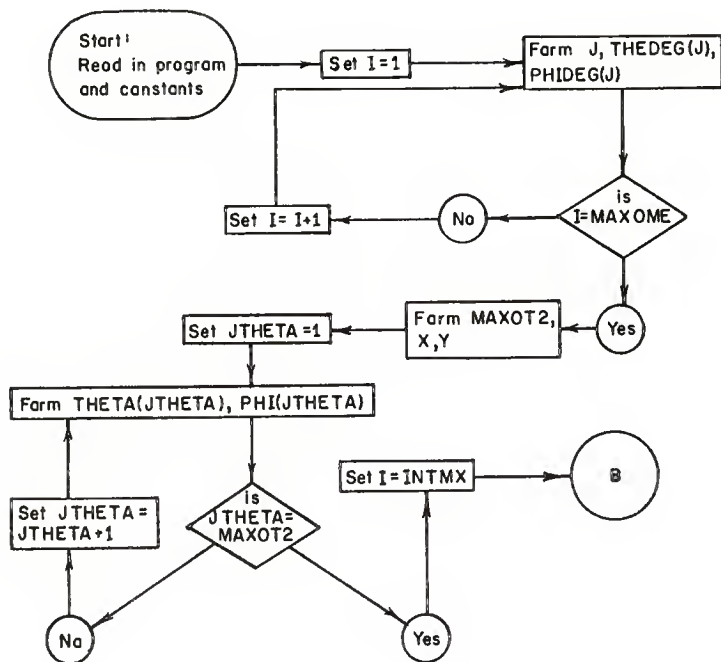
Symbol*	Explanation
KMAX	Degree of Gaussian Quadrature Utilized, $K_{\max}$
CHRTNO	Christoffel Numbers, $a_k$

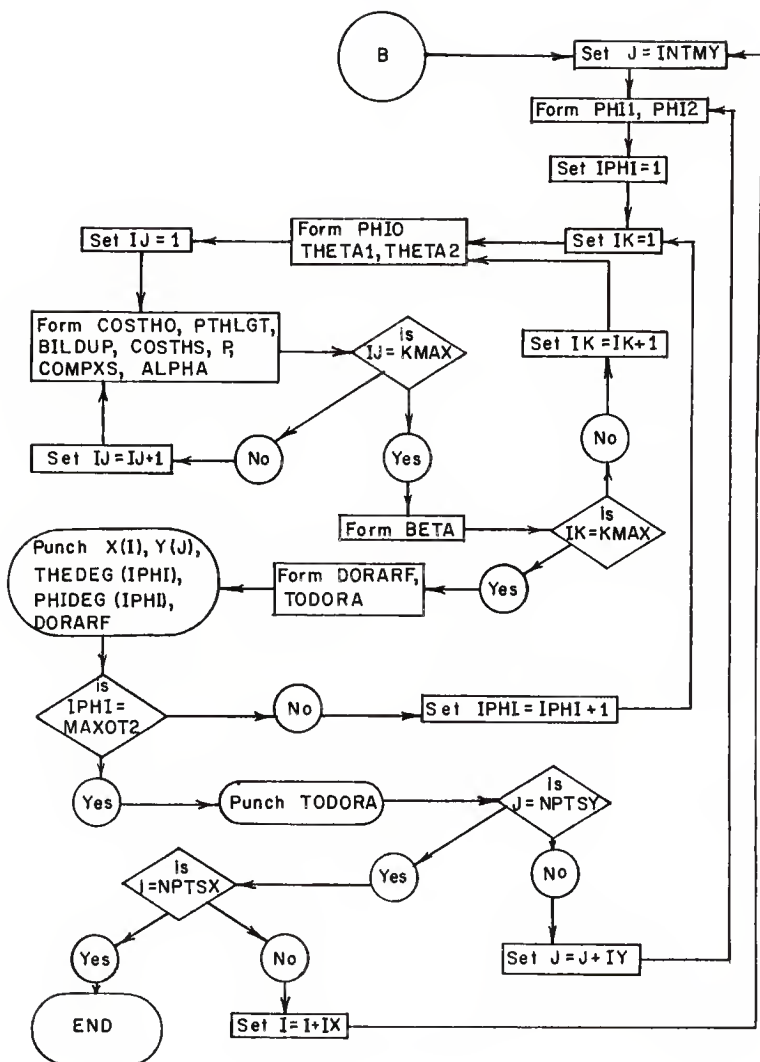
Table 17 cont.

Symbol*	Explanation
OLEGNP	Zeroes of the Legendre Polynomials, $x_k$
MAXOT2	Total Number of Solid Angles Calculated About a Point on the Ceiling
IK	Fixed Point Incident Azimuthal Angle Integration Variable
PHIO	Incident Azimuthal Angle, $\Phi$
IJ	Fixed Point Incident Polar Angle Integration Variable
COSTHO	Cosine of the Incident Polar Angle, $\cos\Theta$
DORARF	Dose Rate Reflected into a Given Solid Angle ( $D_o$ )

\*Additional utilized symbols are defined in Table 8 and Table 13

LOGIC DIAGRAM FOR THE DIFFERENTIAL REFLECTED DOSE  
RATE AT ANY POINT ON A BLOCKHOUSE CEILING





```

C      DIFFERENTIAL REFLECTED DOSE RATE, 3/28/63 BY J.A. BARAN
      DIMENSION THEDEG(99),PHIDEG(99),X(101), Y(200), THETA(99),
      1PHI(99), SIN THE(99),COS THE(99), CLEGNP(10),CHRTNC(10)
      10 FORMAT (F6.3)
      18 FORMAT (20I3)
      19 FORMAT (2F7.2)
      20 FORMAT (F12.9,F13.10)
      22 FORMAT(F11.8)
      700 FORMAT(4E18.10)
      710 FORMAT(/,48H SUM OF DIFFERENTIAL DOSE RATES = F10.
      18,/)
      714 FORMAT (60H X Y THETA PHI DIFF.DO
      1RARF ,/)
      715 FORMAT (10H F6.2, F9.2, F10.2, F10.2, F13.8)
      30 READ 10, EC
C      INPUT ABOVE IS 1 CARD
      READ 20, C, CPRIME
C      INPUT ABOVE IS 1 CARD
      READ 700, ACHD,BCHD,R,H,V,XMAX, YMAX
C      INPUT ABOVE IS 2 CARDS
      READ 18, KMAX, NPTSX, NPTSY, INTMX, INTMY,IX,IY, MAXCME
C      INPUT ABOVE IS 1 CARD
      DC16I=1,KMAX
      READ22,CHRTNC(I)
      16 READ22,CLEGNP(I)
C      INPUT ABOVE IS 12 CARDS
      DC 21 I=1,MAXCME
      J = MAXCME + I
      READ 19, THEDEG(I), PHIDEG(I)
      THEDEG(J) = THEDEG(I)
      21 PHIDEG(J) = 180. + PHIDEG(I)
C      THIS LOOP CONVERTS THE SOLID ANGLE LIMITS TO RADIAN AND UTILIZES
C      SYMMETRY TO EXPAND THE SOLID ANGLES TO COVER THE HEMISPHERE
      MAXCT2 = MAXCME * 2
      DC 14 I=INTMX, NPTSX, IX
      14 X(I)= I-1
      DC 15 I=INTMY, NPTSY, IY
      15 Y(I) = I
C      THESE LOOPS CALCULATE THE X AND Y CO-ORDINATES OF INTEREST
      DC 76JTHETA=1,MAXCT2
      THETA(JTHETA) = THEDEG(JTHETA)/57.295779
      SIN THE(JTHETA)=SINF(THETA(JTHETA))
      COS THE(JTHETA)=COSF(THETA(JTHETA))
      76 PHI(JTHETA) = PHIDEG(JTHETA)/57.295779
      DC 760 I=INTMX, NPTSX, IX
      DC 720 J=INTMY, NPTSY, IY
C      THESE LOOPS REPEAT THE ENTIRE CALCULATION FOR DIFFERENT (X,Y,
C      WHERE THE DIFFERENTIAL REFLECTED DOSE RATES ARE CALCULATED
      IF (SENSE SWITCH 1) 86, 87
      86 PAUSE
      87 PHI1=ATANF((X(I)-R)/Y(J)) + 3.1415927
      PHI2=ATANF((X(I)+R)/Y(J)) + 3.1415927

```

```

PHI1P2 = PHI1 + PHI2
PHI2M1 = PHI2 - PHI1
TDCORA = 0.
PUNCH 714
DO 65 IPHI = 1, MAXOME
DO 65 IPHI = 1, MAXOT2
C THIS LOOP REPEATS THE CALCULATIONS FOR EACH SOLID ANGLE
  BETA = 0.
  DO 5 IK=1,KMAX
C THIS LOOP PERFORMS THE INTEGRATION OVER INCIDENT AZIMUTHAL ANGLES
  IF (SENSE SWITCH 1) 88, 89
88 PAUSE
89 ALPHA = 0.
  PHIC= (PHI2M1*CLEGNP(IK)/2.) + (PHI1P2/2.)
  THETA1=ATANF(Y(J)/((H+V)*ABSF(COSF(PHIC-3.1415927))))
  THETA2=ATANF(Y(J)/((H-V)*ABSF(COSF(PHIC-3.1415927))))
  CT1PT2 = COSF(THETA1)+COSF(THETA2)
  CT2MT1 = COSF(THETA2)-COSF(THETA1)
  DO 4 IJ=1,KMAX
C THIS LOOP PERFORMS THE INTEGRATION OVER INCIDENT POLAR ANGLES
  COSTHC=((CT2MT1)*CLEGNP(IJ)/2.)+(CT1PT2*0.5)
  SINHC = SQRTF(1.-COSTHC*COSTHC)
  PTHLGT=0.01825/COSTHC
  BILDUP=1.+ACHD*PTHLGT*EXPF(BCHD*PTHLGT)
  COSTHS = (SINHC*COSF(PHI(IPHI)-PHIC+3.1415927)*SINTHE(IPHI))
  1 - (COSTHC*COSTHE(IPHI))
  P=1./((1.+(EC*(1.-COSTHS)/0.511))
  COMPS=(3.970562)*(P**2)*(1.+(P**2)-P*(1.-(COSTHS**2)))
  ALPHA1 = (0.1917+0.0095*COSTHC)*(C*COMPS+CPRIME)*CHRTNC(IJ)
  1* BILDUP / (EXPF( PTHLGT )*(COSTHC + COSTHE(IPHI)))
  4 ALPHA = ALPHA + ALPHA1
  BETAC=-CT2MT1* ALPHA * CHRTNC(IK)
  5 BETA= BETAC+BETA
  DCRARF = BETA * 5.7723214E-3* PHI2M1
  TDCORA = DCRARF + TDCORA
65 PUNCH 715,X(I),Y(J), THEDEG(IPHI), PHIDEG(IPHI), DOANDI
65 PUNCH 715,X(I),Y(J), THEDEG(IPHI), PHIDEG(IPHI), DCRARF
  PUNCH 710, TDCORA
720 CONTINUE
760 CONTINUE
GO TO 30
END

```

## INPUT DATA

1.252

.064501061 0.0089294690

89.562-2

62.518-3

1.85+0

2.88+0

1.08+0

10.0+0

20.0+0

6 7 15 1 5 3 5 28

.46791393

.23861919

.36076157

.66120939

.17132449

.93246951

.17132449

- .93246951

.36076157

- .66120939

.46791393

- .23861919

7.70 90.00

18.60 90.00

28.30 30.00

28.30 90.00

28.30 150.00

39.60 30.00

39.60 90.00

39.60 150.00

49.80 22.50

49.80 67.50

49.80 112.50

49.80 157.50

59.90 22.50

59.90 67.50

59.90 112.50

59.90 157.50

71.10 15.00

71.10 45.00

71.10 75.00

71.10 105.00

71.10 135.00

71.10 165.00

83.80 15.00

83.80 45.00

83.80 75.00

83.80 105.00

83.80 135.00

83.80 165.00



TABLE 18.  
DIFFERENTIAL REFLECTED DOSE RATE RESULTS

X	Y	THETA	PHI	DIFF.DCRARF
.00	5.00	7.70	90.00	.00001205
.00	5.00	18.60	90.00	.00001255
.00	5.00	28.30	30.00	.00001662
.00	5.00	28.30	90.00	.00001339
.00	5.00	28.30	150.00	.00001168
.00	5.00	39.60	30.00	.00002135
.00	5.00	39.60	90.00	.00001499
.00	5.00	39.60	150.00	.00001246
.00	5.00	49.80	22.50	.00003067
.00	5.00	49.80	67.50	.00002052
.00	5.00	49.80	112.50	.00001530
.00	5.00	49.80	157.50	.00001359
.00	5.00	59.90	22.50	.00004689
.00	5.00	59.90	67.50	.00002604
.00	5.00	59.90	112.50	.00001785
.00	5.00	59.90	157.50	.00001557
.00	5.00	71.10	15.00	.00009413
.00	5.00	71.10	45.00	.00005615
.00	5.00	71.10	75.00	.00003249
.00	5.00	71.10	105.00	.00002364
.00	5.00	71.10	135.00	.00002026
.00	5.00	71.10	165.00	.00001903
.00	5.00	83.80	15.00	.00022883
.00	5.00	83.80	45.00	.00011012
.00	5.00	83.80	75.00	.00005166
.00	5.00	83.80	105.00	.00003446
.00	5.00	83.80	135.00	.00002874
.00	5.00	83.80	165.00	.00002677
.00	5.00	7.70	270.00	.00001205
.00	5.00	18.60	270.00	.00001255
.00	5.00	28.30	210.00	.00001168
.00	5.00	28.30	270.00	.00001339
.00	5.00	28.30	330.00	.00001662
.00	5.00	39.60	210.00	.00001246
.00	5.00	39.60	270.00	.00001499
.00	5.00	39.60	330.00	.00002135
.00	5.00	49.80	202.50	.00001359
.00	5.00	49.80	247.50	.00001530
.00	5.00	49.80	292.50	.00002052
.00	5.00	49.80	337.50	.00003067
.00	5.00	59.90	202.50	.00001557
.00	5.00	59.90	247.50	.00001785
.00	5.00	59.90	292.50	.00002604
.00	5.00	59.90	337.50	.00004689
.00	5.00	71.10	195.00	.00001903
.00	5.00	71.10	225.00	.00002026
.00	5.00	71.10	255.00	.00002364
.00	5.00	71.10	285.00	.00003249
.00	5.00	71.10	315.00	.00005615
.00	5.00	71.10	345.00	.00009413
.00	5.00	83.80	195.00	.00002677
.00	5.00	83.80	225.00	.00002874
.00	5.00	83.80	255.00	.00003446
.00	5.00	83.80	285.00	.00005166
.00	5.00	83.80	315.00	.00011012
.00	5.00	83.80	345.00	.00022883

SUM OF DIFFERENTIAL DOSE RATES = .00205586

TABLE 18 CONT.  
DIFFERENTIAL REFLECTED DOSE RATE RESULTS

X	Y	THETA	PHI	DIFF.DOCRARF
.00	10.00	7.70	90.00	.00000531
.00	10.00	18.60	90.00	.00000553
.00	10.00	28.30	30.00	.00000822
.00	10.00	28.30	90.00	.00000593
.00	10.00	28.30	150.00	.00000494
.00	10.00	39.60	30.00	.00001141
.00	10.00	39.60	90.00	.00000668
.00	10.00	39.60	150.00	.00000528
.00	10.00	49.80	22.50	.00001854
.00	10.00	49.80	67.50	.00000984
.00	10.00	49.80	112.50	.00000668
.00	10.00	49.80	157.50	.00000581
.00	10.00	59.90	22.50	.00003152
.00	10.00	59.90	67.50	.00001278
.00	10.00	59.90	112.50	.00000794
.00	10.00	59.90	157.50	.00000680
.00	10.00	71.10	15.00	.00007550
.00	10.00	71.10	45.00	.00003331
.00	10.00	71.10	75.00	.00001602
.00	10.00	71.10	105.00	.00001104
.00	10.00	71.10	135.00	.00000933
.00	10.00	71.10	165.00	.00000872
.00	10.00	83.80	15.00	.00020750
.00	10.00	83.80	45.00	.00007019
.00	10.00	83.80	75.00	.00002783
.00	10.00	83.80	105.00	.00001800
.00	10.00	83.80	135.00	.00001495
.00	10.00	83.80	165.00	.00001391
.00	10.00	7.70	270.00	.00000531
.00	10.00	18.60	270.00	.00000553
.00	10.00	28.30	210.00	.00000494
.00	10.00	28.30	270.00	.00000593
.00	10.00	28.30	330.00	.00000822
.00	10.00	39.60	210.00	.00000528
.00	10.00	39.60	270.00	.00000668
.00	10.00	39.60	330.00	.00001141
.00	10.00	49.80	202.50	.00000581
.00	10.00	49.80	247.50	.00000668
.00	10.00	49.80	292.50	.00000984
.00	10.00	49.80	337.50	.00001854
.00	10.00	59.90	202.50	.00000680
.00	10.00	59.90	247.50	.00000794
.00	10.00	59.90	292.50	.00001278
.00	10.00	59.90	337.50	.00003152
.00	10.00	71.10	195.00	.00000872
.00	10.00	71.10	225.00	.00000933
.00	10.00	71.10	255.00	.00001104
.00	10.00	71.10	285.00	.00001602
.00	10.00	71.10	315.00	.00003331
.00	10.00	71.10	345.00	.00007550
.00	10.00	83.80	195.00	.00001391
.00	10.00	83.80	225.00	.00001495
.00	10.00	83.80	255.00	.00001800
.00	10.00	83.80	285.00	.00002783
.00	10.00	83.80	315.00	.00007019
.00	10.00	83.80	345.00	.00020750

SUM OF DIFFERENTIAL DOSE RATES = .00131931

TABLE 18 CONT.  
DIFFERENTIAL REFLECTED DOSE RATE RESULTS

X	Y	THETA	PHI	DIFF.DCRARF
.00	15.00	7.70	90.00	.00000283
.00	15.00	18.60	90.00	.00000295
.00	15.00	28.30	30.00	.00000465
.00	15.00	28.30	90.00	.00000317
.00	15.00	28.30	150.00	.00000259
.00	15.00	39.60	30.00	.00000669
.00	15.00	39.60	90.00	.00000358
.00	15.00	39.60	150.00	.00000277
.00	15.00	49.80	22.50	.00001148
.00	15.00	49.80	67.50	.00000546
.00	15.00	49.80	112.50	.00000355
.00	15.00	49.80	157.50	.00000306
.00	15.00	59.90	22.50	.00002033
.00	15.00	59.90	67.50	.00000718
.00	15.00	59.90	112.50	.00000428
.00	15.00	59.90	157.50	.00000364
.00	15.00	71.10	15.00	.00005194
.00	15.00	71.10	45.00	.00002030
.00	15.00	71.10	75.00	.00000910
.00	15.00	71.10	105.00	.00000614
.00	15.00	71.10	135.00	.00000516
.00	15.00	71.10	165.00	.00000482
.00	15.00	83.80	15.00	.00015052
.00	15.00	83.80	45.00	.00004526
.00	15.00	83.80	75.00	.00001708
.00	15.00	83.80	105.00	.00001094
.00	15.00	83.80	135.00	.00000907
.00	15.00	83.80	165.00	.00000844
.00	15.00	7.70	270.00	.00000283
.00	15.00	18.60	270.00	.00000295
.00	15.00	28.30	210.00	.00000259
.00	15.00	28.30	270.00	.00000317
.00	15.00	28.30	330.00	.00000465
.00	15.00	39.60	210.00	.00000277
.00	15.00	39.60	270.00	.00000358
.00	15.00	39.60	330.00	.00000669
.00	15.00	49.80	202.50	.00000306
.00	15.00	49.80	247.50	.00000355
.00	15.00	49.80	292.50	.00000546
.00	15.00	49.80	337.50	.00001148
.00	15.00	59.90	302.50	.00000364
.00	15.00	59.90	247.50	.00000428
.00	15.00	59.90	292.50	.00000718
.00	15.00	59.90	337.50	.00002033
.00	15.00	71.10	195.00	.00000482
.00	15.00	71.10	225.00	.00000516
.00	15.00	71.10	255.00	.00000614
.00	15.00	71.10	285.00	.00000910
.00	15.00	71.10	315.00	.00002030
.00	15.00	71.10	345.00	.00005194
.00	15.00	83.80	195.00	.00000844
.00	15.00	83.80	225.00	.00000907
.00	15.00	83.80	255.00	.00001094
.00	15.00	83.80	285.00	.00001708
.00	15.00	83.80	315.00	.00004526
.00	15.00	83.80	345.00	.00015052

SUM OF DIFFERENTIAL DOSE RATES = .00085421

TABLE 18 CONT.  
DIFFERENTIAL REFLECTED DOSE RATE RESULTS

X	Y	THETA	PHI	DIFF.DCRARF
.00	.00	7.70	90.00	.00000946
.00	.00	18.60	90.00	.00001030
.00	.00	28.30	30.00	.00001366
.00	.00	28.30	90.00	.00001150
.00	.00	28.30	150.00	.00000931
.00	.00	39.60	30.00	.00001864
.00	.00	39.60	90.00	.00001374
.00	.00	39.60	150.00	.00001007
.00	.00	49.80	22.50	.00002714
.00	.00	49.80	67.50	.00002162
.00	.00	49.80	112.50	.00001384
.00	.00	49.80	157.50	.00001095
.00	.00	59.90	22.50	.00004442
.00	.00	59.90	67.50	.00003143
.00	.00	59.90	112.50	.00001684
.00	.00	59.90	157.50	.00001269
.00	.00	71.10	15.00	.00008123
.00	.00	71.10	45.00	.00008198
.00	.00	71.10	75.00	.00004452
.00	.00	71.10	105.00	.00002476
.00	.00	71.10	135.00	.00001792
.00	.00	71.10	165.00	.00001547
.00	.00	83.80	15.00	.00020667
.00	.00	83.80	45.00	.00020578
.00	.00	83.80	75.00	.00008725
.00	.00	83.80	105.00	.00003953
.00	.00	83.80	135.00	.00002660
.00	.00	83.80	165.00	.00002235
.00	.00	7.70	270.00	.00000897
.00	.00	18.60	270.00	.00000903
.00	.00	28.30	210.00	.00000870
.00	.00	28.30	270.00	.00000936
.00	.00	28.30	330.00	.00001160
.00	.00	39.60	210.00	.00000924
.00	.00	39.60	270.00	.00001015
.00	.00	39.60	330.00	.00001391
.00	.00	49.80	202.50	.00001018
.00	.00	49.80	247.50	.00001060
.00	.00	49.80	292.50	.00001267
.00	.00	49.80	337.50	.00001868
.00	.00	59.90	202.50	.00001169
.00	.00	59.90	247.50	.00001223
.00	.00	59.90	292.50	.00001509
.00	.00	59.90	337.50	.00002534
.00	.00	71.10	195.00	.00001457
.00	.00	71.10	225.00	.00001461
.00	.00	71.10	255.00	.00001561
.00	.00	71.10	285.00	.00001832
.00	.00	71.10	315.00	.00002553
.00	.00	71.10	345.00	.00004585
.00	.00	83.80	195.00	.00002090
.00	.00	83.80	225.00	.00002096
.00	.00	83.80	255.00	.00002257
.00	.00	83.80	285.00	.00002717
.00	.00	83.80	315.00	.00004111
.00	.00	83.80	345.00	.00009083

SUM OF DIFFERENTIAL DOSE RATES = .00168663

TABLE 18 CONT.  
DIFFERENTIAL REFLECTED DOSE RATE RESULTS

X	Y	THETA	PHI	DIFF.DCRARF
3.00	10.00	7.70	90.00	.00000490
3.00	10.00	18.60	90.00	.00000528
3.00	10.00	28.30	30.00	.00000793
3.00	10.00	28.30	90.00	.00000583
3.00	10.00	28.30	150.00	.00000459
3.00	10.00	39.60	30.00	.00001165
3.00	10.00	39.60	90.00	.00000684
3.00	10.00	39.60	150.00	.00000493
3.00	10.00	49.80	22.50	.00001939
3.00	10.00	49.80	67.50	.00001121
3.00	10.00	49.80	112.50	.00000668
3.00	10.00	49.80	157.50	.00000541
3.00	10.00	59.90	22.50	.00003545
3.00	10.00	59.90	67.50	.00001582
3.00	10.00	59.90	112.50	.00000809
3.00	10.00	59.90	157.50	.00000636
3.00	10.00	71.10	15.00	.00008116
3.00	10.00	71.10	45.00	.00005021
3.00	10.00	71.10	75.00	.00002068
3.00	10.00	71.10	105.00	.00001181
3.00	10.00	71.10	135.00	.00000910
3.00	10.00	71.10	165.00	.00000812
3.00	10.00	83.80	15.00	.00023559
3.00	10.00	83.80	45.00	.00012411
3.00	10.00	83.80	75.00	.00003927
3.00	10.00	83.80	105.00	.00001989
3.00	10.00	83.80	135.00	.00001482
3.00	10.00	83.80	165.00	.00001309
3.00	10.00	7.70	270.00	.00000470
3.00	10.00	18.60	270.00	.00000477
3.00	10.00	28.30	210.00	.00000438
3.00	10.00	28.30	270.00	.00000499
3.00	10.00	28.30	330.00	.00000686
3.00	10.00	39.60	210.00	.00000467
3.00	10.00	39.60	270.00	.00000549
3.00	10.00	39.60	330.00	.00000891
3.00	10.00	49.80	202.50	.00000517
3.00	10.00	49.80	247.50	.00000562
3.00	10.00	49.80	292.50	.00000745
3.00	10.00	49.80	337.50	.00001359
3.00	10.00	59.90	202.50	.00000606
3.00	10.00	59.90	247.50	.00000663
3.00	10.00	59.90	292.50	.00000922
3.00	10.00	59.90	337.50	.00002082
3.00	10.00	71.10	195.00	.00000785
3.00	10.00	71.10	235.00	.00000808
3.00	10.00	71.10	275.00	.00000899
3.00	10.00	71.10	315.00	.00001147
3.00	10.00	71.10	355.00	.00001945
3.00	10.00	83.80	195.00	.00004655
3.00	10.00	83.80	235.00	.00001262
3.00	10.00	83.80	275.00	.00001302
3.00	10.00	83.80	315.00	.00001460
3.00	10.00	83.80	355.00	.00001922
3.00	10.00	83.80	395.00	.00003635
3.00	10.00	83.80	435.00	.00011223

SUM OF DIFFERENTIAL DOSE RATES = .00121825

TABLE 18 CONT.  
DIFFERENTIAL REFLECTED DOSE RATE RESULTS

X	Y	THETA	PHI	DIFF.DCRARF
3.00	15.00	7.70	90.00	.00000273
3.00	15.00	18.60	90.00	.00000293
3.00	15.00	28.30	30.00	.00000467
3.00	15.00	28.30	90.00	.00000321
3.00	15.00	28.30	150.00	.00000251
3.00	15.00	39.60	30.00	.00000705
3.00	15.00	39.60	90.00	.00000373
3.00	15.00	39.60	150.00	.00000269
3.00	15.00	49.80	22.50	.00001241
3.00	15.00	49.80	67.50	.00000618
3.00	15.00	49.80	112.50	.00000363
3.00	15.00	49.80	157.50	.00000297
3.00	15.00	59.90	22.50	.00002341
3.00	15.00	59.90	67.50	.00000859
3.00	15.00	59.90	112.50	.00000442
3.00	15.00	59.90	157.50	.00000353
3.00	15.00	71.10	15.00	.00005835
3.00	15.00	71.10	45.00	.00002851
3.00	15.00	71.10	75.00	.00001107
3.00	15.00	71.10	105.00	.00000653
3.00	15.00	71.10	135.00	.00000515
3.00	15.00	71.10	165.00	.00000466
3.00	15.00	83.80	15.00	.00017796
3.00	15.00	83.80	45.00	.00007049
3.00	15.00	83.80	75.00	.00002181
3.00	15.00	83.80	105.00	.00001182
3.00	15.00	83.80	135.00	.00000913
3.00	15.00	83.80	165.00	.00000821
3.00	15.00	7.70	270.00	.00000265
3.00	15.00	18.60	270.00	.00000270
3.00	15.00	28.30	210.00	.00000242
3.00	15.00	28.30	270.00	.00000285
3.00	15.00	28.30	330.00	.00000414
3.00	15.00	39.60	210.00	.00000258
3.00	15.00	39.60	270.00	.00000316
3.00	15.00	39.60	330.00	.00000564
3.00	15.00	49.80	202.50	.00000287
3.00	15.00	49.80	247.50	.00000320
3.00	15.00	49.80	292.50	.00000450
3.00	15.00	49.80	337.50	.00000921
3.00	15.00	59.90	202.50	.00000341
3.00	15.00	59.90	247.50	.00000383
3.00	15.00	59.90	292.50	.00000570
3.00	15.00	59.90	337.50	.00001504
3.00	15.00	71.10	195.00	.00000455
3.00	15.00	71.10	225.00	.00000474
3.00	15.00	71.10	255.00	.00000539
3.00	15.00	71.10	285.00	.00000721
3.00	15.00	71.10	315.00	.00001364
3.00	15.00	71.10	345.00	.00003686
3.00	15.00	83.80	195.00	.00000801
3.00	15.00	83.80	225.00	.00000836
3.00	15.00	83.80	255.00	.00000957
3.00	15.00	83.80	285.00	.00001321
3.00	15.00	83.80	315.00	.00002806
3.00	15.00	83.80	345.00	.00009790

SUM OF DIFFERENTIAL DOSE RATES = .00082004

TABLE 18 CCNT.  
DIFFERENTIAL REFLECTED DOSE RATE RESULTS

X	Y	THETA	PHI	DIFF.DCRARF
6.00	5.00	7.70	90.00	.00000526
6.00	5.00	18.60	90.00	.00000598
6.00	5.00	28.30	30.00	.00000768
6.00	5.00	28.30	90.00	.00000705
6.00	5.00	28.30	150.00	.00000532
6.00	5.00	39.60	30.00	.00001069
6.00	5.00	39.60	90.00	.00000913
6.00	5.00	39.60	150.00	.00000587
6.00	5.00	49.80	22.50	.00001486
6.00	5.00	49.80	67.50	.00001608
6.00	5.00	49.80	112.50	.00000931
6.00	5.00	49.80	157.50	.00000640
6.00	5.00	59.90	22.50	.00002379
6.00	5.00	59.90	67.50	.00002690
6.00	5.00	59.90	112.50	.00001211
6.00	5.00	59.90	157.50	.00000757
6.00	5.00	71.10	15.00	.00003724
6.00	5.00	71.10	45.00	.00006489
6.00	5.00	71.10	75.00	.00004595
6.00	5.00	71.10	105.00	.00002074
6.00	5.00	71.10	135.00	.00001210
6.00	5.00	71.10	165.00	.00000932
6.00	5.00	83.80	15.00	.00008343
6.00	5.00	83.80	45.00	.00017957
6.00	5.00	83.80	75.00	.00011140
6.00	5.00	83.80	105.00	.00003815
6.00	5.00	83.80	135.00	.00001934
6.00	5.00	83.80	165.00	.00001427
6.00	5.00	7.70	270.00	.00000477
6.00	5.00	18.60	270.00	.00000470
6.00	5.00	28.30	210.00	.00000467
6.00	5.00	28.30	270.00	.00000481
6.00	5.00	28.30	330.00	.00000585
6.00	5.00	39.60	210.00	.00000497
6.00	5.00	39.60	270.00	.00000515
6.00	5.00	39.60	330.00	.00000672
6.00	5.00	49.80	202.50	.00000555
6.00	5.00	49.80	247.50	.00000590
6.00	5.00	59.90	202.50	.00000618
6.00	5.00	59.90	247.50	.00000856
6.00	5.00	59.90	292.50	.00000644
6.00	5.00	59.90	337.50	.00000637
6.00	5.00	59.90	382.50	.00000727
6.00	5.00	71.10	195.00	.00001084
6.00	5.00	71.10	225.00	.00000829
6.00	5.00	71.10	255.00	.00000798
6.00	5.00	71.10	285.00	.00000817
6.00	5.00	71.10	315.00	.00000898
6.00	5.00	71.10	345.00	.00001114
6.00	5.00	83.80	195.00	.00001750
6.00	5.00	83.80	225.00	.00001252
6.00	5.00	83.80	255.00	.00001201
6.00	5.00	83.80	285.00	.00001232
6.00	5.00	83.80	315.00	.00001367
6.00	5.00	83.80	345.00	.00001751
6.00	5.00	83.80	382.50	.00003059

SUM OF DIFFERENTIAL DOSE RATES = .00106972



TABLE 18 CONT.  
DIFFERENTIAL REFLECTED DOSE RATE RESULTS

X	Y	THETA	PHI	DIFF.DCRARF
6.00	10.00	7.70	90.00	.00000382
6.00	10.00	18.60	90.00	.00000425
6.00	10.00	28.30	30.00	.00000629
6.00	10.00	28.30	90.00	.00000487
6.00	10.00	28.30	150.00	.00000363
6.00	10.00	39.60	30.00	.00000954
6.00	10.00	39.60	90.00	.00000602
6.00	10.00	39.60	150.00	.00000394
6.00	10.00	49.80	22.50	.00001547
6.00	10.00	49.80	67.50	.00001098
6.00	10.00	49.80	112.50	.00000580
6.00	10.00	49.80	157.50	.00000431
6.00	10.00	59.90	22.50	.00002861
6.00	10.00	59.90	67.50	.00001713
6.00	10.00	59.90	112.50	.00000722
6.00	10.00	59.90	157.50	.00000510
6.00	10.00	71.10	15.00	.00005731
6.00	10.00	71.10	45.00	.00005828
6.00	10.00	71.10	75.00	.00002439
6.00	10.00	71.10	105.00	.00001135
6.00	10.00	71.10	135.00	.00000775
6.00	10.00	71.10	165.00	.00000653
6.00	10.00	83.80	15.00	.00016017
6.00	10.00	83.80	45.00	.00016384
6.00	10.00	83.80	75.00	.00005242
6.00	10.00	83.80	105.00	.00002027
6.00	10.00	83.80	135.00	.00001303
6.00	10.00	83.80	165.00	.00001080
6.00	10.00	7.70	270.00	.00000353
6.00	10.00	18.60	270.00	.00000351
6.00	10.00	28.30	210.00	.00000331
6.00	10.00	28.30	270.00	.00000362
6.00	10.00	28.30	330.00	.00000485
6.00	10.00	39.60	210.00	.00000353
6.00	10.00	39.60	270.00	.00000393
6.00	10.00	39.60	330.00	.00000598
6.00	10.00	49.80	202.50	.00000393
6.00	10.00	49.80	247.50	.00000410
6.00	10.00	49.80	292.50	.00000506
6.00	10.00	49.80	337.50	.00000852
6.00	10.00	59.90	202.50	.00000463
6.00	10.00	59.90	247.50	.00000484
6.00	10.00	59.90	292.50	.00000613
6.00	10.00	59.90	337.50	.00001196
6.00	10.00	71.10	195.00	.00000610
6.00	10.00	71.10	225.00	.00000609
6.00	10.00	71.10	255.00	.00000651
6.00	10.00	71.10	285.00	.00000771
6.00	10.00	71.10	315.00	.00001123
6.00	10.00	71.10	345.00	.00002385
6.00	10.00	83.80	195.00	.00001005
6.00	10.00	83.80	225.00	.00001004
6.00	10.00	83.80	255.00	.00001078
6.00	10.00	83.80	285.00	.00001296
6.00	10.00	83.80	315.00	.00001998
6.00	10.00	83.80	345.00	.00005088

SUM OF DIFFERENTIAL DOSE RATES = .00098100



TABLE 18 CONT.  
DIFFERENTIAL REFLECTED DOSE RATE RESULTS

X	Y	THETA	PHI	DIFF.DCRARF
6.00	15.00	7.70	90.00	.00000241
6.00	15.00	18.60	90.00	.00000264
6.00	15.00	28.30	30.00	.00000420
6.00	15.00	28.30	90.00	.00000298
6.00	15.00	28.30	150.00	.00000223
6.00	15.00	39.60	30.00	.00000657
6.00	15.00	39.60	90.00	.00000359
6.00	15.00	39.60	150.00	.00000240
6.00	15.00	49.80	22.50	.00001149
6.00	15.00	49.80	67.50	.00000647
6.00	15.00	49.80	112.50	.00000343
6.00	15.00	49.80	157.50	.00000264
6.00	15.00	59.90	22.50	.000002230
6.00	15.00	59.90	67.50	.00000964
6.00	15.00	59.90	112.50	.00000424
6.00	15.00	59.90	157.50	.00000316
6.00	15.00	71.10	15.00	.00005102
6.00	15.00	71.10	45.00	.00003554
6.00	15.00	71.10	75.00	.00001294
6.00	15.00	71.10	105.00	.00000654
6.00	15.00	71.10	135.00	.00000477
6.00	15.00	71.10	165.00	.00000416
6.00	15.00	83.80	15.00	.00015567
6.00	15.00	83.80	45.00	.00000739
6.00	15.00	83.80	75.00	.000002735
6.00	15.00	83.80	105.00	.00001219
6.00	15.00	83.80	135.00	.00000860
6.00	15.00	83.80	165.00	.00000743
6.00	15.00	7.70	270.00	.00000226
6.00	15.00	18.60	270.00	.00000227
6.00	15.00	28.30	210.00	.00000208
6.00	15.00	28.30	270.00	.00000236
6.00	15.00	28.30	330.00	.00000336
6.00	15.00	39.60	210.00	.00000222
6.00	15.00	39.60	270.00	.00000258
6.00	15.00	39.60	330.00	.00000435
6.00	15.00	49.80	202.50	.00000248
6.00	15.00	49.80	247.50	.00000266
6.00	15.00	49.80	292.50	.00000349
6.00	15.00	49.80	337.50	.00000671
6.00	15.00	59.90	202.50	.00000295
6.00	15.00	59.90	247.50	.00000318
6.00	15.00	59.90	292.50	.00000433
6.00	15.00	59.90	337.50	.00001013
6.00	15.00	71.10	195.00	.00000397
6.00	15.00	71.10	225.00	.00000404
6.00	15.00	71.10	255.00	.00000443
6.00	15.00	71.10	285.00	.00000553
6.00	15.00	71.10	315.00	.00000907
6.00	15.00	71.10	345.00	.00002291
6.00	15.00	83.80	195.00	.00000707
6.00	15.00	83.80	225.00	.00000720
6.00	15.00	83.80	255.00	.00000794
6.00	15.00	83.80	285.00	.00001009
6.00	15.00	83.80	315.00	.00001783
6.00	15.00	83.80	345.00	.00005561

SUM OF DIFFERENTIAL DOSE RATES = .00072733

## APPENDIX K

Description and Explanation of the IBM-1620  
Computer Program Used for Calculating the  
Total Reflected Dose Rate at Point (x,y) on  
the Ceiling of a Blockhouse

The total dose rate reflected from any point of the ceiling is  
given by eq.(4'),

$$D_r(x,y) = \{1.293(\Phi_2 - \Phi_1)D_o / 16\} \sum_{c=1}^{K_{\max}} a_c \sum_{m=1}^{K_{\max}} a_m \sum_{k=1}^{K_{\max}} a_k (\omega_{1k} - \omega_{2k}) \sum_{j=1}^{K_{\max}} a_j \\ \times (0.1917 + 0.0095\omega_{oj}) \exp(-\sum_a (E_o) d / \omega_{oj}) (CK(\Theta_s) + C') \{1 + a' \sum_a (E_o) d \\ \times \exp(b \sum_a (E_o) d / \omega_{oj}) \omega_{oj}\} \{\omega_{oj} + \omega_m\}^{-1} \quad (49)$$

The source program written in FORTRAN II language is listed in this  
appendix. A logic diagram for this program is also shown.

The results obtained for the nine points of interest are presented  
in Table 19. Each of these results required 43 minutes of computer

Table 19. Total reflected dose rate results.

x feet	y feet	Reflected Dose Rate $D_o$
0.00	5.00	0.0020992
0.00	10.00	0.0013809
0.00	15.00	0.0009131
3.00	5.00	0.0017215
3.00	10.00	0.0012473
3.00	15.00	0.0008616
6.00	5.00	0.0011606
6.00	10.00	0.0009931
6.00	15.00	0.0007418

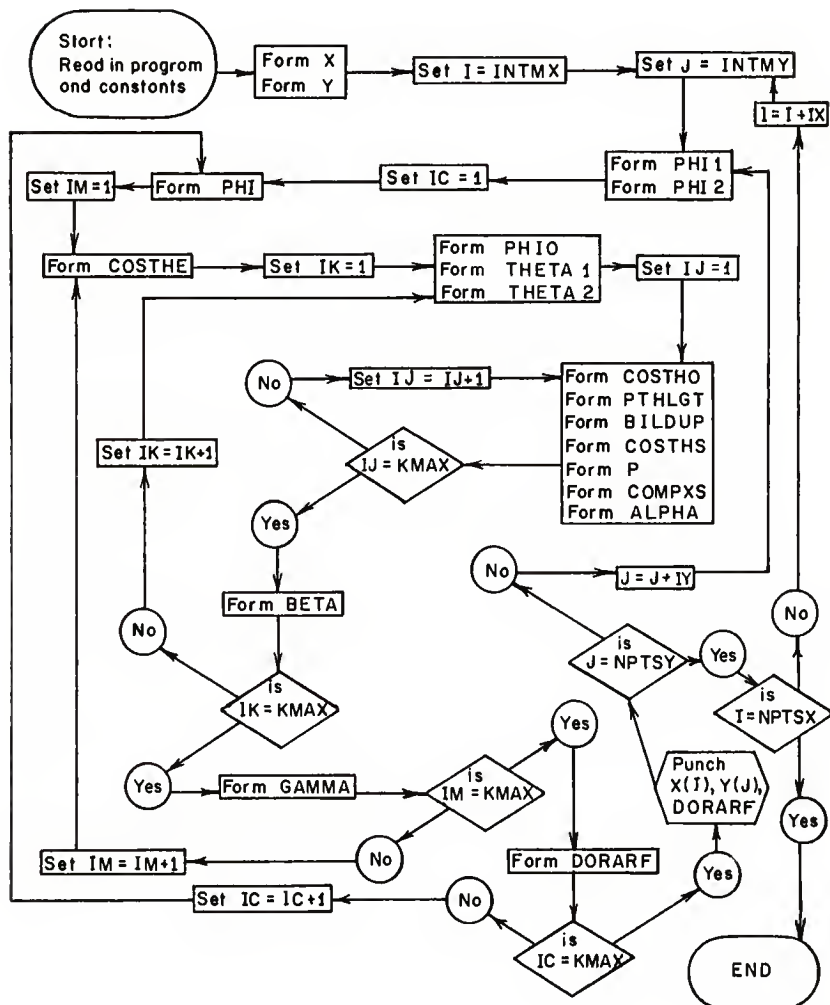
time with a  $K_{\max}$  of six. Table 20 defines the various alphanumeric  
characters utilized in this computer program.

Table 20. Input data and variables required for the IBM-1620 total reflected dose rate computer program.

Symbol*	Explanation
XMAX	Half-width of Structure Measured Parallel to Aperture Plane, $X_{\max}$ (feet)
YMAX	Total Length of Structure Measured Perpendicularly from the Aperture Plane, $Y_{\max}$ (feet)
KMAX	Degree of Gaussian Quadrature Utilized, $K_{\max}$
CHRTNO	Christoffel Numbers, $a_k$
OLEGNP	Zeros of the Legendre <sup>k</sup> Polynomials, $x_k$
IC	Fixed Point Emergent Azimuthal Angle Integration Variable
PHI	Emergent Azimuthal Angle, $\Phi$ (radians)
IM	Fixed Point Emergent Polar Angle Integration Variable
COSTHE	Cosine of Emergent Polar Angle, $\cos\Theta$
IK	Fixed Point Incident Azimuthal Angle Integration Variable
PHIO	Incident Azimuthal Angle, $\Phi_0$ (radians)
IJ	Fixed Point Incident Polar Angle Integration Variable
COSTHO	Cosine of Incident Polar Angle, $\cos\Theta_0$
DORARF	Total Reflected Dose Rate at Ceiling Poaition (x,y)( $D_0$ )

\*Additional utilized alphanumeric symbols are defined in Table 8 and Table 13.

# LOGIC DIAGRAM FOR THE TOTAL REFLECTED DOSE RATE AT ANY POINT ON A BLOCKHOUSE CEILING



```

C      REFLECTED DOSE RATE,3/9/63 BY J.A.BARAN
      DIMENSION X(101), Y(200), CLEGNP(10), CHRTNC(10)
      18 FORMAT (8I3)
      22 FORMAT(F11.8)
      20 FORMAT (F12.9,F13.10, F6.3)
      700 FORMAT(4E18.10)
      715 FORMAT (F28.2,F21.2,F25.7)
      30 READ 20, C, CPRIME, EC
C      INPUT ABOVE IS 2 CARDS
      710 READ 700, ACHD,BCHD,R,H,V,XMAX, YMAX
C      INPUT ABOVE IS 2 CARDS
      READ 18, KMAX,NPTSX, NPTSY, INTMX, INTMY, IX, IY
C      INPUT ABOVE IS 1 CARD
      DC16I=1,KMAX
      READ22,CHRTNC(I)
      16 READ22,CLEGNP(I)
C      INPUT ABOVE IS 12 CARDS
      DC 14 I= INTMX, NPTSX, IX
      14 X(I)= I-1
      DC 15 I= INTMY, NPTSY, IY
      15 Y(I)= I
C      THESE LOOPS CALCULATE THE X AND Y CO-ORDINATES OF INTEREST
      DC 760 I= INTMX, NPTSX, IX
      DC 720 J= INTMY, NPTSY, IY
C      THESE LOOPS REPEAT THE ENTIRE CALCULATION FOR DIFFERENT (X,Y)
      IF (SENSE SWITCH 1) 86, 87
      86 PAUSE
      87 PHI1=ATANF((X(I)-R)/Y(J)) + 3.1415927
      PHI2=ATANF((X(I)+R)/Y(J)) + 3.1415927
      PHI1P2 = PHI1 + PHI2
      PHI2M1 = PHI2 - PHI1
      DORARF=0.
      DC 7 IC=1,KMAX
C      THIS LOOP PERFORMS THE INTEGRATION OVER EMERGENT AZIMUTHAL ANGLES
      PHI=(CLEGNP(IC)*3.1415927) + 3.1415927
      GAMMA = 0.
      DC 6 IM=1,KMAX
C      THIS LOOP PERFORMS THE INTEGRATION OVER EMERGENT POLAR ANGLES
      COSTHE=(CLEGNP(IM)/2.)*0.5
      SIN THE=SQRTF(1.-COSTHE*COSTHE)
      BETA = 0.
      DC 5 IK=1,KMAX
C      THIS LOOP PERFORMS THE INTEGRATION OVER INCIDENT AZIMUTHAL ANGLES
      IF (SENSE SWITCH 1) 88, 89
      88 PAUSE
      89 ALPHA = 0.
      PHIC= (PHI2M1*CLEGNP(IK)/2.) + (PHI1P2/2.)
      THETA1=ATANF(Y(J)/((H+V)*ABSF(COSF(PHIC-3.1415927))))
      THETA2=ATANF(Y(J)/((H-V)*ABSF(COSF(PHIC-3.1415927))))
      CT1PT2 = COSF(THETA1)+COSF(THETA2)
      CT2MT1 = COSF(THETA2)-COSF(THETA1)
      DC 4 IJ=1,KMAX

```

```

C   THIS LOOP PERFORMS THE INTEGRATION OVER INCIDENT POLAR ANGLES
    COSTHC=((CT2MT1          )*(GLEGNP(IJ)/2.)+(CT1PT2*0.5)
    SINTHC = SQRTF(1.-COSTHC*COSTHC)
    PTHLGT=0.01825/COSTHC
    BILDUP=1.+ACHD*PTHLGT*EXPF(BCHD*PTHLGT)
    COSTHS = (SINTHC*COSF(PHI-PHIC+3.1415927)*SINTHE)-(COSTHC*COSTHE)
    P=1./(1.+(EQ*(1.-COSTHS)/0.511))
    COMPTS=(3.970562          )*(P**2)*(1.+(P**2)-P*(1.-(COSTHS**2)))
    ALPHA1 = (0.1917+0.0095*COSTHC)*(C*COMPTS+CPRIME)*CHRTNC(IJ)
1* BILDUP / (EXPF( PTHLGT          )*(COSTHC + COSTHE))
4 ALPHA = ALPHA + ALPHA1
  BETAC=-CT2MT1* ALPHA * CHRTNC(IK)
5 BETA= BETAC+BETA
  GAMMA1 = BETA*CHRTNC(IM)
6 GAMMA=GAMMA + GAMMA1
7 DCRARF=DCRARF+(GAMMA * PHI2M1 * CHRTNC(IC) * 8.08125E-2)
C   THIS ORDER CALCULATES THE REFLECTED DOSE RATE AT A CEILING POINT
720 PUNCH 715,X(I),Y(J),DCRARF
760 CONTINUE
   GO TO 30
END

```

```

      INPUT DATA
      .064501061 0.0089294690 1.252
89.562-2          62.518-3          1.85+0          2.88+0
      1.08+0          10.0+0          20.0+0
      6 7 15 1 5 3 5
      .46791393
      .23861919
      .36076157
      .66120939
      .17132449
      .93246951
      .17132449
      - .93246951
      .36076157
      - .66120939
      .46791393
      - .23861919

```

## APPENDIX L

Description and Explanation of the IBM-1620  
Computer Program Used for Calculating the Total  
Dose Rate at Position (xx,yy,zz) in a Blockhouse

The dose rate from ceiling scattered radiation at any position in  
a blockhouse is given by eq. (54),

$$\begin{aligned}
 D(xx,yy,zz) = & \{1.293(\Phi_2 - \Phi_1)K_{\max} Y_{\max} D_o / 16\pi\} \sum_{c=1}^{K_{\max}} a_c \sum_{m=1}^{K_{\max}} (a_m / \rho^2) \sum_{k=1}^{K_{\max}} a_k (\omega_{1k} - \\
 & \omega_{2k}) \sum_{j=1}^{K_{\max}} a_j (0.1917 + 0.0095 \omega_{oj}) \{1 + a' \sum_a (E_o) d \exp(b \sum_a (E_o) d / \omega_{oj})\} \exp(-\sum_a (E_o) \\
 & \times d / \omega_{oj}) \{CK(\Theta_g) + C'\} \{1 + a' (\sum_a (E') (\rho - t / \cos \Theta) - \sum_c (E') t / \cos \Theta) \\
 & \times \exp(b (\sum_a (E') (\rho - t / \cos \Theta) - \sum_c (E') t / \cos \Theta))\} \exp(-\sum_a (E') (\rho - t / \cos \Theta) \\
 & - \sum_c (E') t / \cos \Theta) \{\omega_{oj} + \cos \Theta\}^{-1}.
 \end{aligned} \quad (54)$$

The FORTRAN II source program which solves eq.(54) is listed in this  
appendix along with the pertinent logic diagram.

Approximately 21 minutes of computer time was required to obtain  
each point with a Gaussian quadrature of six for the y integration and  
three for the x,  $\Theta_o$  and  $\Phi_o$  integrations. These orders of integration  
were of sufficient accuracy for the x = 0 centerline positions. The  
computer required 43 minutes to calculate each point when off the center-  
line where Gaussian quadrature of order six was also required for the x  
integration. Total dose rates were calculated for the detector positions  
three feet above the basement and first floors at the (x,y) co-ordinates:  
(0.1, (0,6), (0,10), (0,14), (0.19), (2,10), (5,10) and (10,10). These  
dose rates are listed in Table 23.

The alphanumeric characters utilized in this program are defined in Table 22.

Table 22. Input data and variables required for the IBM-1620 total dose rate computer program.

Symbo1*	Explanation
XX	Detector Rectangular Co-ordinate Parallel to Aperture Plane, xx (feet)
YY	Detector Rectangular Co-ordinate Perpendicular to Aperture Plane, yy (feet)
ZZ	Perpendicular Distance Measured Positive Downwards from Ceiling, zz (feet)
XINTVL	X Co-ordinate Distance Between Mesh Points (feet)
YINTVL	Y Co-ordinate Distance Between Mesh Points (feet)
ZINTVL	Z Co-ordinate Distance Between Mesh Points (feet)
FLOC2G	Mass Thickness of Blockhouse Floor (g./cm <sup>2</sup> .)
TFLOOR	Thickness of Blockhouse Floor, t (feet)
MAXENG	Number of Emergent Energy Intervals
INTRPT	Number of Interpolation Points for the Average Reflected Energy Determinations
IABSC	Number of Interpolation Points for Determination of the Total Mass Absorption Coefficient
ANCTHE	The Three Incident Polar Angles, $\Theta = 30^\circ, 60^\circ$ and $90^\circ$ for Which the Average Reflected Energy is Tabulated
ENER30	Tabulated Values for the Average Reflected Energy for a $30^\circ$ Incident Polar Angle
ENER60	Tabulated Values for the Average Reflected Energy for a $60^\circ$ Incident Polar Angle
ENER90	Tabulated Values for the Average Reflected Energy for a $90^\circ$ Incident Polar Angle
THENER	Emergent $5^\circ$ Polar Angle Intervals for the Average Reflected Energies
EABSCO	Total Linear Macroscopic Gamma Ray Absorption Coefficients for Concrete; $\Sigma$ (cm <sup>-1</sup> )
EABAIR	Total Linear Macroscopic Gamma Ray Absorption Coefficients for Air at STP, $\Sigma$ (cm <sup>-1</sup> )
CHDENG	Tabulated Build-up Parameter Energies (MeV)
ACHOD	Tabulated Build-up Parameters, a'
BCHOD	Tabulated Build-up Parameters, b
XSYMTY	Has Value of One When XX = 0 and a Value of Two Otherwise
XXSYMT	Has Value of Zero When XX = 0 and a Value of $X_{\max}$ Otherwise
IC	Fixed Point x Co-ordinate Integration Variable
IM	Fixed Point y Co-ordinate Integration Variable
RHO	Distance Between Position (x,y) on the Ceiling and the Position (xx,yy,zz) of the Detector, $\rho$ (feet)

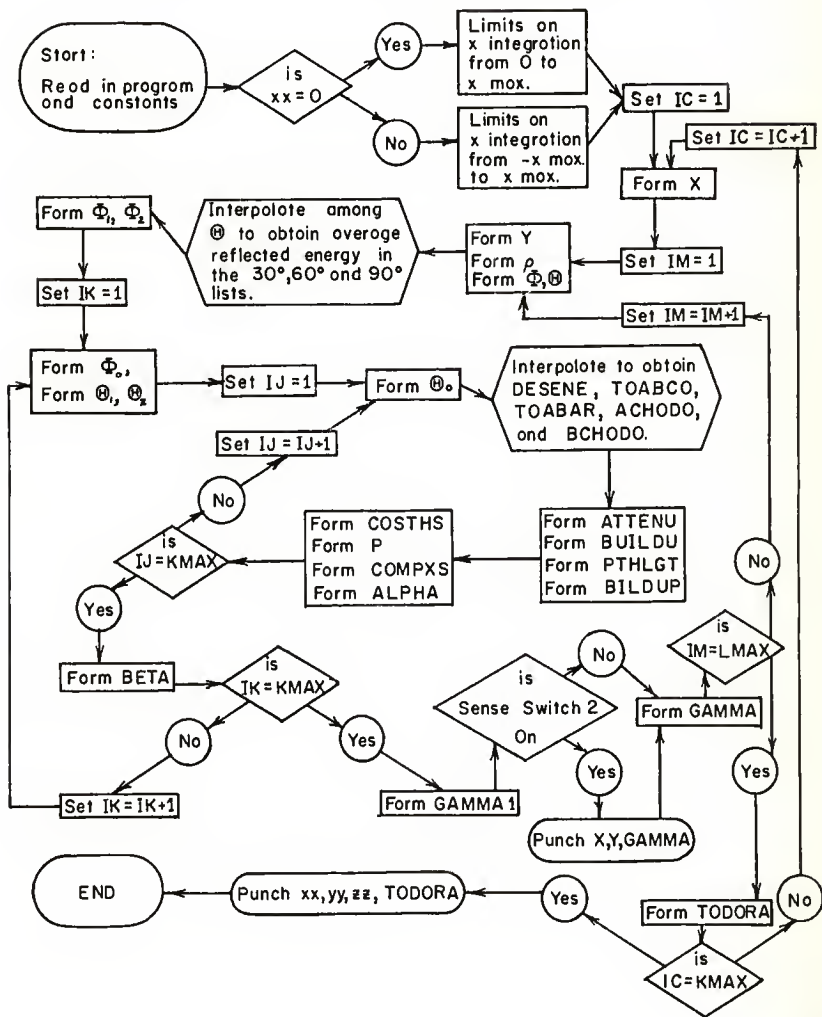


Table 22 cont.

Symbol*	Explanation
PHI	Azimuthal Angle Between Position (x,y) on the Ceiling and the Position (xx,yy,zz) of the Detector, $\Phi$ (radians)
THETA	Polar Angle Between Position (x,y) on the Ceiling and the Position (xx,yy,zz) of the Detector, $\Theta$ (radians)
INTERP	Interpolation Subroutine Discussed in Appendix C
ATTENU	Total Attenuation of Gamma Ray Between Ceiling Position and Detector
PTHLEN	Mean Free Path of Gamma Ray from Ceiling Position to Detector
TODORA	Total Dose Rate, $D(xx,yy,zz)$ ( $D_0$ )

\*Additional utilized alphanumeric symbols are defined in Tables 8, 13 and 20.

# LOGIC DIAGRAM FOR THE TOTAL DOSE RATE AT ANY POINT IN A BLOCKHOUSE



```

C      TOTAL DOSE RATE, D(XX,YY,ZZ)-- 4/3/63 BY J.A. BARAN
      DIMENSION CLEGNP(10), CHRTNC(10), ENER30(20), ENER60(20),
1 ENER90(20), THENER(20), ANCTHE(20), EN(20), EABSCC(20), ABSCEN(20),
1 CHDENG(20), ACHCD(20), BCHCD(20), EABAIR(20), CLEGNL(10), CHRTNL(10)
10  FORMAT (F6.3,F8.6,F10.6)
18  FORMAT (20I3)
19  FORMAT (E10.3)
20  FORMAT (F12.9,F13.10)
21  FORMAT (F12.8)
22  FORMAT(F11.8)
27  FORMAT(F7.4)
700 FORMAT(4E18.10)
714 FORMAT (71H                                X                                Y                                PAR
      1TIAL DOSE RATES )
715 FORMAT (F22.6, F19.6, F24.8)
716 FORMAT (/, 62H                                XX                                YY                                ZZ                                TOTAL
1 DOSE RATE ,/, F22.6, 2F11.6, F14.8)
30  READ 10, E0, EACAEC, XX, YY, ZZ, XINTVL, YINTVL, ZINTVL
C      INPUT ABOVE IS 1 CARD
      READ 20, C, CPRIME
C      INPUT ABOVE IS 1 CARD
710 READ 700, ACHD, BCHD, R, H, V, FLCC2G, XMAX, YMAX, TFLCCR,
1 YDEL, YDD
C      INPUT ABOVE IS 3 CARDS
      READ 18, KMAX, MAXENG, INTRPT, IABSC, LMAX
C      INPUT ABOVE IS 1 CARD
      DC 52 I=1,3
52  READ 21, ANCTHE(I)
C      INPUT ABOVE IS 3 CARDS
      DC 53 I=1, MAXENG
53  READ 19, ENER30(I)
C      INPUT ABOVE IS 18 CARDS
      DC 54 I=1, MAXENG
54  READ 19, ENER60(I)
C      INPUT ABOVE IS 18 CARDS
      DC 55 I=1, MAXENG
55  READ 19, ENER90(I)
C      INPUT ABOVE IS 18 CARDS
      DC 56 I=1, MAXENG
56  READ 21, THENER(I)
C      INPUT ABOVE IS 18 CARDS
      DC 57 I=1, 10
57  READ 27, EABSCC(I)
C      INPUT ABOVE IS 10 CARDS
      DC 63 I=1, 10
63  READ 27, EABAIR(I)
C      INPUT ABOVE IS 10 CARDS
      DC 58 I=1, 10
58  READ 27, ABSCEN(I)
C      INPUT ABOVE IS 10 CARDS
      DC 60 I=1, 3
60  READ 27, CHDENG(I)
C      INPUT ABOVE IS 3 CARDS
      DC 61 I=1, 3
61  READ 27, ACHCD(I)
C      INPUT ABOVE IS 3 CARDS
      DC 62 I=1, 3
62  READ 27, BCHCD(I)
C      INPUT ABOVE IS 3 CARDS
      DC 16 I=1, KMAX
      READ 22, CHRTNC(I)
16  READ 22, CLEGNP(I)
C      INPUT ABOVE IS 6 CARDS
      DC 17 I=1, LMAX
      READ 22, CHRTNL(I)
17  READ 22, CLEGNL(I)
C      INPUT ABOVE IS 6 CARDS
26  IF (SENSE SWITCH 2) 24, 25
24  PUNCH 714
25  TDCORA = 0.

```

```

XSYM TY = 1.
XXSYM = 0.
IF (XX) 67,68,67
68 XSYM TY = 2.
XXSYM = XMAX
THESE ORDERS CHANGE X LIMITS OF INTEGRATION TO 1/2 THE WIDTH
C OF THE BLOCKHOUSE IF THE DETECTOR IS ON THE X=0 CENTERLINE
67 DO 7 IC=1,LMAX
X = (XMAX * CLEGNL(IC) / XSYM TY) + (XXSYM / XSYM TY)
GAMMA = 0.
DO 6 IM=1,LMAX
Y = (YMAX * CLEGNL(IM) * 0.5) + (YMAX * 0.5)
C THESE LOOPS CALCULATE THE X AND Y CO-ORDINATES OF INTEREST
RHC = SQRTF((XX-X)*(XX-X)) + ((YY-Y)*(YY-Y)) + (ZZ*ZZ))
IF (Y - YY) 76,77,76
77 PHI = 1.5707963
GO TO 79
76 PHI = (ATANF ((X -XX) / (Y -YY ))) + 3.1415927
IF(Y-YY) 78,78,79
78 PHI = 3.1415927 + PHI
79 COSPHI = COSF(PHI)
COSTHE = ZZ/RHC
SINTHE = SQRTF(1.-COSTHE**2)
THETA = ATANF (SINTHE/COSTHE)
C CALL INTERP (MAXENG, THENER, ENER30, INTRPT, THETA , E30)
C THIS ORDER INTERPOLATES TO OBTAIN THE AVERAGE REFLECTED ENERGY
C FOR A 30 DEGREE INCIDENT POLAR ANGLE AND THE EMERGENT POLAR
C ANGLE, THETA
IF (SENSE SWITCH 1) 112,113
112 PAUSE
113 EN(1) = E30
CALL INTERP ( MAXENG, THENER, ENER60, INTRPT, THETA , E60)
EN(2) = E60
CALL INTERP ( MAXENG, THENER, ENER90, INTRPT, THETA , E90)
EN(3) = E90
IF (SENSE SWITCH 1) 86, 87
86 PAUSE
87 PHI1=ATANF((X -R)/Y ) + 3.1415927
PHI2=ATANF((X +R)/Y ) + 3.1415927
PHI1P2 = PHI1 + PHI2
PHI2M1 = PHI2 - PHI1
BETA = 0.
DO 5 IK=1,KMAX
C THIS LOOP PERFORMS THE INTEGRATION OVER INCIDENT AZIMUTHAL ANGLES
IF (SENSE SWITCH 1) 88, 89
88 PAUSE
89 ALPHA = 0.
PHIC = (PHI2M1*CLEGNP(1K)/2.) + (PHI1P2/2.)
THETA1=ATANF(Y /((H+V)*ABSF(COSF(PHIC-3.1415927))))
THETA2=ATANF(Y /((H-V)*ABSF(COSF(PHIC-3.1415927))))
CT1PT2 = COSF(THETA1)+COSF(THETA2)
CT2MT1 = COSF(THETA2)-COSF(THETA1)
DO 4 IJ=1,KMAX
C THIS LOOP PERFORMS THE INTEGRATION OVER INCIDENT POLAR ANGLES
COSTHC=((CT2MT1 )*CLEGNP(IJ)/2.)+(CT1PT2*0.5)
SINTHC = SQRTF(1.-COSTHC*COSTHC)
THETAC = ATANF (SINTHC/COSTHC)
CALL INTERP (3, ANCTHE, EN, 2, THETAC, DESENE)
C THIS ORDER INTERPOLATES TO OBTAIN THE AVERAGE REFLECTED ENERGY
CALL INTERP (10, ABSCE, EABSCC, IABSC, DESENE, TCABCC)
C THIS ORDER INTERPOLATES TO OBTAIN THE CONCRETE ATTENUATION COEF.
CALL INTERP (10, ABSCE, EABAIR, IABSC, DESENE, TCABAR)
C THIS ORDER INTERPOLATES TO OBTAIN THE AIR ATTENUATION COEFFICIENT
CALL INTERP (3, CHDENG, ACHOD, 2, DESENE, ACHODC)
C THIS ORDER INTERPOLATES TO OBTAIN THE BUILD-UP CONSTANT,ACHOD
CALL INTERP (3, CHDENG, BCHOD, 2, DESENE, BCHODC)
C THIS ORDER INTERPOLATES TO OBTAIN THE BUILD-UP CONSTANT,BCHOD
ATTENU = 1.
BILDU = 1.
IF (8.5-ZZ) 33,33,28

```

```

33 PTHLEN = TCABCO * FLOC2G / COSTHE
   BUILDU = 1. + ACHODC * PTHLEN * EXPF (BCHODC*PTHLEN)
   ATTENU = EXPF (PTHLEN)
   PTHLEN = TCABAR * (RHC - (TFLOOR/COSTHE)) * 30.48 * 0.001293
   GO TO 29
28 PTHLEN = TCABAR * RHC * 30.48 * 0.001293
29 BUILDU = BUILDU * (1. + ACHODC * PTHLEN * EXPF (BCHODC*PTHLEN))
   ATTENU = ATTENU * EXPF (PTHLEN)
   PTHLGT=0.01825/COSTHC
   BILDUP=1.+ACHD*PTHLGT*EXPF(BCHD*PTHLGT)
   COSTHS = (SINTHC*CSE(PHI-PHIC+3.1415927)*SINTHE)-(COSTHC*COSTHE)
   P=1./(1.+(EC*(1.-COSTHS)/0.511))
   COMPTS=(3.970562)*(P**2)*(1.+(P**2)-P*(1.-COSTHS**2)))
   ALPHA1 = (0.1917+0.0095*COSTHC)*(C*COMPTS+CPRIME)*CHRTNC(IJ)
1 * BILDUP*BILDUP / (EXPF(PTHLGT)*ATTENU*(COSTHC+COSTHE))
4 ALPHA = ALPHA + ALPHA1
5 BETA= BETA - CT2MT1 * ALPHA * CHRTNC(IK)
   GAMMA1 = BETA*CHRTNL(IM) * PHI2M1 * 2.5723417E-2 * XMAX * YMAX
1 * CHRTNL(IC) / (RHC*RHC)
   IF (SENSE SWITCH 2) 720,6
720 PUNCH 715,X ,Y ,GAMMA1
6 GAMMA=GAMMA + GAMMA1
7 TCDORA = TCDORA + GAMMA
   PUNCH 716, XX,YY,ZZ,TCDORA
   IF (ZZ-ZINTVL) 31,31,73
73 ZZ = ZZ - ZINTVL
   GO TO 26
31 ZZ= ZZ+ZINTVL
   IF (SENSE SWITCH 3) 32,34
32 XX= XX+XINTVL
   IF (XMAX-XX) 30,26,26
34 YY = YY + YINTVL
   IF (YMAX-YY) 30,26,26
117 END

```

INPUT DATA							
1.252	0.0268	2.0	10.0	5.166667	5.	3.	8.
.064501061	0.0089294690						
	89.562-2		62.518-3		1.85+0		2.88+0
	1.08+0		26.91+0		10.0+0		20.0+0
	.5+0						

3 18 2 2

.523599  
1.047198  
1.570796

.143+0

.161+0

.143+0

.148+0

.144+0

.150+0

.149+0

.151+0

.159+0

.165+0

.171+0

.156+0

.162+0

.184+0

.190+0

.185+0

.224+0

.243+0

.197+0

.134+0

.168+0

.165+0

.162+0

.177+0

.175+0

.180+0

.175+0

.192+0

.206+0

.207+0

.249+0

.280+0

.269+0

.296+0

.322+0

.401+0

.222+0

.196+0

.208+0

.223+0

.230+0

.241+0

.259+0

.274+0

.277+0

.292+0

.323+0

.360+0

.448+0

.473+0

.523+0

.570+0

.602+0

.640+0

# Continuation of Input Data

.043633

.130900

.218166

.305433

.392699

.479966

.567232

.654499

.741765

.829032

.916298

1.003565

1.090831

1.178097

1.265364

1.352630

1.439897

1.527163

.169

.139

.124

.107

.0954

.0870

.0804

.0706

.0635

.0567

.151

.134

.123

.106

.0953

.0868

.0804

.0706

.0655

.0567

.1

.15

.2

.3

.4

.5

.6

.8

1.0

1.25

.5

1.0

2.0

1.288

.988

.742

.112

.0752

.041

.55555556

.77459667

.88888889

.0

.55555556

.77459667

.17132449

.93246951

.36076157

.66120939

.46791393

.23861919

.46791393

.23861919

.36076157

.66120939

.17132449

.93246951

TABLE 23.  
TOTAL DOSE RATE RESULTS  
5 PER CENT APERTURE

X	Y	PARTIAL DOSE RATES
2.113248	4.226498	.00033801
2.113248	15.773502	.00003821
7.886751	4.226498	.00003529
7.886751	15.773502	.00001960

XX	YY	ZZ	TOTAL DOSE RATE
.000000	10.000000	5.166667	.00043112

X	Y	PARTIAL DOSE RATES
.694318	1.388637	.00003106
.694318	6.600190	.00008251
.694318	13.399810	.00001651
.694318	18.611363	.00000264
3.300094	1.388637	.00002212
3.300094	6.600190	.00008601
3.300094	13.399810	.00002489
3.300094	18.611363	.00000449
6.699905	1.388637	.00000441
6.699905	6.600190	.00002755
6.699905	13.399810	.00001438
6.699905	18.611363	.00000338
9.305681	1.388637	.00000087
9.305681	6.600190	.00000639
9.305681	13.399810	.00000469
9.305681	18.611363	.00000134

XX	YY	ZZ	TOTAL DOSE RATE
.000000	10.000000	5.166667	.00033331

X	Y	PARTIAL DOSE RATES
.469100	.938202	.00001006
.469100	4.615307	.00005370
.469100	10.000000	.00002386
.469100	15.384693	.00000506
.469100	19.061798	.00000112
2.307653	.938202	.00001198
2.307653	4.615307	.00007253
2.307653	10.000000	.00004370
2.307653	15.384693	.00000943
2.307653	19.061798	.00000216
5.000000	.938202	.00000372
5.000000	4.615307	.00003068
5.000000	10.000000	.00003951
5.000000	15.384693	.00000853
5.000000	19.061798	.00000218
7.692346	.938202	.00000097
7.692346	4.615307	.00000921
7.692346	10.000000	.00002488
7.692346	15.384693	.00000488
7.692346	19.061798	.00000142
9.530899	.938202	.00000024
9.530899	4.615307	.00000243
9.530899	10.000000	.00001027
9.530899	15.384693	.00000180
9.530899	19.061798	.00000057

XX	YY	ZZ	TOTAL DOSE RATE
.000000	10.000000	5.166667	.00037501

TABLE 23 CONT.  
TOTAL DOSE RATE RESULTS  
5 PER CENT APERTURE

X	Y	PARTIAL DOSE RATES	
.337652	.675305	.00000377	
.337652	3.387907	.00002961	
.337652	7.613809	.00002461	
.337652	12.386191	.00000767	
.337652	16.612093	.00000207	
.337652	19.324695	.00000055	
1.693953	.675305	.00000594	
1.693953	3.387907	.00004826	
1.693953	7.613809	.00004430	
1.693953	12.386191	.00001500	
1.693953	16.612093	.00000421	
1.693953	19.324695	.00000114	
3.806904	.675305	.00000283	
3.806904	3.387907	.00002726	
3.806904	7.613809	.00003398	
3.806904	12.386191	.00001480	
3.806904	16.612093	.00000474	
3.806904	19.324695	.00000135	
6.193095	.675305	.00000090	
6.193095	3.387907	.00000968	
6.193095	7.613809	.00001629	
6.193095	12.386191	.00000952	
6.193095	16.612093	.00000366	
6.193095	19.324695	.00000112	
8.306046	.675305	.00000029	
8.306046	3.387907	.00000329	
8.306046	7.613809	.00000657	
8.306046	12.386191	.00000475	
8.306046	16.612093	.00000213	
8.306046	19.324695	.00000070	
9.662347	.675305	.00000008	
9.662347	3.387907	.00000097	
9.662347	7.613809	.00000210	
9.662347	12.386191	.00000170	
9.662347	16.612093	.00000083	
9.662347	19.324695	.00000028	
XX	YY	ZZ	TOTAL DOSE RATE
.000000	10.000000	5.166667	.00033712



TABLE 23 CONT.  
TOTAL DOSE RATE RESULTS  
5 PER CENT APERTURE

X	Y	PARTIAL DOSE RATES
1.127016	.675305	.00002439
1.127016	3.387907	.00007680
1.127016	7.613809	.00002771
1.127016	12.386191	.00000816
1.127016	16.612093	.00000276
1.127016	19.324695	.00000084
5.000000	.675305	.00000522
5.000000	3.387907	.00003316
5.000000	7.613809	.00002492
5.000000	12.386191	.00000995
5.000000	16.612093	.00000376
5.000000	19.324695	.00000119
8.872983	.675305	.00000052
8.872983	3.387907	.00000450
8.872983	7.613809	.00000624
8.872983	12.386191	.00000374
8.872983	16.612093	.00000170
8.872983	19.324695	.00000058

XX	YY	ZZ	TOTAL DOSE RATE
.000000	1.000000	5.166667	.00023623

X	Y	PARTIAL DOSE RATES
1.127016	.675305	.00001667
1.127016	3.387907	.00009828
1.127016	7.613809	.00005336
1.127016	12.386191	.00001427
1.127016	16.612093	.00000427
1.127016	19.324695	.00000123
5.000000	.675305	.00000412
5.000000	3.387907	.00003658
5.000000	7.613809	.00003860
5.000000	12.386191	.00001578
5.000000	16.612093	.00000556
5.000000	19.324695	.00000169
8.872983	.675305	.00000046
8.872983	3.387907	.00000468
8.872983	7.613809	.00000802
8.872983	12.386191	.00000520
8.872983	16.612093	.00000233
8.872983	19.324695	.00000078

XX	YY	ZZ	TOTAL DOSE RATE
.000000	6.000000	5.166667	.00031195

TABLE 23 CONT.  
TOTAL DOSE RATE RESULTS  
5 PER CENT APERTURE

X	Y	PARTIAL DOSE RATES
1.127016	.675305	.00001066
1.127016	3.387907	.00008596
1.127016	7.613809	.00007457
1.127016	12.386191	.00002410
1.127016	16.612093	.00000663
1.127016	19.324695	.00000179
5.000000	.675305	.00000296
5.000000	3.387907	.00003058
5.000000	7.613809	.00004494
5.000000	12.386191	.00002281
5.000000	16.612093	.00000800
5.000000	19.324695	.00000235
8.872983	.675305	.00000037
8.872983	3.387907	.00000414
8.872983	7.613809	.00000856
8.872983	12.386191	.00000651
8.872983	16.612093	.00000303
8.872983	19.324695	.00000101

XX	YY	ZZ	TOTAL DOSE RATE
.000000	10.000000	5.166667	.00033905

X	Y	PARTIAL DOSE RATES
1.127016	.675305	.00000715
1.127016	3.387907	.00007065
1.127016	7.613809	.00008982
1.127016	12.386191	.00003795
1.127016	16.612093	.00001111
1.127016	19.324695	.00000284
5.000000	.675305	.00000214
5.000000	3.387907	.00002406
5.000000	7.613809	.00004467
5.000000	12.386191	.00002944
5.000000	16.612093	.00001164
5.000000	19.324695	.00000342
8.872983	.675305	.00000029
8.872983	3.387907	.00000344
8.872983	7.613809	.00000811
8.872983	12.386191	.00000740
8.872983	16.612093	.00000384
8.872983	19.324695	.00000131

XX	YY	ZZ	TOTAL DOSE RATE
.000000	14.000000	5.166667	.00035936

TABLE 23 CONT.  
TOTAL DOSE RATE RESULTS  
5 PER CENT APERTURE

X	Y	PARTIAL DOSE RATES	
1.127016	.675305	.00000472	
1.127016	3.387907	.00005427	
1.127016	7.613809	.00009159	
1.127016	12.386191	.00005961	
1.127016	16.612093	.00002060	
1.127016	19.324695	.00000544	
5.000000	.675305	.00000149	
5.000000	3.387907	.00001800	
5.000000	7.613809	.00004089	
5.000000	12.386191	.00003503	
5.000000	16.612093	.00001666	
5.000000	19.324695	.00000532	
8.872983	.675305	.00000022	
8.872983	3.387907	.00000268	
8.872983	7.613809	.00000704	
8.872983	12.386191	.00000761	
8.872983	16.612093	.00000463	
8.872983	19.324695	.00000172	
XX	YY	ZZ	TOTAL DOSE RATE
.000000	19.000000	5.166667	.00037759

TABLE 23 CONT.  
TOTAL DOSE RATE RESULTS  
5 PER CENT APERTURE

X	Y	PARTIAL DOSE RATES	
-9.324695	.675305	.00000008	
-9.324695	3.387907	.00000091	
-9.324695	7.613809	.00000187	
-9.324695	12.386191	.00000151	
-9.324695	16.612093	.00000076	
-9.324695	19.324695	.00000026	
-6.612093	.675305	.00000049	
-6.612093	3.387907	.00000510	
-6.612093	7.613809	.00000861	
-6.612093	12.386191	.00000549	
-6.612093	16.612093	.00000233	
-6.612093	19.324695	.00000075	
-2.386191	.675305	.00000512	
-2.386191	3.387907	.00004011	
-2.386191	7.613809	.00003878	
-2.386191	12.386191	.00001528	
-2.386191	16.612093	.00000483	
-2.386191	19.324695	.00000137	
2.386191	.675305	.00000637	
2.386191	3.387907	.00005859	
2.386191	7.613809	.00005947	
2.386191	12.386191	.00001998	
2.386191	16.612093	.00000552	
2.386191	19.324695	.00000149	
6.612093	.675305	.00000068	
6.612093	3.387907	.00000782	
6.612093	7.613809	.00001439	
6.612093	12.386191	.00000834	
6.612093	16.612093	.00000305	
6.612093	19.324695	.00000091	
9.324695	.675305	.00000011	
9.324695	3.387907	.00000133	
9.324695	7.613809	.00000292	
9.324695	12.386191	.00000223	
9.324695	16.612093	.00000101	
9.324695	19.324695	.00000033	
XX	YY	ZZ	TOTAL DOSE RATE
2.000000	10.000000	5.166667	.00032834

TABLE 23 CONT.  
TOTAL DOSE RATE RESULTS  
5 PER CENT APERTURE

X	Y	PARTIAL DOSE RATES	
-9.324695	.675305	.00000006	
-9.324695	3.387907	.00000070	
-9.324695	7.613809	.00000142	
-9.324695	12.386191	.00000117	
-9.324695	16.612093	.00000062	
-9.324695	19.324695	.00000022	
-6.612093	.675305	.00000038	
-6.612093	3.387907	.00000381	
-6.612093	7.613809	.00000621	
-6.612093	12.386191	.00000414	
-6.612093	16.612093	.00000190	
-6.612093	19.324695	.00000063	
-2.386191	.675305	.00000408	
-2.386191	3.387907	.00002862	
-2.386191	7.613809	.00002627	
-2.386191	12.386191	.00001137	
-2.386191	16.612093	.00000403	
-2.386191	19.324695	.00000120	
2.386191	.675305	.00000682	
2.386191	3.387907	.00006687	
2.386191	7.613809	.00006053	
2.386191	12.386191	.00001890	
2.386191	16.612093	.00000535	
2.386191	19.324695	.00000146	
6.612093	.675305	.00000084	
6.612093	3.387907	.00001085	
6.612093	7.613809	.00002161	
6.612093	12.386191	.00001098	
6.612093	16.612093	.00000351	
6.612093	19.324695	.00000100	
9.324695	.675305	.00000014	
9.324695	3.387907	.00000181	
9.324695	7.613809	.00000432	
9.324695	12.386191	.00000309	
9.324695	16.612093	.00000123	
9.324695	19.324695	.00000038	
XX	YY	ZZ	TOTAL DOSE RATE
5.000000	10.000000	5.166667	.00031671

TABLE 23 CONT.  
TOTAL DOSE RATE RESULTS  
5 PER CENT APERTURE

X	Y	PARTIAL DOSE RATES	
-9.324695	.675305	.00000004	
-9.324695	3.387907	.00000048	
-9.324695	7.613809	.00000096	
-9.324695	12.386191	.00000082	
-9.324695	16.612093	.00000046	
-9.324695	19.324695	.00000017	
-6.612093	.675305	.00000026	
-6.612093	3.387907	.00000249	
-6.612093	7.613809	.00000396	
-6.612093	12.386191	.00000278	
-6.612093	16.612093	.00000138	
-6.612093	19.324695	.00000048	
-2.386191	.675305	.00000270	
-2.386191	3.387907	.00001690	
-2.386191	7.613809	.00001495	
-2.386191	12.386191	.00000719	
-2.386191	16.612093	.00000291	
-2.386191	19.324695	.00000093	
2.386191	.675305	.00000649	
2.386191	3.387907	.00005847	
2.386191	7.613809	.00003920	
2.386191	12.386191	.00001287	
2.386191	16.612093	.00000423	
2.386191	19.324695	.00000124	
6.612093	.675305	.00000113	
6.612093	3.387907	.00001813	
6.612093	7.613809	.00003255	
6.612093	12.386191	.00001158	
6.612093	16.612093	.00000354	
6.612093	19.324695	.00000100	
9.324695	.675305	.00000020	
9.324695	3.387907	.00000311	
9.324695	7.613809	.00000840	
9.324695	12.386191	.00000452	
9.324695	16.612093	.00000149	
9.324695	19.324695	.00000043	
XX	YY	ZZ	TOTAL DOSE RATE
10.000000	10.000000	5.166667	.00026862

TABLE 23 CONT.  
TOTAL DOSE RATE RESULTS  
5 PER CENT APERTURE

X	Y	PARTIAL DOSE RATES	
1.127016	.675305	.00000095	
1.127016	3.387907	.00000342	
1.127016	7.613809	.00000178	
1.127016	12.386191	.00000050	
1.127016	16.612093	.00000013	
1.127016	19.324695	.00000003	
5.000000	.675305	.00000027	
5.000000	3.387907	.00000185	
5.000000	7.613809	.00000167	
5.000000	12.386191	.00000057	
5.000000	16.612093	.00000018	
5.000000	19.324695	.00000004	
8.872983	.675305	.00000003	
8.872983	3.387907	.00000030	
8.872983	7.613809	.00000039	
8.872983	12.386191	.00000019	
8.872983	16.612093	.00000007	
8.872983	19.324695	.00000002	
XX	YY	ZZ	TOTAL DOSE RATE
.000000	1.000000	13.166667	.00001248

X	Y	PARTIAL DOSE RATES	
1.127016	.675305	.00000067	
1.127016	3.387907	.00000387	
1.127016	7.613809	.00000240	
1.127016	12.386191	.00000096	
1.127016	16.612093	.00000027	
1.127016	19.324695	.00000006	
5.000000	.675305	.00000023	
5.000000	3.387907	.00000197	
5.000000	7.613809	.00000230	
5.000000	12.386191	.00000109	
5.000000	16.612093	.00000033	
5.000000	19.324695	.00000009	
8.872983	.675305	.00000002	
8.872983	3.387907	.00000031	
8.872983	7.613809	.00000054	
8.872983	12.386191	.00000032	
8.872983	16.612093	.00000012	
8.872983	19.324695	.00000003	
XX	YY	ZZ	TOTAL DOSE RATE
.000000	6.000000	13.166667	.00001568

TABLE 23 CONT.  
TOTAL DOSE RATE RESULTS  
5 PER CENT APERTURE

X	Y	PARTIAL DOSE RATES
1.127016	.675305	.00000042
1.127016	3.387907	.000000319
1.127016	7.613809	.000000289
1.127016	12.386191	.000000128
1.127016	16.612093	.000000046
1.127016	19.324695	.000000012
5.000000	.675305	.000000015
5.000000	3.387907	.000000166
5.000000	7.613809	.000000250
5.000000	12.386191	.000000144
5.000000	16.612093	.000000054
5.000000	19.324695	.000000015
8.872983	.675305	.000000002
8.872983	3.387907	.000000025
8.872983	7.613809	.000000056
8.872983	12.386191	.000000043
8.872983	16.612093	.000000019
8.872983	19.324695	.000000005

XX	YY	ZZ	TOTAL DOSE RATE
.0000000	10.000000	13.166667	.00001638

X	Y	PARTIAL DOSE RATES
1.127016	.675305	.000000024
1.127016	3.387907	.000000208
1.127016	7.613809	.000000289
1.127016	12.386191	.000000147
1.127016	16.612093	.000000062
1.127016	19.324695	.000000018
5.000000	.675305	.000000009
5.000000	3.387907	.000000111
5.000000	7.613809	.000000236
5.000000	12.386191	.000000168
5.000000	16.612093	.000000076
5.000000	19.324695	.000000023
8.872983	.675305	.000000001
8.872983	3.387907	.000000017
8.872983	7.613809	.000000048
8.872983	12.386191	.000000048
8.872983	16.612093	.000000025
8.872983	19.324695	.000000008

XX	YY	ZZ	TOTAL DOSE RATE
.0000000	14.000000	13.166667	.00001526



TABLE 23 CONT.  
TOTAL DOSE RATE RESULTS  
5 PER CENT APERTURE

X	Y	PARTIAL DOSE RATES	
.337652	.675305	.00000003	
.337652	3.387907	.00000038	
.337652	7.613809	.00000070	
.337652	12.386191	.00000054	
.337652	16.612093	.00000024	
.337652	19.324695	.00000009	
1.693953	.675305	.00000005	
1.693953	3.387907	.00000067	
1.693953	7.613809	.00000133	
1.693953	12.386191	.00000108	
1.693953	16.612093	.00000050	
1.693953	19.324695	.00000015	
3.806904	.675305	.00000003	
3.806904	3.387907	.00000049	
3.806904	7.613809	.00000116	
3.806904	12.386191	.00000108	
3.806904	16.612093	.00000056	
3.806904	19.324695	.00000019	
6.193095	.675305	.00000001	
6.193095	3.387907	.00000022	
6.193095	7.613809	.00000061	
6.193095	12.386191	.00000068	
6.193095	16.612093	.00000041	
6.193095	19.324695	.00000015	
8.306046	.675305	0.00000000	
8.306046	3.387907	.00000008	
8.306046	7.613809	.00000025	
8.306046	12.386191	.00000032	
8.306046	16.612093	.00000021	
8.306046	19.324695	.00000008	
9.662347	.675305	0.00000000	
9.662347	3.387907	.00000002	
9.662347	7.613809	.00000008	
9.662347	12.386191	.00000010	
9.662347	16.612093	.00000007	
9.662347	19.324695	.00000003	
XX	YY	ZZ	TOTAL DOSE RATE
.000000	19.000000	13.166667	.00001276

TABLE 23 CONT.  
TOTAL DOSE RATE RESULTS  
5 PER CENT APERTURE

-9.324695	.675305	0.00000000
-9.324695	3.387907	.00000003
-9.324695	7.613809	.00000007
-9.324695	12.386191	.00000006
-9.324695	16.612093	.00000003
-9.324695	19.324695	.00000001
-6.612093	.675305	.00000001
-6.612093	3.387907	.00000020
-6.612093	7.613809	.00000036
-6.612093	12.386191	.00000024
-6.612093	16.612093	.00000010
-6.612093	19.324695	.00000003
-2.386191	.675305	.00000016
-2.386191	3.387907	.00000130
-2.386191	7.613809	.00000152
-2.386191	12.386191	.00000075
-2.386191	16.612093	.00000026
-2.386191	19.324695	.00000007
2.386191	.675305	.00000026
2.386191	3.387907	.00000227
2.386191	7.613809	.00000232
2.386191	12.386191	.00000105
2.386191	16.612093	.00000037
2.386191	19.324695	.00000009
6.612093	.675305	.00000004
6.612093	3.387907	.00000057
6.612093	7.613809	.00000099
6.612093	12.386191	.00000061
6.612093	16.612093	.00000024
6.612093	19.324695	.00000006
9.324695	.675305	0.00000000
9.324695	3.387907	.00000011
9.324695	7.613809	.00000025
9.324695	12.386191	.00000019
9.324695	16.612093	.00000008
9.324695	19.324695	.00000002

XX	YY	ZZ	TOTAL DOSE RATE
5.000000	10.000000	13.166667	.00001487

TABLE 23 CONT.  
TOTAL DOSE RATE RESULTS  
5 PER CENT APERTURE

X	Y	PARTIAL DOSE RATES	
-9.324695	.675305	0.00000000	
-9.324695	3.387907	.00000001	
-9.324695	7.613809	.00000003	
-9.324695	12.386191	.00000003	
-9.324695	16.612093	.00000001	
-9.324695	19.324695	0.00000000	
-6.612093	.675305	0.00000000	
-6.612093	3.387907	.00000009	
-6.612093	7.613809	.00000017	
-6.612093	12.386191	.00000013	
-6.612093	16.612093	.00000006	
-6.612093	19.324695	.00000001	
-2.386191	.675305	.00000008	
-2.386191	3.387907	.00000066	
-2.386191	7.613809	.00000077	
-2.386191	12.386191	.00000040	
-2.386191	16.612093	.00000015	
-2.386191	19.324695	.00000004	
2.386191	.675305	.00000019	
2.386191	3.387907	.00000169	
2.386191	7.613809	.00000179	
2.386191	12.386191	.00000080	
2.386191	16.612093	.00000027	
2.386191	19.324695	.00000007	
6.612093	.675305	.00000005	
6.612093	3.387907	.00000066	
6.612093	7.613809	.00000112	
6.612093	12.386191	.00000064	
6.612093	16.612093	.00000024	
6.612093	19.324695	.00000006	
9.324695	.675305	.00000001	
9.324695	3.387907	.00000015	
9.324695	7.613809	.00000032	
9.324695	12.386191	.00000023	
9.324695	16.612093	.00000010	
9.324695	19.324695	.00000002	
XX	YY	ZZ	TOTAL DOSE RATE
10.000000	10.000000	13.166667	.00001122

TABLE 23 CONT.  
TOTAL DOSE RATE RESULTS  
60 PER CENT APERTURE

X	Y	PARTIAL DOSE RATES
1.127016	.675305	.00063415
1.127016	3.387907	.00109058
1.127016	7.613809	.00075629
1.127016	12.386191	.00025516
1.127016	16.612093	.00007386
1.127016	19.324695	.00002039
5.000000	.675305	.00081115
5.000000	3.387907	.00137922
5.000000	7.613809	.00074970
5.000000	12.386191	.00027826
5.000000	16.612093	.00009428
5.000000	19.324695	.00002770
8.872983	.675305	.00038830
8.872983	3.387907	.00028342
8.872983	7.613809	.00018394
8.872983	12.386191	.00009314
8.872983	16.612093	.00003885
8.872983	19.324695	.00001258

XX	YY	ZZ	TOTAL DOSE RATE
.000000	10.000000	5.166667	.00717106

X	Y	PARTIAL DOSE RATES
1.127016	.675305	.00001942
1.127016	3.387907	.00003672
1.127016	7.613809	.00002945
1.127016	12.386191	.00001384
1.127016	16.612093	.00000511
1.127016	19.324695	.00000136
5.000000	.675305	.00002673
5.000000	3.387907	.00004685
5.000000	7.613809	.00003630
5.000000	12.386191	.00001738
5.000000	16.612093	.00000639
5.000000	19.324695	.00000179
8.872983	.675305	.00001067
8.872983	3.387907	.00001269
8.872983	7.613809	.00001112
8.872983	12.386191	.00000609
8.872983	16.612093	.00000243
8.872983	19.324695	.00000071

XX	YY	ZZ	TOTAL DOSE RATE
.000000	10.000000	13.166667	.00028515

## APPENDIX M

Description and Explanation of the IBM-1620  
Computer Program Used to Calculate the First  
Order Exponential Integral

The first and second order exponential integrals,  $E_1(x)$  and  $E_2(x)$ , were encountered in the study of the total incident dose rate on the ceiling, eq.(38). This appendix describes the subroutine written to obtain the  $E_1$  function, Subroutine E1(ARGT, EARGT). Here ARG T is the argument of the  $E_1$  function and EARGT is the value of the function for this argument. Second order exponential integrals were obtained from the recursion relationship,

$$E_2(x) = e^{-x} - x E_1(x). \quad (89)$$

Two different expressions were utilized to obtain  $E_1(x)$  for different arguments (22). When the argument of  $E_1$  was less than one, the following infinite series was utilized.

$$E_1(x) = -0.57721566 - \ln x + x - (x^2/4) + (x^3/18) - \dots \quad (90)$$

The number of terms considered was determined by requiring that the ratio of the absolute value of the last term to the complete series be less than a specified value. This value was set at  $1 \times 10^{-5}$  in this subroutine. The  $E_1$  function for values of the argument greater than or equal to one (26) is given by the expression,

$$E_1(x) = (e^{-x}/x) \{ a_0 + a_1 x + a_2 x^2 + a_3 x^3 + x^4 \} \\ \times \{ b_0 + b_1 x + b_2 x^2 + b_3 x^3 + x^4 \}^{-1} \quad (91)$$

where

$$\begin{aligned} a_0 &= 0.26777373 & b_0 &= 3.9584969 \\ a_1 &= 8.6347609 & b_1 &= 21.099653 \\ a_2 &= 18.059017 & b_2 &= 25.632956 \\ a_3 &= 8.5733287 & b_3 &= 9.5733223 \end{aligned}$$

Eq.(91) is accurate to within the limitations of the computer.

The program printout of this subroutine is as follows:

```
C      E1 SUBROUTINE, 3/16/63 BY J.A.BARAN
      SUBROUTINE E1(ARGT,EARGH)
      IF(ARGT-1.) 730, 729, 729
729  EARGH = (0.26777373 + (8.6347609*ARGT) + (18.059017*ARGT*ARGT)+(
      18.5733287*(ARGT**3)) + (ARGT**4)) / ((EXP(ARGT)) * ARG * (3.9584
      1969 + (21.099653 * ARG) + (25.632956 * ARG * ARG) + (9.5733223
      1 * (ARG * ARG * ARG)) + (ARGT**4)))
      GO TO 765
730  EARGH = -0.57721566-LCGF(ARGT)+ARGT-(((ARGT**2)/4.)+(ARGT**3)/
      118.)
      QFACT=24
      Q=4
740  ERE1=(((ARGT**Q)/(QFACT*Q))/EARGH
      IF(ERE1-1.E-5) 765,750,750
750  N=Q
      EARGH =EARGH +((-1.)*(N+1))*((ARGT**Q)/(QFACT*Q))
      Q=Q+1.
      QFACT=QFACT*Q
      GO TO 740
765  RETURN
      END
```

## APPENDIX N

## Protection Factor of the KSU Blockhouse

The protection factor,  $P_f$ , of the KSU blockhouse illustrated in Figure 1 can be obtained by utilizing the methodology and design curves of reference 2. The protection factor is the coefficient which, when multiplied by the dose rate in a protected area (shelter area), will equal the dose rate which would be received by a detector located at the standard unprotected position three feet above the center of a smooth, uniformly contaminated area of infinite extent. Reference 2 utilizes a series of design curves to obtain reduction factors (inverse of protection factors). The reduction factor in this thesis for a given detector position would be merely the dose rate divided by  $D_o$ .

The protection factor of the KSU blockhouse with no apertures was experimentally measured (4) to be 5.7 at about three feet above the center of the first floor and 370 at three feet above the center of the basement floor. The results obtained (4) utilizing Reference 2 are 6.8 for the first floor and 1000 for the basement. With an aperture in a wall, the ground contribution through that portion of the wall which is actually occupied by the windows but is assumed to be solid is subtracted from the ground contribution through the wall assuming it has no windows (2). This subtraction yields the ground contribution through that portion of the wall not occupied by windows. The skyshine contribution through the windows themselves are next added to this quantity. Although this technique can be followed straightforwardly, it is rather laborious and does not give a very good physical picture of what is actually going on.

In contrast to this, an "Equivalent Building Method" developed by

LeDoux (24) gives a very good feel for the effect of windows in walls. The ratio of total window area to total wall area is first calculated. This ratio is called the aperture fraction. The detector is assumed to be at the sill height of the window. An equivalent wall mass thickness is obtained graphically which corrects for the effect of the aperture. This equivalent wall mass thickness is mainly a function of the actual wall mass thickness, the aperture fraction and the structure area. The experimentally measured wall thickness for the KSU blockhouse is 69 pounds per square foot (psf). The curves of reference (24) indicate that an aperture fraction of 0.6 for this structure would result in an equivalent mass thickness of about 61 psf. That is, removing 60% of the wall above the detector location results in a decrease in wall mass thickness by only about 12%. This result is indicative not only of the small proportion of radiation incident on the detector from skyshine, but also of the fact that radiation penetrating walls of such low mass thicknesses are so lowered in energy that the wall attenuation is nearly overcome by the higher attenuation coefficients of the transmitted radiation.

The protection factors in the KSU blockhouse with a 0.6 aperture fraction above the level of the detector would therefore be decreased by approximately 20% to about 300 at the central 3' level in the basement and about 4.7 at the central 3' level on the first floor.



BLOCKHOUSE DOSAGE CONTRIBUTIONS RESULTING FROM  
WINDOW-COLLIMATED, CEILING SCATTERED FALLOUT RADIATION

by

JAMES ANDREW BARAN

B. S., Case Institute of Technology, 1960

---

AN ABSTRACT OF  
A MASTER'S THESIS

submitted in partial fulfillment of the  
requirements for the degree

MASTER OF SCIENCE

Department of Nuclear Engineering

KANSAS STATE UNIVERSITY

Manhattan, Kansas

1963

## ABSTRACT

The theory of the penetration of fallout gamma radiation into structures has been extensively studied and formulated in the past few years. This monograph considers one aspect of this theory which has not been investigated--the contribution of radiation dose rate in a protective structure resulting from fallout radiation entering the structure through apertures in vertical walls and reflecting off the ceiling of the structure. This problem is known as the "ceiling shine" problem.

FORTRAN II digital computer programs are written whereby the differential and total (incident and reflected) aperture-collimated, dose rate contributions at the ceiling of an idealized concrete structure are determined. A program was also written for the aperture-collimated, ceiling scattered dose rate at any point in the structure. Results are graphically presented for the case of the concrete blockhouse presently erected at the Kansas State University Nuclear Engineering Shielding Facility (a 20' x 20' x 8' structure with basement and a window centered horizontally in one wall). This window covers approximately 5% of the area of one wall.

The average total dose rate albedo of the concrete blockhouse ceiling for incident cobalt-60 gamma photons was determined from the derived differential dose rate albedo to be fourteen per cent. The window-collimated radiation incident on the ceiling was just under one per cent of the dose rate outside the structure at the standard position three feet above the contaminated plane. Approximately one tenth of one per cent of this outside radiation was thus reflected at a given ceiling point.

The total dose rate from this window-collimated, ceiling scattered radiation was determined for two traverses along the blockhouse center-lines for the detector positioned three feet above the first floor and three feet above the basement floor. These window-collimated, ceiling scattered dose rates were compared with the experimental total dose rates received by the detector in the blockhouse surrounded by an infinite plane field of cobalt-60 contamination. The window-collimated, ceiling scattered dose rates for the above described blockhouse with a five per cent aperture in each of the four walls were approximately one per cent of the total on the first floor and about two per cent of the total in the basement. When the window was increased in size to cover sixty per cent of the wall area with its lower edge higher above the ground than the detector position, the window-collimated, ceiling scattered radiation was about twelve per cent of the total on the first floor and about twenty-six per cent of the total in the basement.